

Production and purification of four cytokines from recombinant *Escherichia coli*

Der Naturwissenschaften Fakult ä
der Gottfried Wilhelm Leibniz Universit ä Hannover

zur Erlangung des Grades
Doktorin der Naturwissenschaften
Dr. rer. nat.

genehmigte Dissertation
von

Dipl.-Biol. Yangxi Zhao
geboren am 01.03.1982 in Sichuan, China

Hannover, 2012

Referent

Prof. Dr. Thomas Scheper

Institut für Technische Chemie

Gottfried Wilhelm Leibniz Universität Hannover

Korreferentin

Prof. Dr. Ursula Rinas

Institut für Technische Chemie

Gottfried Wilhelm Leibniz Universität Hannover

Tag der Promotion: 17.12.2012

Eigenständigkeitserklärung

Ich versichere, dass ich diese Dissertation selbstständig und nur unter Verwendung der angegebenen Hilfsmittel und Quellen durchgeführt habe.

Diese Arbeit wurde nicht als Diplomarbeit oder ähnliche Prüfungsarbeit verwendet.

Hannover, im Oktober 2012

Acknowledgements

It was a pleasure for me to make this dissertation at the Institute for Technical Chemistry (TCI) at Leibniz University of Hanover. First of all, I would like to thank my advisor, Prof. Dr. Thomas Scheper. He patiently provided the vision, encouragement and advice necessary for me to proceed through the Ph.D study and complete my dissertation. I learned a lot during this time and I am convinced that this knowledge will help me in the future.

I am grateful to Prof. Dr. Ursula Rinas for her valuable suggestions and discussions of my practical work and the reviewing of my thesis. I am happy to have had such a supportive co-supervisor.

I would like to thank Prof. Dr. Jürgen Alves for being my third examiner.

My thanks to the people from Medical School Hanover (MHH) for their kind cooperation. Prof. Dr. Denise Hilfiker-Kleiner and Dr. Axel Schambach provided the plasmids of 16-kDa hPRL and hActivin A, respectively. The team of Prof. Dr. Denise Hilfiker-Kleiner did the excellent work with testing the bioactivity of 16-kDa hPRL. Dr. Motimer Korf-Klingebiel made the plasmids of mHSS1 and Fam163a and without his work with Dr. Marc Reboll in testing the activity of purified mHSS1 and Fam163a, I could not have accomplished this work.

Additionally, thanks go to Mr. Manfred Nimtz from Helmholtz-Center for Infection Research for his support in identification of Fam163a via mass spectrometry.

I would also to thank all the colleagues in our institute for the wonderful time. My special thanks to Dr. Magda Tomala for her kind help at the beginning of my work. Many thanks to Dr. Yanhong Li for the collaboration on the downstreaming processes of mHSS1. Also thanks to Dr. Ran Chen and Maria Zahid, who were always ready to help me solve various problems in the laboratory. Also I am appreciative of Dr. Johanna Walter, Satish Kumar Nemani, Ana Leticia de Souza Vanz and Wendy Musgnove, who spent a lot of time in reading and correcting the grammatical mistakes of my thesis.

I would also like to give my appreciation to Dr. Sascha Beutel for his support of my work. As well as thanks to Martin Pähler and Martina Weiß for their efforts in purchasing of chemicals and technical assistance.

Finally, I wish to thank my parents, my parents-in-law and my husband for their continued encouragement and support. Without them I could not have finished this work.

Abstract

Cytokines belong to a class of proteins which have essential functions throughout the body. They can influence tissue development, hematopoiesis and the immune defense. Sometimes, cytokines can cause programmed cell death and also certain diseases.

In the present work, the production and purification process using recombinant *E. coli* strains was developed for four cytokines: 16-kDa human prolactin (hPRL), human Activin A (hActivin A), murine hematopoietic signal peptide-containing secreted 1 (mHSS1), as well as murine protein family with sequence similarity 163, member A (Fam163a).

For the purification of 16-kDa hPRL, a combination of anion exchange membrane chromatography and size exclusion chromatography was applied. An affinity chromatography procedure was used in the polishing step to remove endotoxins. Finally, the apoptotic activity of purified 16-kDa hPRL was verified *in vitro* and *in vivo*.

Activin A is one of the most important hematopoietic cytokines. The human HSS1 and Fam163a have exhibited pro-angiogenetic activity. The current strategy for obtaining of the three cytokines is based exclusively on production in eukaryotic cells. Within this thesis, for the first time, the production of these three cytokines as thioredoxin (Trx) fusion proteins in *E. coli* was attempted. As an initial step in the production process, the cultivation conditions of the recombinant bacteria were optimized. hActivin A was entirely produced in form of inclusion bodies, whereas Fam163a was produced almost as completely soluble fusion protein. The fusion with Trx allowed production of soluble mHSS1 but only in small amounts compared with the insoluble part.

The inclusion bodies of Trx-hActivin A were used as the starting material for purification. After renaturation and purification of his-tagged fusion protein via immobilized metal ion affinity chromatography (IMAC) based on membrane adsorber technology, the fusion protein was subsequently cleaved with the tobacco etch virus (TEV)-protease. The released hActivin A did not maintain its solubility in the absence of the Trx fusion partner.

Due to degradation, the purity of IMAC purified Trx-Fam163a was poor. After cleavage of the fusion protein, the released Fam163a was successfully isolated via immunoprecipitation using anti-his antibody beads. The target protein was detected in the flow through and the recovery

Abstract

was limited using this method. However, the bioactivity of purified Fam163a was proven via scratch assay.

Instead of soluble Trx-mHSS1, the inclusion bodies were applied to the purification process. The fusion protein was purified under optimized denaturing conditions following refolding *in vitro*. Subsequently, Trx-mHSS1 was cleaved using TEV-protease, resulting in the release of soluble mHSS1 and Trx. The isolation of mHSS1 was achieved by another IMAC. Finally, the angiogenic effect of purified mHSS1 was confirmed using different activity assays.

Key words: recombinant cytokines; fusion protein; thioredoxin

Zusammenfassung

Zytokine gehören zu einer Klasse von Proteinen, die im ganzen Körper essentielle Funktionen haben. Sie können die Gewebeentwicklung, die Blutbildung und die Immunabwehr beeinflussen. Manchmal können Zytokine den programmierten Zelltod oder auch bestimmte Krankheiten verursachen.

Im Rahmen dieser Arbeit wurde der Produktions- und Aufreinigungsprozess für vier Zytokine unter Verwendung rekombinanter *E. coli* Stämme durchgeführt: 16-kDa humanes Prolaktin (hPRL), humanes Activin A (hActivin A), murines Hematopoietic Signal Peptide-containing Secreted 1 (mHSS1), sowie murines Protein Family With Sequence Similarity 163, Member A (Fam163a).

Für die Aufreinigung von 16-kDa hPRL wurde eine Kombination von Anionenaustauschermembran- und Größenausschlusschromatographie eingesetzt. Außerdem wurde eine Affinitätschromatographie als Polierschritt zum Entfernen von Endotoxinen verwendet. Abschließend wurde die apoptotische Aktivität des aufgereinigten 16-kDa hPRL *in vitro* und *in vivo* nachgewiesen.

Activin A ist eines der wichtigsten Zytokine im Bereich der Blutbildung. Die humanen HSS1 und Fam163a zeigten Aktivität bei der Angiogenese. Bisher basierte die Gewinnung der drei Zytokine ausschließlich auf der Produktion in eukaryotischen Zellen. In der vorliegenden Arbeit wurde erstmalig versucht, die drei Zytokine jeweils als Thioredoxin (Trx)-Fusionsprotein in *E. coli* zu produzieren. Als Teil des ersten Prozessschrittes wurden die Kultivierungsbedingungen der rekombinanten Bakterien optimiert. hActivin A wurde vollständig in Form von Einschlusskörpern produziert, während Fam163a nahezu komplett als lösliches Fusionsprotein gebildet wurde. Die Fusion mit Trx ermöglichte die Produktion von löslichem mHSS1. Allerdings war die Menge im Vergleich zum unlöslichen Teil sehr klein.

Die Einschlusskörper von Trx-hActivin A wurden als Ausgangsmaterial für die Aufreinigung verwendet. Nach der Renaturierung und Aufreinigung des His-getaggten Fusionsproteins mittels immobilisierter Metallaffinitätschromatographie (IMAC) basierend auf Membranadsorber Technik erfolgte die Spaltung des Proteins mit Tobacco Etch Virus (TEV)-Protease. Ohne Fusion mit Trx konnte hActivin A seine Löslichkeit nicht beibehalten.

Aufgrund von Abbauprozessen war die Reinheit des mittels IMAC-aufgereinigten

Zusammenfassung

Trx-Fam163a gering. Nach Spaltung des Fusionsproteins wurde das freigesetzte Fam163a mittels Immunopräzipitation unter Verwendung von Anti-His-Antikörper-Beads erfolgreich isoliert. Das Zielprotein wurde in Durchfluss detektiert wobei die Rückgewinnung mit dieser Methode limitiert war. Jedoch wurde die Bioaktivität des aufgereinigten Fam163a mittels Scratch Assay bestätigt.

Anstatt des löslichen Trx-mHSS1 wurden die entsprechenden Einschlusskörper für den Aufreinigungsprozess eingesetzt. Das Fusionsprotein wurde unter optimierten Denaturierungsbedingungen aufgereinigt und es folgte die Renaturierung *in vitro*. Anschließend wurde Trx-mHSS1 mittels TEV-Protease zur Freisetzung von Trx und löslichem mHSS1 gespalten. Die Isolierung von mHSS1 erfolgte mittels einer zweiten IMAC. Schließlich wurden die angiogenen Effekte durch verschiedene Aktivitätsassays bestätigt.

Schlagworte: rekombinante Zytokine; Fusionsprotein; Thioredoxin

Abbreviations

Activin β A	Activin A monomer (β A chain)
AEC	anion exchange chromatography
AP	alkaline phosphatase
APS	ammonium persulfate
AU	arbitrary units
BACE	bovine adrenal cortex endothelial cells
bFGF	basic fibroblast growth factor
BMP-2	bone morphogenetic protein-2
BrdU	bromodeoxyuridine
BSA	bovine serum albumin
°C	degree Celsius
CCL2	C-C motif chemokine ligand 2
CD	cathepsin-D
CFU-GEMM	colony forming units granulocyte erythroid macrophage megakaryocyte
CXCL1	C-X-C motif chemokine ligand 1
CXCR4	C-X-C motif chemokine receptor 4
Da	dalton
DCM	dry cell mass
DDT	dichlorodiphenyltrichloroethane
DNA	deoxyribonucleic acid
DNB	defined non-inducing broth
DsbA	protein disulfide isomerase 1
<i>E. coli</i>	<i>Escherichia coli</i>
EDTA	ethylenediaminetetraacetic acid
EGF	epidermal growth factor
FAM163A	human protein family with sequence similarity 163, member A
Fam163a	murine protein family with sequence similarity 163, member A
FCS	foetal calf serum
FPLC	fast protein liquid chromatography
Fr.	fraction
FS	fractional shortening
g	gram
g	gravity
GSH	reduced glutathione
GSSG	oxidized glutathione
GST	glutathione S-transferase
HACEC	human arterial coronary endothelial cells
HEK	human embryo kidney

Abbreviations

HPLC	high performance liquid chromatography
HRV3C	human rhinovirus
HSM1	hematopoietic signal peptide containing membrane domain-containing 1
HSS1	hematopoietic signal peptide-containing secreted 1
IDA	iminodiacetic acid
I κ B- α	inhibitor of nuclear factor- κ B
IL-6	interleukin-6
IMAC	immobilized metal ion affinity chromatography
IPTG	isopropyl- β -D-thiogalactopyranosid
k	kilo (10^3)
L	liter
LAL	limulus amebocyte lysate
LB	Luria Bertani
LC	Langerhans cells
LPS	lipopolysaccharides
LVEDD	left ventricular internal dimensions at end-diastole
LVESD	left ventricular internal dimensions at end-systole
μ	micro
m	mili
M	molar
(m/v)	weight per volume
MBP	maltose-binding protein
min	minute
MnSOD	manganese superoxide dismutase
MS	mass spectrometry
MS/MS	tandem mass spectrometry
n	nano
NDSP	neuroblastoma-derived secretory protein
NF κ B	nuclear factor- κ B
NRCM	neonatal rat cardiomyocytes
NusA	transcription termination anti-termination factor
OD	optical density
PAGE	polyacrylamide gel electrophoresis
PCR	polymerase chain reaction
pET	plasmid expression by T7-RNA-polymerase
PMSF	phenylmethanesulfonylfluoride
PPCM	peripartum cardiomyopathy
PRL	prolactin
PVDF	polyvinylidendifluorid
RNA	ribonucleic acid
ROS	reactive oxygen species

Abbreviations

rpm	revolutions per minute
SARS-CoV3CL (pro)	3C-like protease of severe acute respiratory syndrome coronavirus
S-DAB	simple-to-prepare defined autoinduction broth
SDS	sodium dodecyl sulfate
SEC	size exclusion chromatography
sec	second
sh FAM163A	small hairpin RNA against FAM163A
SPARC	secreted protein acidic and rich in cysteines
STAT3	signal transducer and activator of transcription 3
SUMO	small ubiquitin-related modifier protein
TB	Terrific broth
TBS	Tris buffered saline
TCA	trichloroacetic acid
TDCA/Na	taurodeoxycholic acid sodium salt
TEMED	N, N, N', N'-tetramethylethylenediamine
TEV	tobacco etch virus
TGF- α	transforming growth factor- α
TNF	tumor necrosis factor
Trx	thioredoxin
V	volt
(v/v)	volume per volume
VEGF	vascular endothelial growth factor
WB	Western Blot

Table of contents

1	INTRODUCTION AND AIM OF THE WORK.....	1
2	THEORETICAL BACKGROUND.....	3
2.1	Cytokines.....	3
2.1.1	16-kDa Prolactin	3
2.1.2	Activin A.....	6
2.1.3	Protein family with sequence similarity 163, member A.....	9
2.1.4	Hematopoietic signal peptide-containing secreted 1.....	11
2.2	Production of recombinant proteins in <i>E.coli</i>	13
2.2.1	Inclusion bodies.....	13
2.2.2	Refolding of inclusion bodies.....	14
2.2.3	Improving solubility of recombinant proteins.....	16
3	EXPERIMENTS.....	19
3.1	Production of 16-kDa human prolactin.....	19
3.1.1	Expression of 16-kDa hPRL.....	20
3.1.2	Purification of 16-kDa hPRL from inclusion bodies.....	20
3.1.2.1	Anion exchange chromatography	20
3.1.2.2	Size exclusion chromatography.....	22
3.1.3	Endotoxin assay and removal of endotoxin.....	24
3.1.4	Test of biological activity.....	24
3.1.4.1	<i>In vitro</i>	25
3.1.4.2	<i>In vivo</i>	26
3.1.5	Summary.....	27
3.2	Production of cytokines using thioredoxin as fusion partner.....	29
3.2.1	Construction of expression vector.....	30
3.2.2	Production of human Activin A.....	31
3.2.2.1	Expression of Trx-hActivin β A.....	31
3.2.2.2	Purification of Trx-hActivin β A from inclusion bodies.....	32
3.2.2.3	Cleavage of Trx-hActivin β A.....	34
3.2.2.4	Summary.....	35
3.2.3	Production of murine protein family with sequence similarity 163, member A.....	36
3.2.3.1	Expression of Trx-Fam163a.....	36
3.2.3.2	Purification of soluble Trx-Fam163a.....	38
3.2.3.2.1	Screening with Vivaspure MCM <i>ini</i>	38
3.2.3.2.2	Degradation of Trx-Fam163a.....	39

Table of contents

3.2.3.2.3	Upscaling of immobilized metal ion affinity chromatography.....	44
3.2.3.3	Cleavage of Trx-Fam163a.....	45
3.2.3.4	Purification of Fam163a.....	49
3.2.3.4.1	Immobilized metal ion affinity chromatography.....	49
3.2.3.4.2	Immuoprecipitation.....	50
3.2.3.5	Test of biological activity.....	53
3.2.3.6	Summary.....	55
3.2.4	Production of murine hematopoietic signal peptide-containing secreted	
1.....		58
3.2.4.1	Expression of Trx-mHSS1.....	58
3.2.4.1.1	IPTG-induction.....	58
3.2.4.1.2	Autoinduction.....	62
3.2.4.2	Purification of Trx-mHSS1.....	64
3.2.4.2.1	Purification of soluble Trx-mHSS1.....	64
3.2.4.2.2	Purification of Trx-mHSS1 from inclusion bodies.....	66
3.2.4.3	Cleavage of Trx-mHSS1.....	71
3.2.4.4	Purification of mHSS1.....	74
3.2.4.4.1	Screening with Vivawell 8-Strips.....	74
3.2.4.4.2	Upscaling of immobilized metal ion affinity chromatography.....	74
3.2.4.5	Size exclusion-HPLC.....	77
3.2.4.6	Test of biological activity.....	78
3.2.4.6.1	Proliferation.....	79
3.2.4.6.2	Tube formation.....	80
3.2.4.6.3	Mouse aortic ring assay.....	81
3.2.4.6.4	Scratch assay.....	82
3.2.4.7	Summary.....	84
4	SUMMARY AND OUTLOOK.....	86
5	APPENDIX.....	90
5.1	Materials.....	90
5.1.1	Chemicals.....	90
5.1.2	Consumable materials.....	91
5.1.3	Enzymes.....	92
5.1.4	Antibodies.....	92
5.1.5	Molecular weight markers.....	92
5.1.6	Columns and membrane adsorbers.....	93
5.2	Equipments.....	93

Table of contents

5.3	Bacterial strain.....	93
5.4	Expression vectors.....	94
5.5	Methods.....	96
5.5.1	Working with recombinant <i>E.coli</i> strains.....	96
5.5.1.1	Media compositions.....	96
5.5.1.2	Transformation.....	97
5.5.1.3	Cultivation of <i>E. coli</i> and expression of recombinant proteins.....	98
5.5.1.4	Cell lysis.....	98
5.5.1.5	Washing and solubilization of cell pellets.....	99
5.5.2	Electrophoresis and staining.....	100
5.5.2.1	Native-PAGE.....	100
5.5.2.2	SDS-PAGE.....	101
5.5.2.3	Staining.....	102
5.5.3	Western Blot.....	103
5.5.4	Determination of protein concentration.....	104
5.5.4.1	Bradford assay.....	104
5.5.4.2	Densitometric analysis.....	104
5.5.5	Purification with Vivaspure MCM <i>ini</i>	105
5.5.6	Purification with Vivawell 8- <i>Strips</i>	106
5.5.7	Purification using FPLC.....	107
5.5.7.1	Anion exchange chromatography.....	107
5.5.7.2	Size exclusion chromatography.....	108
5.5.7.3	Immobilized metal ion affinity chromatography.....	108
5.5.8	Endotoxin assay and removal of endotoxin.....	112
5.5.9	Dialysis.....	112
5.5.10	Cleavage of fusion proteins.....	112
5.5.11	Protease inhibitor.....	113
5.5.12	Immunoprecipitation.....	113
5.5.12.1	Anti-his tag beads.....	113
5.5.12.2	Protein G.....	113
5.5.13	TCA precipitation.....	115
5.5.14	Size exclusion-HPLC.....	115
6	REFERENCES.....	116

1 INTRODUCTION AND AIM OF THE WORK

Cytokines are a class of signaling proteins that are used extensively in cellular communication, immune function and embryogenesis (1, 2). They can be classified into families by structure as follows: the interferons, the chemokines, the members of the tumor necrosis factor (TNF) family, the haematopoietins, the epidermal growth factor (EGF) family and transforming growth factor- α (TGF- α) family and the cysteine knots (including TGF- β , vascular endothelial growth factor (VEGF) (3-5).

Cytokines have been applied not only into various research areas but also directly for therapeutic purposes. For instance, the cytokines which can inhibit growth of tumor cells have been used in cancer therapy (6). The restoration of the damaged tissues or organs depends on the application of cytokines which regulate the proliferation and differentiation of cells. Additionally, cytokines play a critical important role in treatments with stem cell transplantation (7). On the other hand, some cytokines demonstrate negative effects on tissues. They can lead to apoptosis of cells, which can be associated with diseases and tumors (8, 9). In some cases, the increase of cytokine expression serves as a useful biomarker for clinical prognosis (10).

Due to the varied and extensive applications, there is a great need for cytokines which have been well studied. The development of recombinant protein technologies has contributed to large-scale production of cytokines. Moreover, in recent years more and more new proteins have been discovered and characterized as cytokines and their properties and potential function will be investigated.

16-kDa prolactin (PRL), a proteolytic N-terminal fragment of intact PRL, is identified as cytokine, and its apoptotic effect associated with peripartum cardiomyopathy (PPCM) has received more and more attention from the research community (11, 12). There have been reports about production of the protein previously (13), but this protein was produced from *E. coli* and often contained endotoxins, which are cytotoxic to endothelial cells (14).

1 Introduction and aim of the work

Activin A is a well known cytokine of the TGF- β superfamily, which consists of two homodimeric β A subunits and plays an important role in haematopoiesis (15, 16). It induces hemoglobin synthesis (17) and potentiates the proliferation and differentiation of erythroid (18). Moreover, Activin A takes part in mesoderm induction (19), neural cell differentiation (20), bone remodeling (21). The production of Activin A has been already described in literature and biologically active Activin A was obtained exclusively from eukaryotic cells (22). However, no paper about successful production of Activin A in *E. coli* has been published.

Hematopoietic signal peptide-containing secreted 1(HSS1) and protein family with sequence similarity 163, member A (FAM163A), are two novel cytokines which have no structural homology to any known proteins. HSS1 is reported to regulate tumor growth (23) and FAM163A can promote neuroblastoma cell proliferation (24). Recently, both cytokines expressed by human embryo kidney (HEK) cells have been found to exhibit pro-angiogenic activities. So they are expected to be employed into reperfusion of the cardiac coronary artery. So far, there has been no report about production of both cytokines in *E. coli*.

The aim of this work is the development, optimization and performance of the production and purification processes of four cytokines in *E. coli*. The work comprises of two parts. In the first part, the production of 16-kDa human prolactin (hPRL) is to be optimized and the endotoxin in protein solution is to be removed. Finally, biological activity of purified 16-kDa hPRL is to be tested.

The second part comprises of production of human Activin A (hActivin A), murine HSS1 (mHSS1) and murine FAM163A (Fam163a). These target proteins are fused with the solubility tag thioredoxin (Trx) and expected to be expressed as soluble fusion proteins. After the separation of fusion partners the bioactivities of target cytokines are to be tested. Particular care should be taken to identify and prevent the difficulties in the entire process, including cultivation, cleavage of fusion protein and subsequent purification.

2 THEORETICAL BACKGROUND

2.1 Cytokines

Cytokines are proteins, peptides, or glycoproteins that are secreted by specific cells of diverse embryological origin and produced widely throughout the body. They are a category of signaling molecules used extensively in cellular communication and they affect their target cells by binding to specific receptors, triggering the receptors to deliver signals to the cell in which it is expressed. Cytokines are divided into groups depending firstly on their biologic activity: interferons, interleukins and growth factors (3). 16-kDa PRL, Activin A and HSS1, also FAM163A are members of the last family which plays important roles in the regulation of anti-angiogenesis, angiogenesis and haematopoiesis.

2.1.1 16-kDa Prolactin

Prolactin was originally identified as a lactotrophic hormone secreted by the pituitary gland (25, 26). There are several forms of PRL after post-translational modification such as glycosylation (27), phosphorylation (28) and proteolysis (29). 16-kDa PRL was first discovered more than 20 years ago as a proteolytic fragment from intact 23-kDa rat PRL by acidified mammary extracts (30).

Structure

16-kDa PRL consisting of 146 amino acids is produced by the removal of about a quarter of 23-kDa PRL molecule with 199 amino acids from the C-terminus as shown in Fig. 2.1. The protease responsible for the cleavage was identified as cathepsin D (CD) (12, 29, 31). There are only 3 cysteines left in the sequence and the single disulfide bond involves Cys-4 and Cys-11 at the N-terminus is primarily responsible for the tertiary structure of the protein.

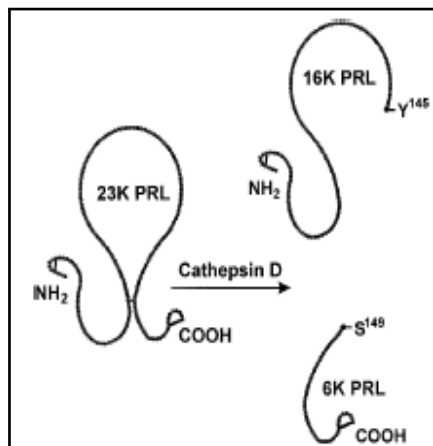


Fig. 2.1 Proteolytical cleavage of 23-kDa PRL into a N-terminal 16 kDa fragment and a C-terminal 7 kDa fragment (31).

16-kDa PRL and anti-angiogenesis

Angiogenesis is an important process of proliferation and differentiation and is identified as the formation of new capillaries from preexisting blood vessels (32). 16-kDa PRL found in the hypothalamus of rats and mice and in the pituitary glands and circulation of humans inhibits angiogenesis, including capillary endothelial cell migration and organization into microvessels (33).

Ferara *et al.* first reported the anti-angiogenic activity of rat 16-kDa PRL. It was shown to inhibit the growth of cultured bovine adrenal cortex endothelial cells (BACE) stimulated by basic fibroblast growth factor (bFGF) in a dose-dependent manner, the best characterized cytokine simulating angiogenesis. In contrast, the intact rat 23-kDa PRL had no effect on these cells (34). The recombinant human 16-kDa PRL inhibited the basal growth of bovine and human vascular endothelial cells *in vitro* even at very low concentrations (35, 36). *In vivo*, normal development of capillaries in chicken embryo chorioallantoic membrane was also inhibited by the recombinant human 16-kDa PRL (37).

In addition, 16-kDa PRL could stimulate cell apoptosis (38-40) and the programmed death of BACE cells could be induced by 16-kDa PRL, because it could activate the nuclear factor- κ B

2 Theoretical background

(NF- κ B) by causing degradation of its inhibitor (IkB- α) (40). It inhibits serum-induced DNA synthesis in adult bovine aortic endothelial cells and this inhibition is associated with cell cycle arrest at both the G₀–G₁ and the G₂–M phases (41).

16-kDa PRL and peripartum cardiomyopathy

PPCM is characterized by an acute onset of heart failure in women in the late stages of pregnancy up to several months postpartum (42, 43). It involves systolic dysfunction of the heart and a decrease of the left ventricular ejection fraction with associated congestive heart failure (44) and an increased risk of atrial and ventricular arrhythmias, thromboembolic events (45), and even sudden cardiac death (46).

It has been reported that, 16-kDa PRL caused PPCM (12) as shown in Fig. 2.2. PPCM is resultant in transgenic mice defective in the signal transducer and activator of transcription 3 (STAT3). STAT3 is involved in protection from oxidative stress by upregulation of antioxidative enzymes such as reactive oxygen species (ROS) and scavenging enzyme manganese superoxide dismutase (MnSOD) (47, 48). Consecutive lack of anti-oxidative enzymes, protective factors in the post-natal heart, induces increased oxidative stress which in turn enhances CD activity. This leads to proteolytic cleavage of 23-kDa PRL into its detrimental 16 kDa form which induces endothelial cell apoptosis, capillary dissociation, and vasoconstriction (49).

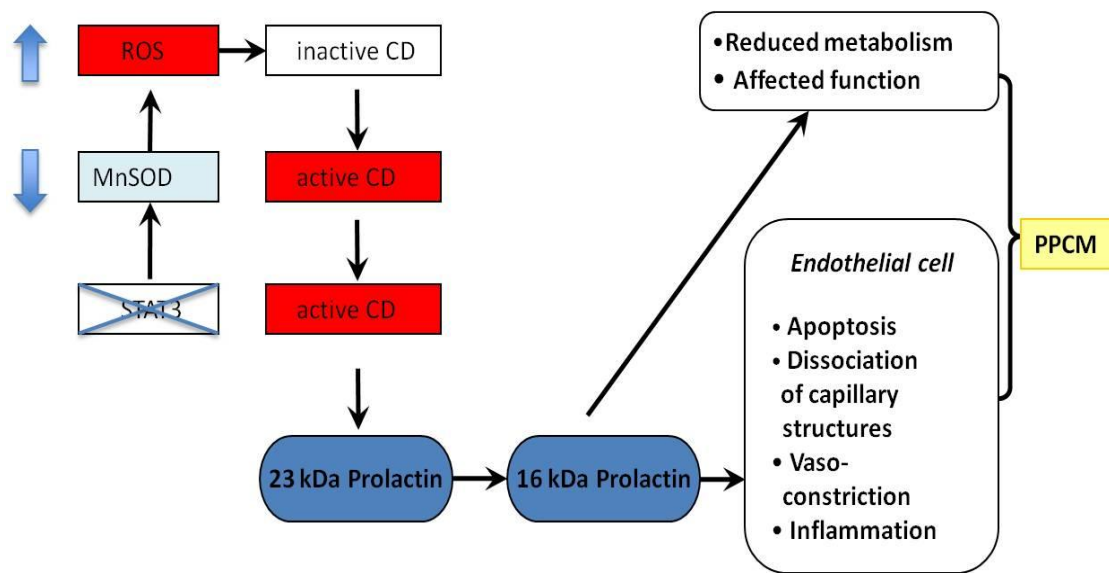


Fig. 2.2 Schematic model for the development of PPCM (12).

2.1.2 Activin A

Activin A is a protein initially discovered in follicular fluid with the capability to suppress follicle stimulating hormone (50). It was then identified as a member of the TGF- β superfamily of cytokines and that the receptors for Activin A signaling were members belonging to TGF- β receptor superfamily (51). This protein is also called erythroid differentiation protein because it can regulate the growth of erythroids (18, 52).

Structure

Human Activin A (hActivin A) is a homodimer protein consisting of 2 β A-polypeptide chains comprised of 116 amino acids as shown in Fig. 2.3.A (53, 54). Each polypeptide contains 9 Cys-residues. Between Cys-314 and Cys-322, Cys-321 and Cys-391, Cys-350 and Cys-423, Cys-354 and Cys-425 there are 4 intramolecular disulfide bonds (55), which are important to the bioactive conformation of Activin A. Cys-390 can form an interchain to another polypeptide with an intermolecular disulfide bond (53, 56). The mature human β A chain (hActivin β A) shares 100% amino acid sequence identity with bovine, feline, mouse, porcine and rat β A (16).

2 Theoretical background

The structure of Activin A dimer is shown in Fig. 2.3.B. Each β_A -monomer comprises of two pairs of anti-parallel β -sheets, forming first a short and a long finger. These slightly curved finger-like projections stretch out from the cysteine-knot core of the molecule creating concave and convex surfaces for receptor and monomer interactions. The α -helix (wrist region) of the monomers sits in the contralateral concave surfaces created by the finger-like projections of the β -sheets (57).

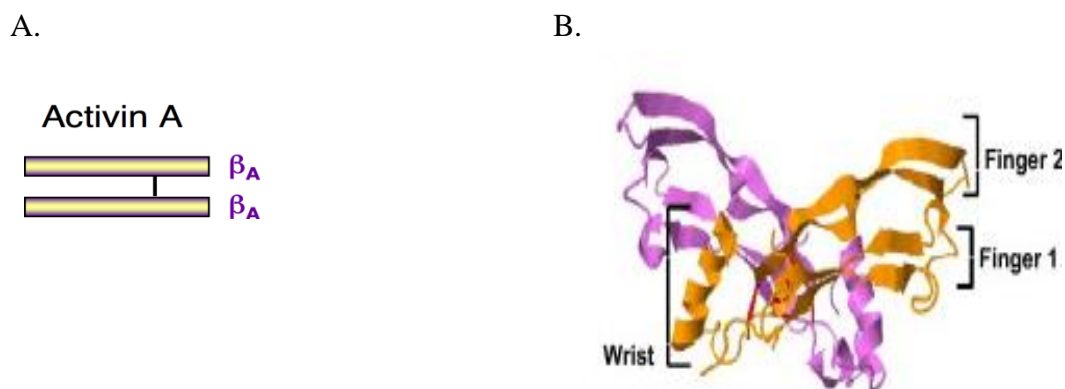


Fig. 2.3 A. Schematic diagram of the 1-D structures of Activin A (53). The black line between the monomers represents a disulfide bond. B. Structure of Activin A dimer (57). The characteristic finger (anti-parallel β -sheets) and wrist (α -helical) regions of the molecule are noted. The disulphide bonds are marked in red.

Activin A and haematopoiesis

Haematopoiesis is the process of forming blood cells, which occurs during embryogenesis and throughout life (58). Defects in haematopoiesis can result in some of the most common and serious human diseases, including anaemia (59) and leukaemia (60). All blood cells are derived from a common progenitor, the haematopoietic stem cell (61). The production of hematopoietic cells is under the tight control of a group of hematopoietic cytokines. Like other members in TGF- β superfamily, Activin A shows functional similarity and is well known to play important roles in regulation of hematopoiesis.

Activin A functions as a morphogen during embryonal development, inducing the formation of different structures including the hemopoietic system (62). Activin A expression is induced

2 Theoretical background

during hemopoietic differentiation (63) and different cell types within the hemopoietic system are under the influence of Activin A, for example, megakaryocytes, B-cells, T-cells and erythrocytes.

Broxmeyer *et al.* were first to show that Activin A enhanced the formation of colony forming units granulocyte erythroid macrophage megakaryocytes (CFU-GEMM), whereas it did not affect CFU granulocyte macrophage numbers (64, 65). Through experiments performed on tumor cells, including human myeloma cells and mouse hybridoma and plasmacytoma cell lines, Activin A was observed to cause apoptotic death in cells of the B lineage and that the mechanism was identified as cell cycle arrest induced by Activin A (66). In T-cells, Activin A cooperated with interleukin-6 (IL-6) which is a stimulator of T-cell proliferation. When both Activin A and IL-6 are added to thymocyte cultures, proliferation is enhanced (67). Moreover, previous studies have suggested Activin A enhances erythropoiesis. It induced the differentiation of erythroleukemia cells at low concentrations (1-10 ng/mL) (68), increased hemoglobin synthesis (17, 69) and transcription of globin genes (70).

Further bioactivities and distribution

Activin A is also involved in skin morphogenesis and wound healing, inducing the differentiation of human monocytes into Langerhans cells (LC), which represent a well characterized subset of dendritic cells located in the epidermis of skin and mucosae (71). Moreover, the functions of Activin A in embryonic stem cells are also well-known. It induces mesoderm and endoderm in mouse embryoid bodies (72). Furthermore, Activin A has been used to induce human embryonic stem cells to differentiate into definitive endoderm in culture (73).

Activin A is widely expressed in cells including fibroblasts, endothelial cells, hepatocytes, macrophages, bone marrow monocytes etc (74). The bioactivities of the factor are observed in adult tissues, such as reproductive organs, brain, heart and liver (74).

Production of Activin A

Due to various functional roles and potential therapeutic applications, significant amounts of purified recombinant Activin A are needed. Activin A was initially isolated based on small-scale high-performance liquid chromatography (HPLC) from porcine ovarian follicular fluid and ovine amniotic fluid (75). Subsequently, recombinant human Activin A has been produced in several mammalian cell line expression systems. In addition, uncleaved high molecular weight precursor forms of Activin A are produced in mammalian cells (76). The recombinant human Activin A is also reported to be produced in baculovirus-insect cells (77) as well as bovine Activin A (78). However, in this study it was observed that insect cells producing Activin A have a more rapid rate of lysis than other cells, suggesting a possible consequence of the role of Activin A in apoptosis (77). Production of human Activin A using engineered *Pichia pastoris* has become very popular in the recent years. This microbial system can be easily modified using genetic engineering and the Activin A produced is folded correctly and bio-functional. Furthermore, higher yields of immunoreactive protein were detected compared to the other three approaches mentioned above (22).

Production of recombinant Activin A in *E. coli* has been attempted and the expression of the Activin A monomer in the bacterial system without any strategy resulted in significant formation of aggregates (79). Obtaining of bioactive Activin A has also been achieved by refolding solubilized Activin β A which was only described in a patent (80)

2.1.3 Protein family with sequence similarity 163, member A

FAM163A belongs to proteins of the FAM163 family and was first discovered as neuroblastoma-derived secretory protein (NDSP) (24), which is secreted by cells of neuroblastoma, the most common extracranial solid tumor in children (81, 82). The gene of FAM163A was found on human chromosome 1 at open reading frame 76 (24), so it has the alternative name C1orf76.

Structure

Human FAM163A consists of 167 amino acids. The sequence of this protein in mouse is well conserved in human. The homologue containing 168 amino acids was also identified, which shares over 80% protein homology with human FAM163A and the first 37 amino acids in both protein sequences are identical (24).

Sequence analysis of the protein revealed that the first 30 amino acids are consistent with a signal peptide with a putative cleavage site between leucine 30 and glutamine 31(24). Downstream from the signal peptide, there is a C-C motif at position Cys-34 and Cys-35 and 6 additional cysteine groups suggesting that FAM163A may be a part of the C-C family of chemokines (83). These 8 cysteines have the potential to form 4 intramolecular disulfide bonds.

FAM163A in angiogenesis

Angiogenesis is necessary for many physiological processes, including embryonic vascular development and differentiation, wound healing and organ regeneration (84). The stimulation of angiogenesis is performed by various cytokines and FAM163A was found to promote angiogenesis.

To identify factors secreted from C-X-C motif chemokine receptor 4 (CXCR4) positive cells of bone marrow from patients with cell therapy after acute myocardial infarction, ProteinChip arrays were performed by the team of Prof. Dr. Kai Wollert (Department of Cardiology and Angiology, Hanover Medical School). Subsequently, out of 280 secreted proteins represented on the ProteinChip arrays 230 genes of proteins were amplified with specific primer and transfected in HEK cells. By analysis of pro-angiogenic activity, FAM163A was identified as one of 10 overexpressed proteins in the conditioned supernatants, which stimulated and induced the proliferation of human arterial coronary endothelial cells (HACEC) and the sprouting of capillaries.

Further bioactivities and distribution

The protein can promote neuroblastoma cell proliferation. To inhibit FAM163A expression in the neuroblastoma cells, a small hairpin RNA against FAM163A (sh FAM163A) was produced in these cell lines. And FAM163A inhibition by shFAM163A was able to cause phenotypic changes of cells (24).

The mRNA expression of FAM 163A was tested in 18 normal adult tissues and the transcript levels of this protein were found to be very low in normal tissues such as the adrenal gland, cerebrum, colon, ileum and ovary (24). Additionally, It was reported that, FAM163A was expressed in tumor cells and that compared to other cell types the expression of FAM163A were 2-to 4-fold higher in supernatant of neuroblastoma (24). So the increasing FAM163A expression levels in neuroblastoma tumor stages 1- 4 were detected and this suggested that this protein may serve as a useful biomarker for neuroblastoma (24).

2.1.4 Hematopoietic signal peptide-containing secreted 1

The growth factor HSS1 was first discovered during a search for novel proteins expressed in murine hematopoietic stem cells (85). This protein exhibits structural properties or motifs characteristic of a cytokine but has no structural homology to any known protein or protein class in the current protein database. Human HSS1 (hHSS1) has an alternative name INM02 (86) and it is also called C19orf63 because this protein resides on chromosome 19 at open reading frame 63 (23).

Structure

The amino acid sequence for hHSS1 comprises of 254 amino acids (23, 86). It was reported that the amino acid sequences of mHSS1 and hHSS1 share 86% identity with each other (23). The signal peptide is represented by approximately the first 27 amino acids, which is cleaved into the mature proteins and indicates the secretability of HSS1. There are 4 cysteines in this protein.

2 Theoretical background

Moreover, HSS1 is glycosylated, as the predicted sequence presents two possible glycosylation sites at residues 182 and 198 (23).

hHSS1 has a splice variant hematopoietic signal peptide containing membrane domain-containing 1 (hHSM1), which contains a membrane spanning domain and comprises of 262 amino acids (23). Most notable is a polyglycine stretch at the carboxyl terminal end of hHSM1, which is predicted to be located at the intracellular membrane and may play a role in intracellular signaling. This isoform was also amplified by polymerase chain reaction (PCR) from cDNA libraries, confirmed for both human and mouse (23).

Bioactivities and distribution

Like FAM163A, hHSS1 is also one of 10 proteins which could promote pro-angiogenesis in tested cells (described in 2.1.3, FAM163A in angiogenesis). Moreover, the protein has been reported to suppress neuroblastomas (23, 87). The effect of hHSS1 on the well studied glioma-derived cell lines A172 and U87 cells was investigated. It was reported that the growth of pcDNA3.1-hHSS1 transfected A172 cells was dramatically decreased relative to mock-transfected clones. In addition to a reduction in proliferation, expression of the hHSS1 gene in U87 cells induced morphological changes and the detection of cell aggregate formation in U87 cells that probably reflected the loss of contact inhibition in these cells (23). Thus, these observations suggested that hHSS1 has a function in the modulation of tumor growth and suppression. Additionally, hHSS1 is expressed in normal brain tissues (88) but cannot be detected in glioblastoma cell lines, suggesting that it could function as a diagnostic marker for the above-mentioned cancers (23). More specifically, the deletion of the region of human chromosome 19 that encompasses the genes encoding HSS1 is associated with the presence of ovarian cancer (89, 90).

The mRNA corresponding to the hHSS1 was found to be ubiquitously expressed (87). Specifically, the mRNA corresponding to the polypeptides of the invention were found to be expressed in bone marrow, colon with mucosal lining, fetal liver, leukocyte, lymph node, ovary, prostate, small intestine, spleen, testis, thymus and tonsil (86, 87).

2.2 Production of recombinant proteins in *E. coli*

2.2.1 Inclusion bodies

The overexpressed proteins often result in the formation of aggregates. These have been reported in different host systems, not only in *E. coli*, but also in bacillus, yeast, insect cells etc (91). The proteins overexpressed in *E. coli* accumulate as inclusion bodies and in many cases the inclusion bodies constitute 20% to 50% of the total cellular protein of the cell (92). In addition to the heterologous protein, very low amounts of host proteins, ribosomal components and DNA/RNA fragments are also found in inclusion bodies (93).

The exact reason for protein aggregation into inclusion body formation in *E. coli* is not clear yet. The high local concentration of protein synthesis in the cytoplasm of *E. coli* cells, and the lack of mammalian post-translational modifying enzymes and foldases during high-level expression of protein could be the main reasons for intracellular aggregation (94). In cases of proteins containing more cysteines, the reducing environment of bacterial cytosol prevents formation of disulfide bonds necessary for proper folding (95). There has been no direct correlation between formation of inclusion bodies and properties of proteins, such as molecular weight, hydrophobicity, folding pathways and so on (96). A great variety of experimental approaches indicates that the formation of inclusion bodies results from partially folded intermediates in the intracellular folding pathways of the protein and not from the completely unfolded or native protein (95, 97, 98). Although protein expression in the form of inclusion bodies is undesirable, it is convenient and effective to isolate the protein of interest from inclusion bodies. Subsequently, it is necessary to convert the inactive misfolded proteins from inclusion bodies into the soluble active form by renaturation. In some cases, this way can result in high recoveries.

2.2.2 Refolding of inclusion bodies

Refolding is a process, where the protein with incorrect conformation folds into its characteristic and functional structure. Proteins from inclusion bodies are commonly solubilized by high concentrations of chaotropic agents such as guanidinium hydrochloride or urea. Then the solubilized protein solution must be transferred into conditions that allow the formation of the native state. Refolding of protein can either be carried out before or after purification and the techniques of protein renaturation includes dilution, dialysis, chromatographic methods etc. Disulfide bonded proteins need special requirements.

Dilution

For small-scale refolding of protein, dilution is the simplest method and it helps to reduce protein aggregates. Most frequently, protein refolding by dilution is performed with the final protein concentration 10-50 $\mu\text{g mL}^{-1}$ (99). However, scale-up of protein refolding is limited by this method and a lot of refolding buffer and additional cost-intensive concentration steps are required. Pulse renaturation, where a small amount of solubilized protein is added in pulses or continuously into the refolding buffer, helps to improve the yields of refolded recombinant protein. It has been reported that this process was successfully applied to the recovery of γ -interferon (100) and lysozyme (101).

Dialysis

The most commonly used method for removal of the solubilizing agent is dialysis. During dialysis the denaturant concentration decreases with time to the concentration in the refolding solvent. As the concentration of denaturant is decreased, the rate of folding into the intermediate and native structures increases. Refolding via dialysis is preferred performed in a stepwise manner. This method has been successfully used for refolding antibodies (102). The unfolded protein sample is first brought to equilibrium using a high concentration of denaturant,

2 Theoretical background

then with an intermediate concentration and then with low concentration. The difference from the one-step dialysis is the establishment of equilibrium at each denaturant concentration.

Protein refolding based on chromatography

Besides dilution and dialysis, refolding can be also performed by chromatography. Refolding via chromatographic processes is attractive because it can be easily automated and can often be combined with simultaneous partial purification. In some cases, they are much more efficient than traditional refolding strategies (103). Generally, after the denatured proteins of interest bind to the matrix, refolding using a decreasing denaturant gradient and optimization of elution leads to purification of protein in bioactive form. For example, refolding of lysozyme and interleukin-2 have been successfully achieved by use of size exclusion chromatography (101) and ion exchange chromatography (104), respectively. Using nickel-chelating chromatography the renaturation and purification of secreted protein acidic and rich in cysteines (SPARC) has also been reported (105).

Disulfide bonded proteins

In the presence of reducing agents such as dichlorodiphenyltrichloroethane (DDT) and β -mercaptonethanol, the non-native disulfide bonds of disulfide-containing proteins are disrupted. For efficient formation of disulfide bonded proteins an oxidizing agent is necessary. Oxidization can be achieved by adding a mixture of oxidized and reduced thiol reagents, such as reduced/ oxidized glutathione (GSH/GSSG), cysteine/cystine, cysteamine/cystamine (106). For example, GSH/GSSG at a total concentration of 5-15 mM with a ratio of 2:1 and 5:1 is very popular for protein renaturation and these conditions allow rapid disulfide exchange reactions until the protein reaches its native stable form (107-109).

2.2.3 Improving solubility of recombinant proteins

Temperature and medium

The production of soluble proteins is under the influence of cellular metabolism of the host, which can be controlled by a number of environmental factors. At first, temperature plays an important role for the correct folding of expressed proteins. When *E. coli* cells are cultivated at high temperatures, the cells grow too fast and overexpressed recombinant proteins lacking the required accessories cannot fold into their native forms. It is well known that, the aggregation of recombinant proteins is limited at reduced temperatures. Additionally, medium composition is critical for protein production. For example, Terrific broth (TB) medium could not only result in higher cell density but also improve the solubility of trypsin-streptavidin compared with the regular Luria Bertani (LB) medium (110).

Fusion proteins

In response to the rapidly growing field of proteomics, the application of recombinant proteins has greatly increased in recent years. Fusion of target proteins with many different proteins has been widely used for the purification of recombinant proteins. Proteins fused with glutathione S-transferase (GST) (111) or maltose-binding protein (MBP) (112) were discovered early. The solubility of different eukaryotic polypeptides could be improved with the help of these fusion partners (111-113) and the proteins purified by one-step affinity chromatography and eluted with 10 mM GSH or maltose respectively.

Also hydrophilic tags, such as transcription termination anti-termination factor (NusA) or protein disulfide isomerase 1(DsbA) have been well described. Usually, *E. coli* NusA protein promotes hairpin folding and termination, while DsbA increases the solubility of the target protein in the cytoplasm and periplasm of *E. coli* (114, 115). Recently, a fusion system with small ubiquitin-related modifier protein (SUMO) containing an external hydrophilic surface that facilitates efficient expression of recombinant proteins in *E. coli* has been described (116). Several proteins, including the 3C-like protease of severe acute respiratory syndrome

2 Theoretical background

coronavirus (SARS-CoV3CL (pro)), nucleocapsid, and membrane proteins, have been recombinantly expressed using the SUMO fusion system (117). However, proteins with these tags cannot be purified with a specific affinity matrix and the fusion construct must be used in combination with a small affinity tag for purification.

Thioredoxin fusion protein

Fusion with Trx which is also a hydrophilic tag, is a very popular strategy in protein expression. The Trx of *E. coli* remains soluble even when overexpressed and has accumulated 40% of the total cellular proteins (118). In contrast to other fusion partners like GST (26kDa) and MBP (40kDa) Trx is small (12 kDa in native form) which represents a relatively modest portion of any fusion protein. Trx has inherent thermal stability and its tertiary structure reveals that both the N- and C- terminus of Trx are accessible on the molecule's surface, in good positions for potential fusions to other proteins (119, 120).

A wide variety of secreted mammalian cytokines and growth factors have been successfully produced in soluble form in *E. coli* cytoplasm as C-terminal fusions to Trx, especially the cytokines rich in cysteins (120). The mechanism is shown in Fig. 2.4. The Trx at the N-terminus is translated first. The reduced Trx binds to a target protein via the hydrophobic interaction surface, followed by nucleophilic attack of the N-terminal active site thiolate on the target disulfide in a thiol-disulfide exchange reaction, resulting in a transient protein-protein mixed disulfide. Intramolecular attack by the second thiol group of Trx results in oxidized Trx and the reduced target protein (121). Moreover, it has been found that Trx fusion proteins are not only soluble, but also exhibit high levels of bioactivity, such as fusion with bone morphogenetic protein-2 (BMP-2) (122).

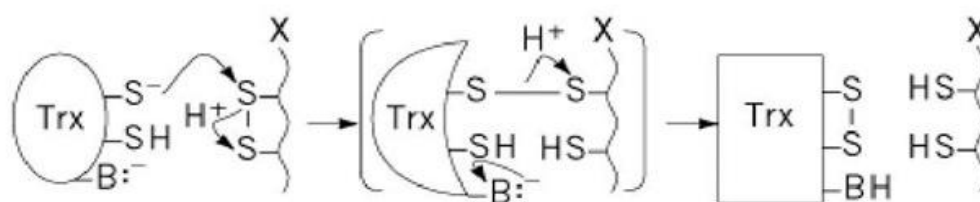


Fig. 2.4 Mechanism of reduction of the disulfide bond of a protein substrate (X) by Trx (121).

Cleavage of fusion protein

Generally, the fusion partner should be cleaved from the target protein. The removal of the tag from a protein of interest can be accomplished with a site-specific protease and the cleavage should not reduce the bioactivity. The most commonly used proteases are enterokinase (123), tobacco etch virus (TEV)-protease (124), thrombin (125) and human rhinovirus (HRV3C) (126)

TEV-protease is the common name of the 27 kDa catalytic domain of the nuclear inclusion protein encoded by the tobacco etch virus. The seven-amino-acid sequence E-N-L-Y-Q-G-S in the fusion protein would be recognized by TEV-protease and the two fragments can be separated from each other (124). The efficiency of cleavage is dependent on both the fusion partner and the protein of interest. It is reported that TEV-protease demonstrates a relatively flat activity at pH values between 4 and 9 and temperatures between 4°C and 34°C (127).

3. EXPERIMENTS

3.1 Production of 16-kDa human Prolactin

16-kDa hPRL is a monomer, a non-glycosylated polypeptide with 140 amino acids and an N-terminal proteolytic fragment of full-length 23-kDa hPRL. The recombinant *E. coli* BL21 (DE3) pT7L-16-kDa hPRL was used for production and the vector contained a synthetic 16-kDa hPRL cDNA-sequence with an inducible T7 promoter (40).

3.1.1 Expression of 16-kDa hPRL

The main culture with TB medium was inoculated with pre-culture and then incubated at 37 °C. When OD₆₀₀ reached 1.5, protein expression was induced by adding 0.5 mM isopropyl-β-D-thiogalactopyranosid (IPTG). After expression at 37 °C for 4 h, the bacterial cells were harvested by centrifugation and the pellets were suspended in lysis buffer and then ruptured by sonication. The soluble part was separated from the insoluble part by high-speed centrifugation. For detection of 16-kDa hPRL expression, the soluble and insoluble fractions of cell lysate were analyzed by sodium dodecyl sulfate-polyacrylamide gel electrophoresis (SDS-PAGE) with blue silver staining. The protein fractions before induction were used as reference as shown in Fig. 3.1.

The result of SDS-PAGE analysis shows, 4 h after induction the recombinant protein was expressed in TB medium, which quickly resulted in high cell density. The protein detected at 16 kDa was found accumulated in inclusion bodies which were found to be 76% of the total insoluble proteins by densitometric analysis via Software Gel-Pro Analyzer 6.0 (see Appendix 5.5.4.2).

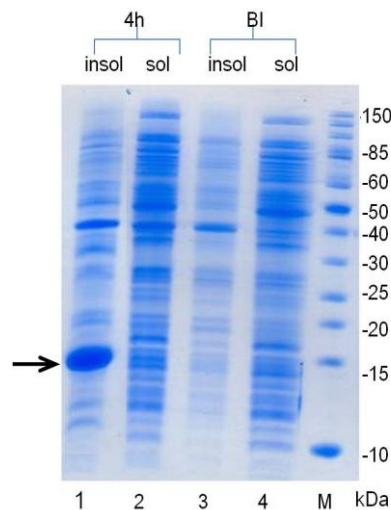


Fig. 3.1 Expression of 16-kDa hPRL in TB medium at 37 °C after 4 h induction presented using 12% SDS-PAGE with blue silver staining. The cell lysate before induction (lanes 3 and 4) and 4 h after induction (lanes 1 and 2) are shown. The black arrow indicates 16-kDa hPRL. BI: before induction; insol: insoluble fraction; sol: soluble fraction; M, protein molecular marker (Fermentas SM0661).

Moreover, the medium composition played an important role of 16-kDa hPRL expression. For example, in LB medium there was neither soluble nor insoluble 16-kDa hPRL production identified at all tested temperatures (18 °C, 26 °C and 37 °C) during 12 h of culture. The obtained pellets of inclusion bodies were washed twice in wash buffer and then solubilized for the following purification of 16-kDa hPRL by 2-step chromatography.

3.1.2 Purification of 16-kDa hPRL from inclusion bodies

3.1.2.1 Anion exchange chromatography

For the first purification, an anion exchange chromatography (AEC) using a membrane absorber filled with strong anion exchangers was employed. 16-kDa hPRL has an isoelectric point of 5.9 acting as an acidic protein and is strongly negatively charged at the basic pH. The solubilized protein sample was loaded onto the membrane absorber connected to a fast performance liquid chromatography (FPLC) system. The membrane was equilibrated with binding buffer prior to use. The proteins which did not bind to the membrane were washed away with the same buffer. Subsequently, a gradient elution with NaCl was performed (0-1 M)

3 Experiments

as shown in Fig. 3.2. The FPLC protocol is found in Appendix 5.5.7.1.

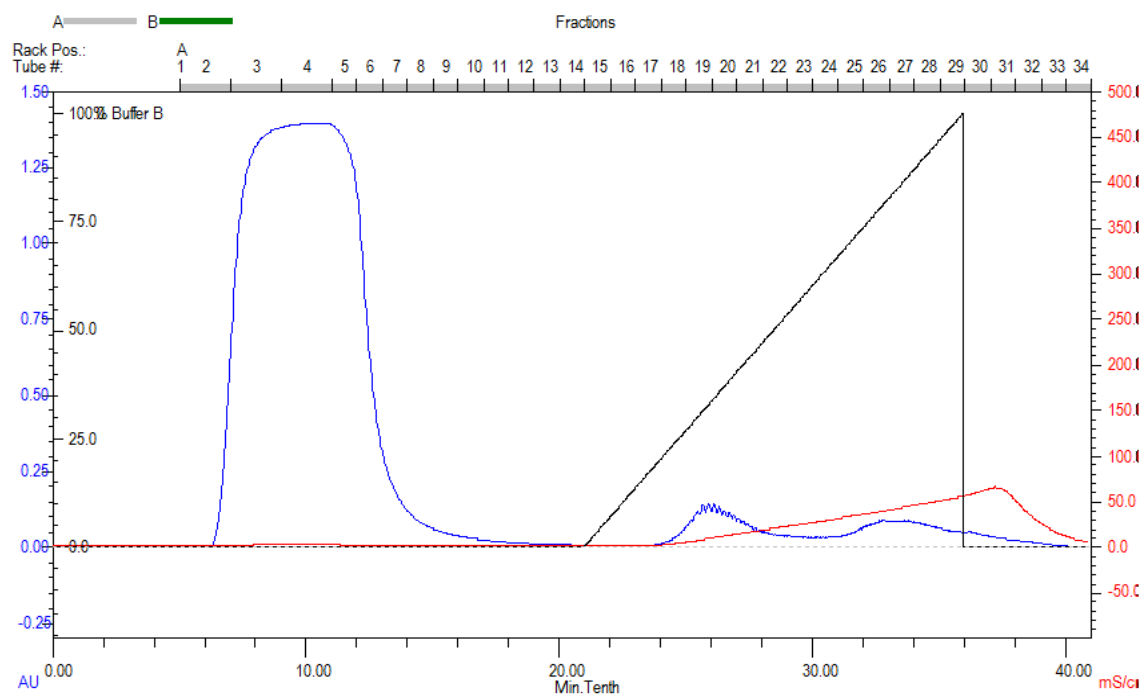


Fig. 3.2 Chromatogram of AEC-purification of 16-kDa hPRL from solubilized inclusion bodies. The UV-absorption (AU) and conductivity (mS/cm^2) dependent on time are shown.

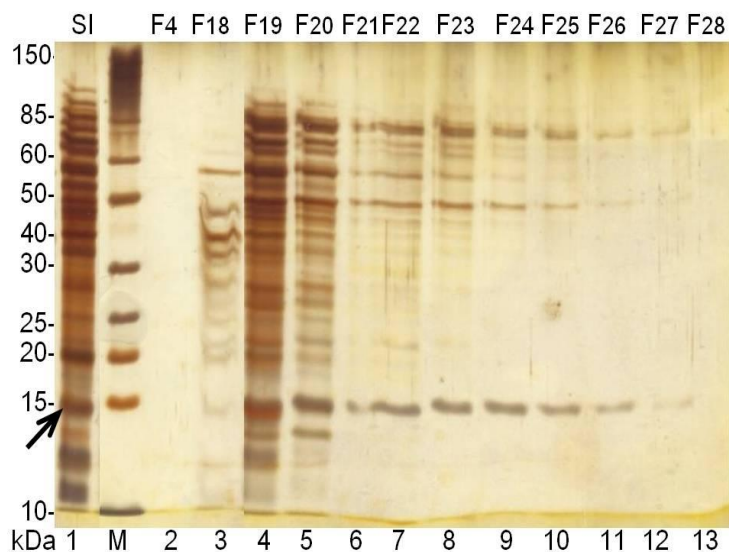


Fig.3.3 AEC-purification of 16-kDa hPRL from solubilized inclusion bodies presented using 12% SDS-PAGE with silver staining. The black arrow indicates 16-kDa hPRL. SI: solubilized inclusion bodies; F, fraction; M, protein marker (Fermentas SM0661).

3 Experiments

The solubilized inclusion bodies before purification and the elution fractions were analyzed by SDS-PAGE using silver staining as shown in Fig. 3.3. No detection of 16-kDa hPRL in the flow through indicated a good binding between this protein and its ligand. 16-kDa hPRL was eluted in a wide range of NaCl concentration. The high concentration protein was eluted from 0.2 M to 0.4 M NaCl but these fractions also contained many impurities from host cells (Fr. 18-20). The fractions from the second peak eluted with 0.4-0.8 M NaCl were pooled for the following refolding step.

The pooled protein solution was introduced into a dialysis membrane and the refolding was performed by a two-step dialysis over 72 h. For the first 6 h, the proteins were dialyzed against 10 volumes binding buffer to reduce the concentration of NaCl. Then, the urea in the protein solution was removed by dialysis against 500 volumes dialysis buffer with 20 mM ethanolamine, pH 9.0. It was necessary to refresh the buffer at least 4 times. After the proteins were slowly refolded into their bioactive form, the buffer was changed to 50 mM NH_4HCO_3 , 100 mM NaCl, pH 7.5. Finally, the protein solution was concentrated via ultra filtration before the second purification.

3.1.2.2 Size exclusion chromatography

The second purification was carried out on size exclusion chromatography (SEC) and the 16-kDa hPRL was expected to be separated from other impurities by passing through the column at different time points according to their molecular masses. The concentrated protein solution was loaded onto the column which was previously equilibrated with buffer. The protocol is seen in Appendix 5.5.7.2 and in Fig. 3.4 the chromatogram of the SEC is shown.

3 Experiments

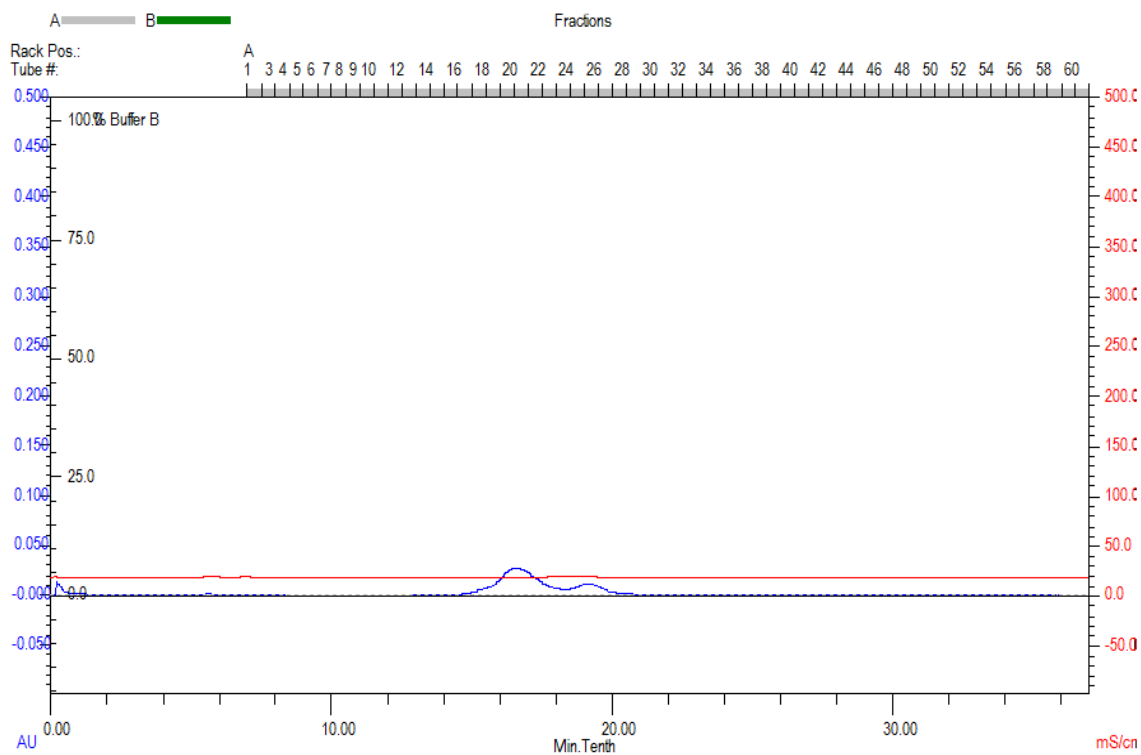


Fig. 3.4 Chromatogram of SEC-purification of 16-kDa hPRL from concentrate after refolding. The UV-absorption (AU) and conductivity (mS/cm^2) dependent on time are shown.

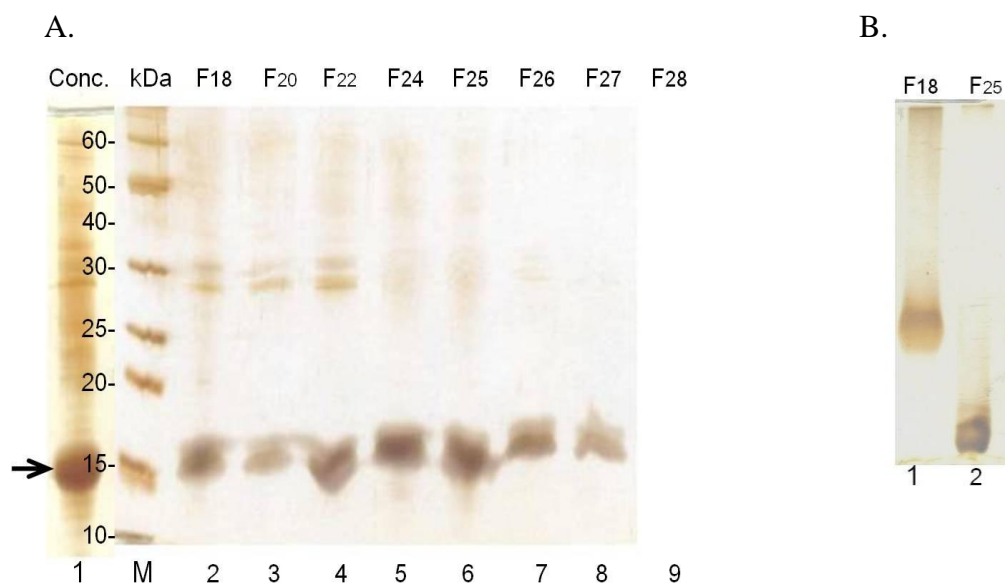


Fig. 3.5 A. SEC-purification of 16-kDa hPRL from concentrate after refolding presented using 12% SDS-PAGE with blue staining. The black arrow indicates 16-kDa hPRL. B. Native-PAGE analysis of Fr. 18 and Fr. 25 (12 % with silver staining). Conc.: protein concentrate after renaturation; F, fraction; M, protein marker (Fermentas SM0661).

3 Experiments

As shown in Fig. 3.5.A, two peaks were detected respectively at 20 and 25 min. Subsequently, the fractions from the peaks are analyzed by SDS-PAGE and silver staining. In the first peak, 16-kDa hPRL and the contaminating proteins (mainly near 30 kDa) were washed down together (Fr. 18- 22). The clean fractions of 16-kDa hPRL, free of any impurities were proven to be in the second peak with lower UV-value.

To determine whether the interchain disulfide bond was formed between two 16-kDa hPRL molecules, which resulted in the products in peak 1, the band locations of Fr. 18 and Fr. 25 were analyzed by native-PAGE with silver staining. From Fig. 3.5.B it can be observed that the position of the band from Fr. 25 is lower than from Fr. 18. So it suggests that the protein in peak 2 is a monomer with correct refolding and that a dimer has been formed from the protein in peak 1, which was first washed down from the column. Subsequently, the 16-kDa hPRL in peak 2 was pooled and dialyzed against 20 mM ethanolamine pH 9.0.

3.1.3 Endotoxin assay and removal of endotoxin

Endotoxin, also called lipopolysaccharides (LPS), is a major contaminant in recombinant proteins in *E. coli* (128). The presence of a low endotoxin level (10 EU mL^{-1} , 1 ng mL^{-1}) in recombinant protein preparations can cause negative effects in host organism such as endotoxin shock, tissue injury and even death (128-130). So it is essential to determine the endotoxin concentration and remove it prior to testing the bioactivity of purified protein solution. In this work, the endotoxin concentration in the purified 16-kDa hPRL was detected by means of limulus amoebocyte lysate (LAL)-Test. A commercial reaction kit was effective in removing endotoxin where the protein solution was passed through a column and the endotoxin bound to the affinity matrix (see in Appendix 5.5.8). The final product of 16-kDa hPRL (0.528 mg mL^{-1} , concentration determined by Bradford assay described in Appendix 5.5.4.1) was revealed below 0.1 EU mL^{-1} while immediately after two-step chromatography $1.2 \times 10^4 \text{ EU mL}^{-1}$ was measured. Finally, the sample was stored at $-20 \text{ }^\circ\text{C}$ with 15% glycerol (end concentration) until use.

3 Experiments

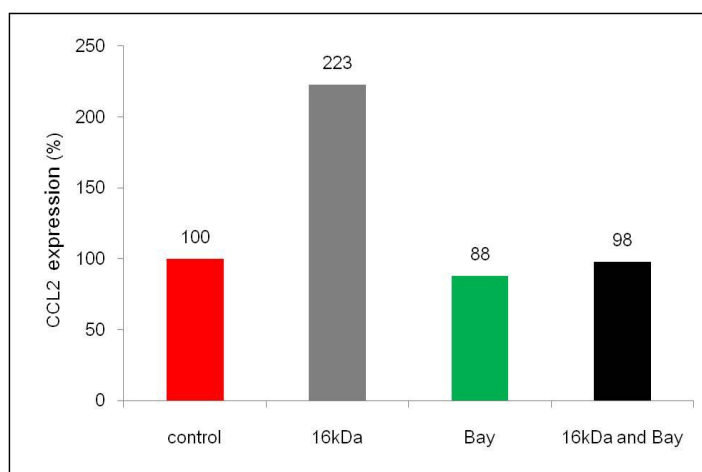
3.1.4 Test of biological activity

The tests of biological activity of purified recombinant 16-kDa hPRL were performed by the team of Prof. Denise Hilfiker-Kleiner (Department of Molecular Cardiology and Angiology, Hanover Medical School). *In vitro*, its effect on NF- κ B activation in neonatal rat cardiomyocytes (NRCM) was investigated. *In vivo*, the fractional shortening (FS) in the left ventricular of wild type mice was evaluated after injected with purified 16-kDa hPRL over 7 days.

3.1.4.1 *In vitro*

The expression of C-C motif chemokine ligand 2 (CCL2) is under the control of NF κ B, which is well known to be the cause of inflammation and cell death (131). The CCL2 expression levels in NRCM exposed to 16-kDa hPRL and only with Bay (a pharmacological inhibitor of NF κ B) were determined via PCR and parallel the CCL2 expression without any stimulation factors was used as the control. The result of CCL2 expression levels is shown in Fig. 3.6.A. Additionally, after NRCM was stimulated with purified protein for 1 h, the expression of I κ B- α was detected by Western Blot (WB) as shown in Fig. 3.6.B.

A.



B.

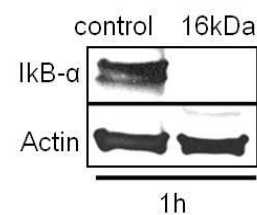


Fig. 3.6 A. The evaluation of CCL2 expression in NRCM treated with 16-kDa hPRL (10 nM) or Bay (1 μ M) as % of the control. The untreated cells were used as control. 16kDa, purified 16-kDa hPRL. B. WB of I κ B- α 1 h after stimulation of NRCM with purified 16-kDa hPRL and actin as a control.

3 Experiments

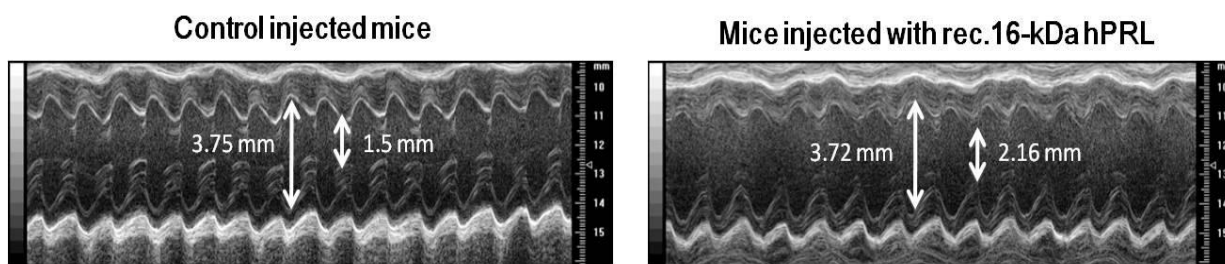
Fig. 3.6.A shows that the CCL2 expression in untreated NRCM was recorded as 100%. When the cells were treated with only purified 16-kDa hPRL, NF κ B was activated and the expression of CCL2 was strongly induced with 223% of the control. However, treatment with 1 μ M Bay only caused significant decrease of expression of CCL2. Moreover, a noticeable decrease of CCL2 expression incubated with Bay for 1 h before addition of 10 nM 16-kDa hPRL to the cells and treated NRCM could be observed. Additionally, the result of the WB demonstrates that after NRCM were stimulated with purified protein for 1 h, no I κ B- α expression was detected by anti-I κ B- α antibody in cell lysate, meanwhile actin served as control and was detected in both fractions before and after stimulation.

3.1.4.2 *In vivo*

The echocardiography of wild type mice, which were injected with purified 16-kDa hPRL for 7 days was performed. The control mice were injected with a control peptide (an E. coli protein). The left ventricular internal dimensions at end-systole and end-diastole (LVESD and LVEDD) were measured digitally on the M-mode tracings and averaged from at least 3 cardiac cycles and the FS was calculated using:

$$[(LVEDD - LVESD)/LVEDD] \times 100 (\%).$$

A.



3 Experiments

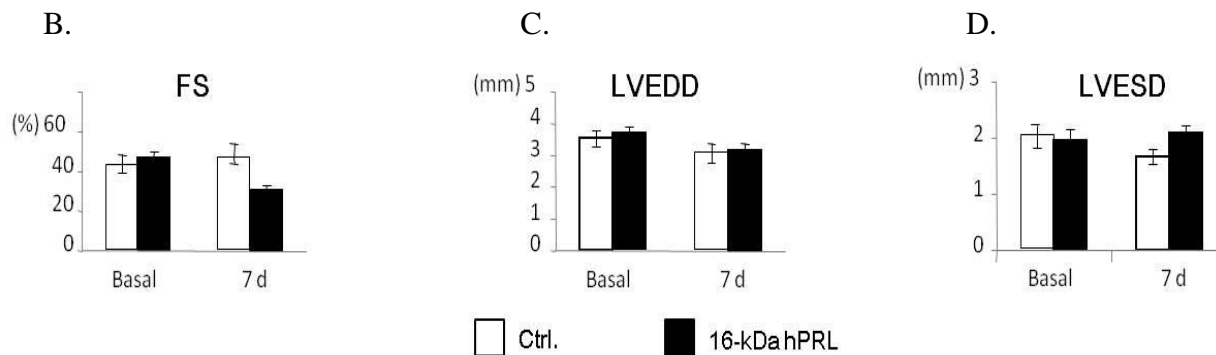


Fig. 3.7 A. Representative M-mode echocardiograms of mice after 7 days of injection with control peptide and purified recombinant 16-kDa hPRL (50 μ g every 3 days, total dose 100 μ g). B. FS in n=4 mice per intervention. C. LVEDD value. D. LVEDS value. White bars, control peptide injected mice; black bars, 16-kDa hPRL injected mice.

Representative M-mode echocardiograms after 7 days of observation are shown in Fig. 3.7.A decrease in LVEDD from 3.75 to 3.72 mm and an increase in LVEDS from 1.50 to 2.16 mm were observed from the mice injected with 16-kDa hPRL for 7 days, whereas both values of LVEDD and LVEDS in the control peptide injected mice were reduced. The reduced percentage of FS indicates statistically significant impairment of the left ventricular in the 16-kDa hPRL injected mice compared with the control mice.

3.1.5 Summary

The pT7L-16-kDa hPRL was transformed in *E. coli* BL21 (DE3) and the cells were cultivated in TB medium in shake flask to a high cell density. The 16-kDa hPRL was produced as insoluble inclusion bodies and subsequently a 2-step chromatography purification was carried out. Firstly, an anion exchange chromatography based on membrane adsorber resulted in the removal of most impurities. After refolding and concentration followed by size exclusion chromatography, the pure 16-kDa hPRL was obtained. Fig. 3.8 shows the flow diagram of the production process.

100 mL culture corresponded to 0.41 g wet cell biomass, of which 0.66 mg bioactive 16-kDa

3 Experiments

hPRL can be recovered with a purity of 95% as estimated by SDS-PAGE, and the endotoxin level was less than 0.1 EU mL^{-1} .

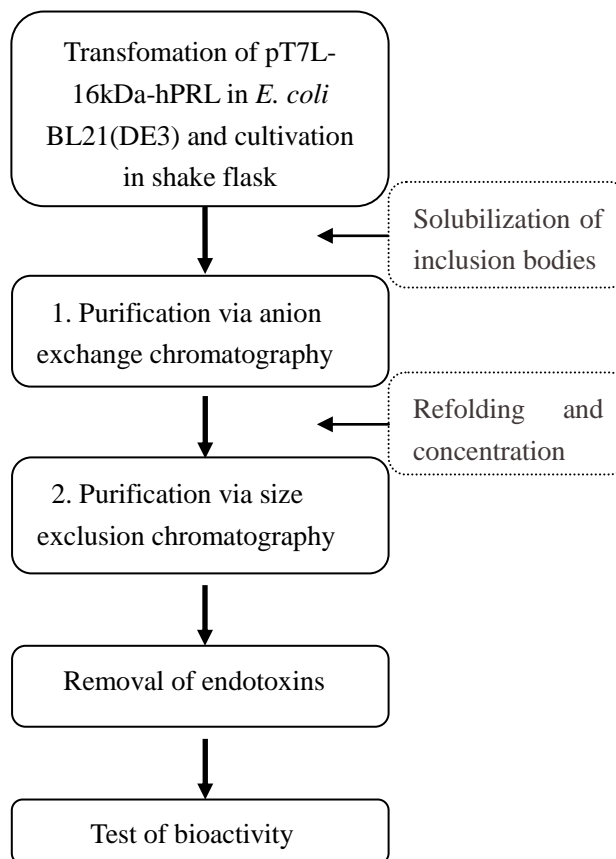


Fig. 3.8 The flow chart of 16-kDa hPRL production process.

The bioactivity of purified 16-kDa hPRL was confirmed successfully *in vitro* and *in vivo*. Significant expression of CCL2 in NRCM treated with 16-kDa hPRL was detected while a decrease in CCL2 expression was observed when cells were pre-treated with Bay, an inhibitor of NF- κ B indicating 16-kDa hPRL was involved in mediating the apoptotic action of NRCM through the NF- κ B signal pathway. *In vivo*, systematic injection of recombinant 16-kDa hPRL induced cardiac dysfunction in normoxic wild type mice.

3.2 Production of cytokines using thioredoxin as fusion partner

Activin A is a glycosylated disulfide linked 26 kDa homodimer, each peptide contains 116 amino acids with 9 cysteines. So far, the successful direct production of Activin A described in literature has been exclusively in eukaryotic expression systems. Attempts to produce the Activin A monomer (Activin β A) in *E. coli* resulted in inclusion bodies in the cytoplasm of bacteria. As this cysteine-rich protein could not generate correct disulfide bonds, the proteins must then be solubilized *in vitro* and renatured before further purification. However, these steps make the overall process more complex and expensive.

FAM163A contains 167 amino acids with 8 cysteines, which share over 80% protein homology with mouse. hHSS1 is a single chain polypeptide containing 254 amino acids with 3 cysteines and the sequence homology between hHSS1 and mHSS1 reaches 86%. It is not known, whether FAM163A and HSS1 from different species can exchange with one another. To our knowledge there have been no reports about expression of both proteins in *E. coli*.

In the present study a new process for production of hActivin A, Fam163a and mHSS1 in *E. coli* was established and optimized. It was expected that the three proteins would be expressed as fusion proteins with Trx as a fusion partner. Trx can regulate the redox state in bacterial cytoplasm and contribute to correct formation of disulfide bridges in these three cytokines. In the presence of this tag, synthesis of the target cytokines in inclusion bodies could be prevented and their solubility could be improved.

For production of hActivin A, Fam163a and mHSS1 several steps were involved. After construction of the expression vector and the synthesis of fusion protein in recombinant *E. coli*, the fusion protein was purified via immobilized metal ion affinity chromatography (IMAC) prior to cleavage where the target cytokine was released. Finally, the isolated proteins of interest were employed in bioactivity tests.

3 Experiments

3.2.1 Construction of expression vector

The expression vector pET32b-Trx-6×his-TEV-Target Protein was transformed into the host cell *E. coli* BL21(DE3) for production of hActivin A, mHSS1 and Fam163a. The complete vector map is presented in Appendix 5.4. The genes corresponding to the three cytokines were fused with N-terminal Trx and they were expected to be expressed as a soluble fusion protein in *E. coli*. After amplification, the cDNA PCR products of hActivin β A, mHSS1 and Fam163a were inserted into plasmid pET32b as BamHI/XhoI fragments which already contained a Trx encoding sequence and a gene marker for selection by ampicillin. The genes of the target proteins were incorporated immediately downstream of Trx which was marked with a 6×his tag and a TEV-protease recognition sequence. This strategy was expected to enable the target proteins to be released from his-tagged Trx after purification of fusion proteins.

The fusion constructs of hActivin β A, Fam163a and mHSS1 (without the signal sequences) consist of 762, 790 and 1060 base pairs respectively, are under the control of a T7 promoter. The sequences of base pairs and amino acids of the three proteins are also given in Appendix 5.4 and Fig. 3.9 shows the schematic diagram of the fusion protein. The recombinant protein contains a Trx-6×his tag at the N-terminal, target protein at the C-terminal and a TEV-protease cleavage site of seven amino acids between them. Since the size of Trx is 14.5 kDa, the expected sizes of Trx fusion with Fam163a and mHSS1 should be 29.3 kDa and 39 kDa respectively. And Trx- hActivin β A results in a molecular size of 27.5 kDa.

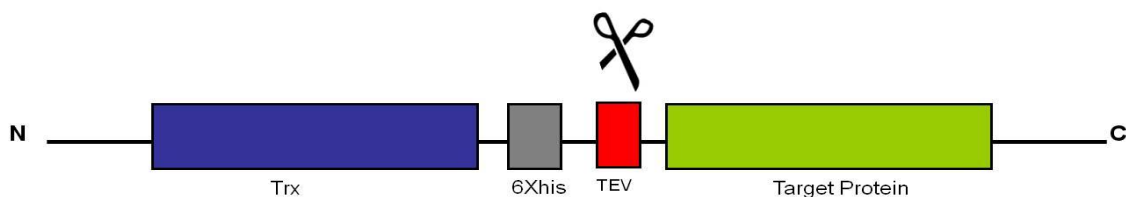


Fig. 3.9 Schematic representation of the expressed fusion protein with the important elements. The site for cleavage of the fusion protein is marked with a scissors symbol.

The results and discussion of productions of hActivin A, Fam163a and mHSS1 are separately presented in the following chapters. The detailed protocols and description of performance can be found in the Appendix.

3.2.2 Production of human Activin A

3.2.2.1 Expression of Trx-hActivin β A

After the plasmid pET32b-Trx-6 \times his-TEV-hActivin β A was transformed in *E. coli* BL21(DE3), the cultivation of the recombinant *E. coli* was performed in LB medium at 26 °C. The cells were collected at 2, 4, 6, 8 and 12 h after IPTG induction and the OD₆₀₀ of the samples were adjusted with lysis buffer to the same value. After cell disruption by sonication, the separated soluble and insoluble fractions of cell lysate were analyzed by SDS-PAGE as shown in Fig. 3.10.

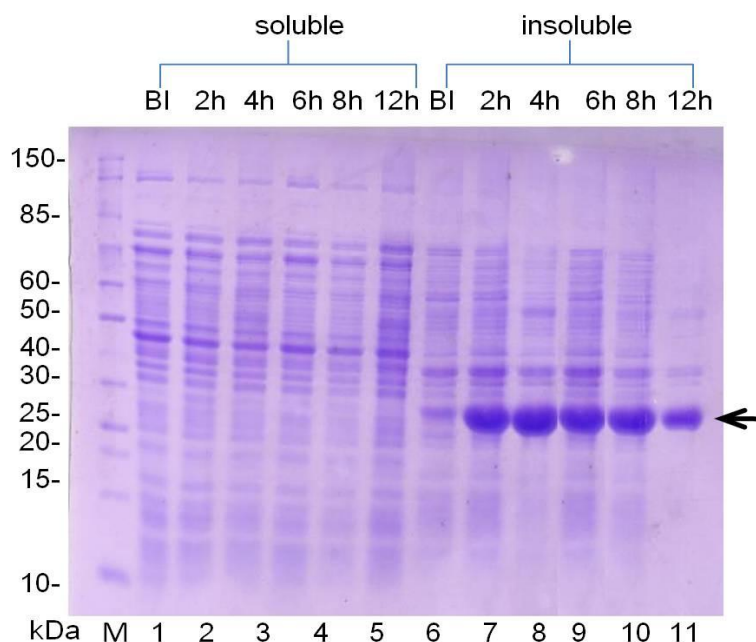


Fig. 3.10 Time course of Trx-hActivin β A production in LB medium at 26 °C presented using 12% SDS-PAGE with coomassie staining. The black arrow indicates Trx-hActivin β A. The soluble (lane1) and insoluble (lane 6) fractions before induction; soluble (lanes 2-5) and insoluble fractions (lanes 7-11) 2, 4, 6, 8 and 12 h after induction, respectively. BI, before induction; M, protein marker (Fermentas SM0661).

No soluble Trx-hActivin β A was detected during the cultivation. However, 2 h immediately after IPTG induction, all of the expressed Trx-hActivin β A with expected size 27.5 kDa was accumulated as inclusion bodies and the concentration of insoluble fusion protein reached its maximum 6 h after induction.

3 Experiments

The cultivation of the recombinant *E. coli* was also performed in LB medium at 18°C and 37°C and both temperatures had no effect in increasing the amount of soluble fusion protein. Moreover, TB medium was tested for production of Trx-hActivin β A and the *E. coli* cells grew more quickly in this medium than in LB medium at all tested temperatures. Unfortunately, Trx-hActivin β A was produced entirely as insoluble product and the change of medium did not make any improvement of Trx-hActivin β A solubility (gels not shown).

3.2.2.2 Purification of Trx-hActivin β A from inclusion bodies

Since the fusion with Trx did not improve production of soluble hActivin β A, bioactive Trx-Activin β A was to be alternatively achieved by purification of previously *in vitro* refolded inclusion bodies. The inclusion bodies of Trx-Activin β A were washed twice and the concentration of solubilized fusion protein was estimated by densitometric analysis. After the intramolecular and intermolecular disulfide bonds in hActivin β A were completely reduced, the fusion protein was diluted to 100 $\mu\text{g mL}^{-1}$ with solubilization buffer without DTT and then dialyzed against a 500-fold excess volume of refolding buffer at 4 °C for 48 h during which the buffer was refreshed at least 4 times. TDCA/Na was also added to the refolding buffer, which was reported to improve hActivin β A renaturation significantly (80).

IMAC using membrane absorber with ligand iminodiacetic acid (Sartobind IDA-75) was performed for the purification of Trx-hActivin β A. The protein solution was concentrated via ultrafiltration prior to purification and the concentrate was applied to IDA-75 with a binding capacity of 3 mg protein connected to a FPLC system. The membrane was preloaded with Zn^{2+} and equilibrated with binding buffer. After removal of non-specifically bound proteins on IDA-75 with binding buffer and wash buffer, the target protein was finally eluted with imidazole. The composition of refolding buffer and the FPLC protocol are seen Appendix 5.5.7.3 "Purification of Trx-hActivin β A". In Fig. 3.11 is presented the chromatogram of the IMAC-purification and Fig. 3.12 shows the SDS-PAGE analysis with silver staining of the chosen fractions.

3 Experiments

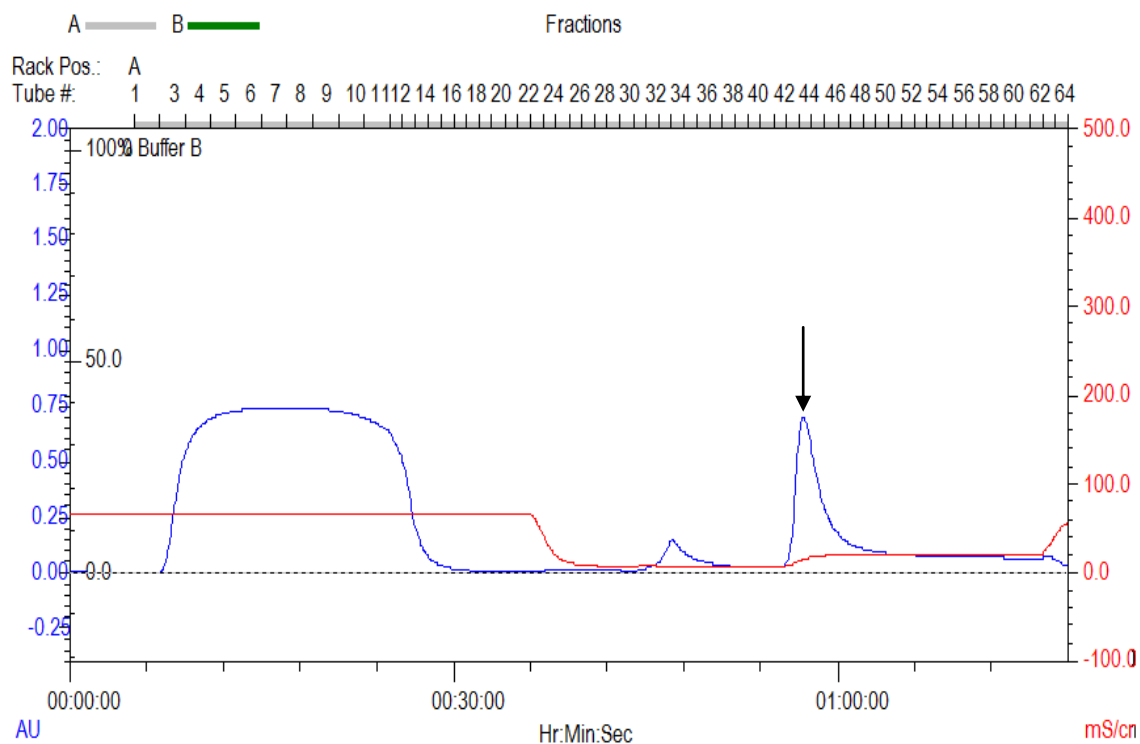


Fig. 3.11 Chromatogram of IMAC-purification of Trx-hActivin β A from refolded inclusion bodies. The UV-absorption (AU) and conductivity (mS/cm^2) dependent on time are shown. The arrow indicates the elution peak of Trx-hActivin β A.

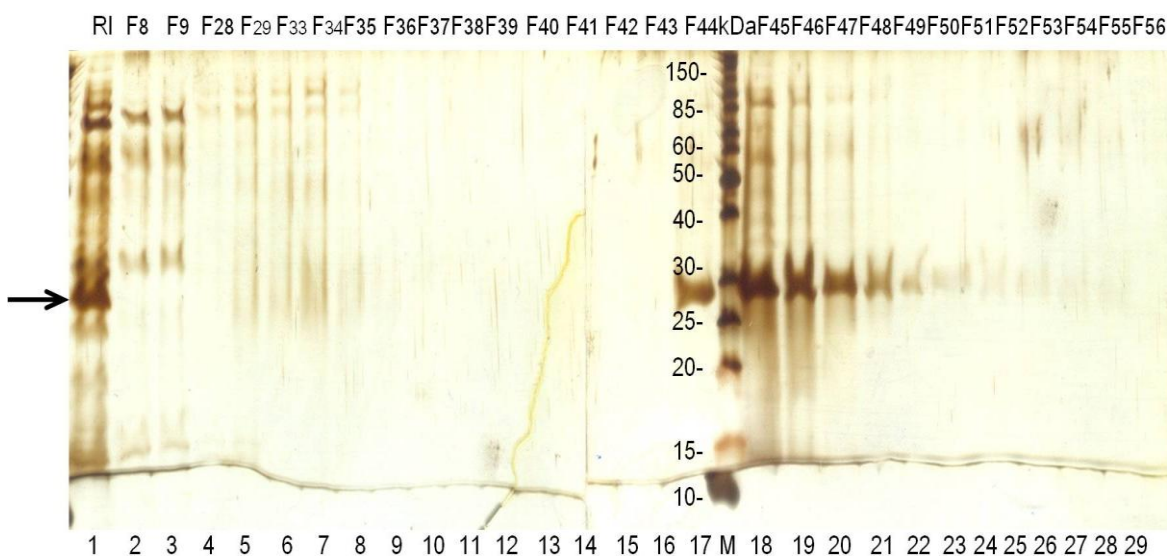


Fig. 3.12 IMAC-purification of Trx-hActivin β A from refolded inclusion bodies presented using 12% SDS-PAGE with silver staining. The arrow indicates Trx-hActivin β A. RI: refolded inclusion bodies before purification; F, fraction; M, protein marker (Fermentas SM0661).

3 Experiments

The fusion protein Trx-hActivin β A could be purified from refolded inclusion bodies via IMAC. The fractions Fr. 46-49 containing the majority of the pure Trx-hActivin β A were pooled and dialyzed overnight against 25 mM Tris-HCl, pH 8.0 at 4 °C for the removal of imidazole. The concentration of fusion protein was determined by Bradford assay.

3.2.2.3 Cleavage of Trx-hActivin β A

For release of hActivin β A, the purified fusion protein must be cleaved in the next process step. The Trx, as well as 6 \times his tag, should be separated from hActivin β A as a common fragment. In this work, the commercial *AcTEV*TM-protease was employed for cleavage of Trx-hActivin β A because of its site-specific-activity and stability. Additionally, with an N-terminal 6 \times his tag it can be easily removed in the subsequent IMAC. DTT in the buffer was replaced with 5 mM GSH/1 mM GSSG, so that more reducing power for TEV-protease could be provided. The cleavage was performed at 10 °C for 8 h and the protocol is seen in Appendix 5.5.10.

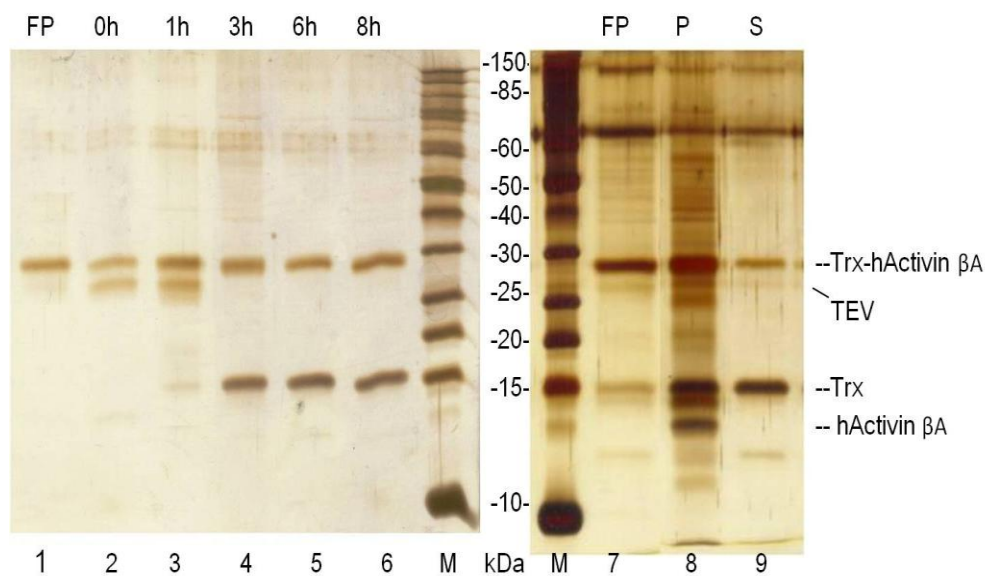


Fig. 3.13 Time course of Trx-hActivin β A cleavage with *AcTEV*TM-protease at 10 °C and centrifugation of cleavage products presented using 12% SDS-PAGE with silver staining. Lanes 1 and 7, purified Trx-hActivin β A; lanes 2-6, the samples 0, 2, 4, 6 and 8 h after addition of *AcTEV*TM-protease; lanes 8 and 9: pellet and supernatant after centrifugation of cleavage products. FP: fusion protein; P, pellet; S, supernatant; M, protein marker (Fermentas SM0661).

3 Experiments

As seen in Fig. 3.13, already after 1 h the released Trx with 14.5 kDa could be detected whose intensity reached a maximum at 3 h and remained stable during further incubation. The band of TEV-protease disappeared after 3 h and during the tested 8 h no protein band at 13 kDa corresponding Activin β A could be seen.

After the cleavage products of fusion protein for 3 h were centrifuged, the supernatant and pellet were analyzed by SDS-PAGE as shown in lane 8 and 9. The 14.5 kDa Trx and the incompletely digested fusion protein at 27.5 kDa are found in supernatant whereas various species are present in pellet: fusion protein, Trx and released hActivin β A at 13 kDa as well as an unknown protein at 25 and 14 kDa. The detection of Trx-hActivin β A in pellet indicates that perhaps part of the fusion proteins has formed soluble mini-aggregates via refolding which is resistant to cleavage with TEV-protease. It seemed that, Activin β A was only soluble as long as fused with Trx and they had precipitated after being released from Trx.

3.2.2.4 Summary

Activin A is a homodimer of the TGF- β family which is well known to play an important role of haematopoiesis. The cDNA of hActivin β A was fused with Trx and transformed into *E. coli* BL21(DE3). Trx-hActivin β A was produced entirely insoluble. Since the temperature and medium change did not improve the solubility of fusion protein, the inclusion bodies were used as starting material for purification.

Trx-hActivin β A was refolded by dialysis prior to purification of fusion protein via IMAC and the renaturation process was performed based on the description in a patent for refolding of hActivin A without any fusion partner. It is claimed that, with this method 24% of hActivin A produced in *E. coli* had reconstituted into its natural form which was confirmed by measuring of its biological activity. It was observed that the released hActivin β A after cleavage of the fusion protein with TEV-protease was detected only in insoluble part. It indicated that the method provided in the patent maybe had made the renaturation of Trx-hActivin β A possible and hActivin β A had changed its conformation as soon as it was released from Trx. Based on this result the work was terminated.

3 Experiments

3.2.3 Production of murine protein family with sequence similarity 163, member A**3.2.3.1 Expression of Trx-Fam163a**

After the plasmid pET32b-Trx-6×his-TEV-Fam163a was transformed in *E. coli* BL(DE3), the cultivation of the recombinant *E. coli* was performed in LB medium at three different temperatures (18 °C, 26 °C and 37 °C). The expression of fusion protein was induced with 0.25 mM IPTG when OD₆₀₀ reached 0.6. The collected cells were lysed with *BugBuster™ Protein Extraction Reagent*. Subsequently, the soluble and insoluble fractions of cell lysate were separated.

Cultivation at 37 °C

The production of Trx-Fam163a was performed in LB medium at 37 °C. The cells were collected at 1, 3, 6, 9 and 16 h after IPTG induction. The soluble and insoluble fractions of cell lysate were analyzed by SDS-PAGE and the result is observed in Fig. 3.14.

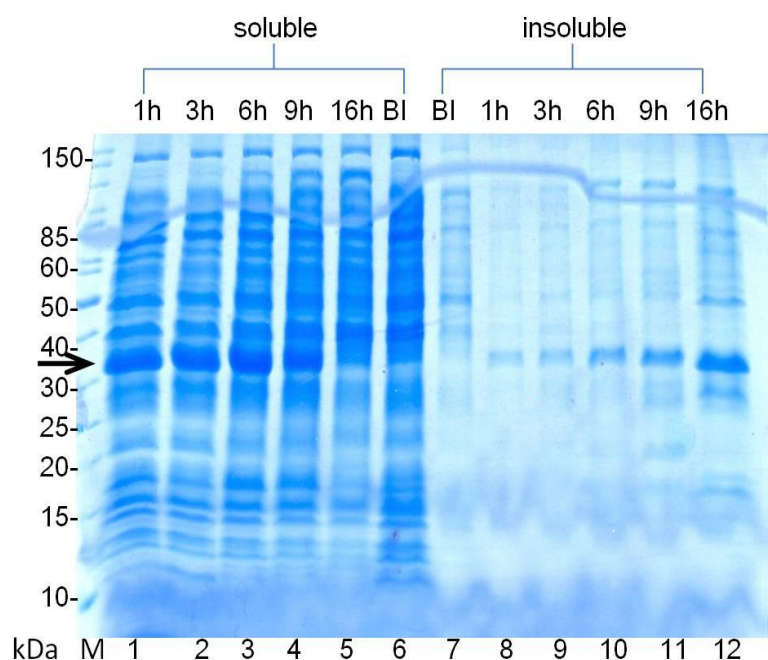


Fig. 3.14 Time course of Trx-Fam163a production in LB medium at 37 °C presented using 12% SDS-PAGE with blue silver staining. The soluble (lane 6) and insoluble (lane 7) fractions before induction; soluble (lanes 1-5) and insoluble fractions (lanes 8-12) 1, 3, 6, 9 and 16 h after induction, respectively. The arrow indicates Trx-Fam163a. BI, before induction; M, protein marker (Fermentas SM0661).

3 Experiments

A significant expression of soluble Trx-Fam163a had already been detected 1 h after IPTG induction with a molecular weight of about 30 kDa, which matched the expected size of the fusion protein. The band intensity increased in the first few hours and the highest concentration of fusion protein was present 6 h after induction. Trx-Fam163a as a soluble fraction decreased gradually over time and at the end of cultivation its band could be not detected.

By contrast, the production of insoluble fusion protein continued to rise during the cultivation period. Over 90 % Trx-Fam163a was produced in soluble form 1 h after induction while the level of inclusion bodies development was very low. 6 h after induction the production of insoluble fusion protein had a share of about 10% of the total amount when the concentration of soluble Trx-Fam163a reached its maximum. At the end of cultivation Trx-Fam163a was found exclusively accumulated in inclusion bodies and a part of them were degraded into smaller proteins at 27 and 17 kDa.

Cultivation at 26 °C and 18 °C

The production of soluble Trx-Fam163a in LB medium at 26 °C and 18 °C are shown in Fig. 3.15.

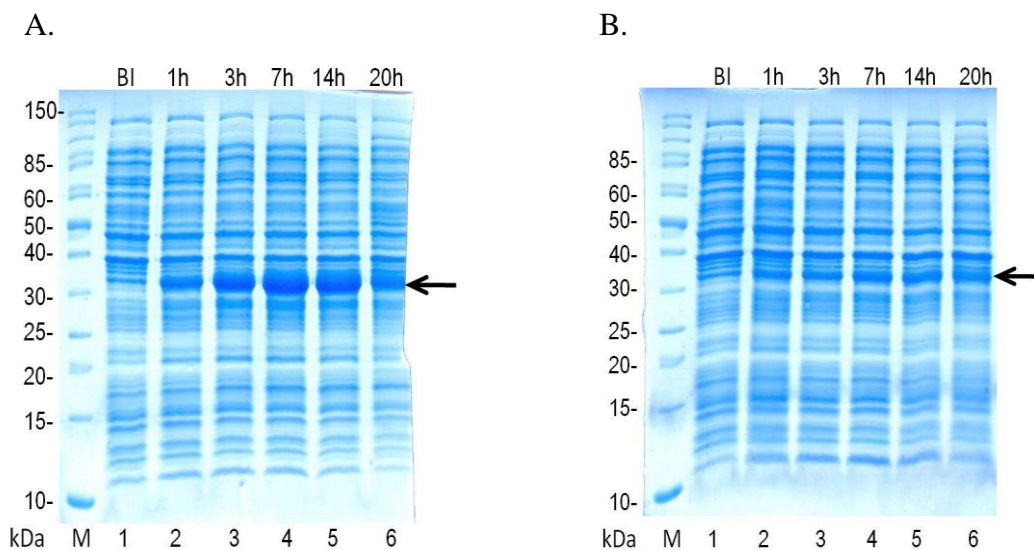


Fig. 3.15 Time course of Trx-Fam163a production in LB medium at 26 °C (A) and 18 °C (B) presented using 12% SDS-PAGE with blue silver staining. The fractions before induction (lane 1) and after induction (lanes 2-6) are shown. The arrow indicates Trx-Fam163a. BI, before induction; M, protein marker (Fermentas SM0661).

3 Experiments

The synthesis of soluble Trx-Fam163a at 26 °C also began already 1 h after IPTG induction but overexpression of the fusion protein was postponed to after 3 h. In comparison with expression at 37 °C where Trx-Fam163a degradation was profound after 9 h, even prolonging induction at 26 °C for 14 h Trx-Fam163a a soluble fraction is seen to be stable. As a consequence of low temperature at 18 °C, there was no significant production of soluble Trx-Fam163a visible on the gel during the tested time.

In conclusion, an overexpression of soluble Fam163a with Trx as fusion partner was observed at 37 °C and 26 °C in LB medium while the insoluble fusion protein was quite little. Compared to 37 °C, the overexpression of fusion protein at 26 °C was postponed a few hours. However, the lower temperature did not have any beneficial effect on production of soluble Trx-Fam163a and no significant synthesis of soluble fusion protein at 18 °C was detected.

3.2.3.2 Purification of soluble Trx-Fam163a

3.2.3.2.1 Screening via Vivaspure MCMini

The purification of his-tagged Trx-Fam163a from fresh soluble fraction of cell lysate in analytical scale was performed with the help of Vivaspure MCMini spin column pre-packed with Ni-IDA agarose in a microfuge. The purification was based on the protocol described in Appendix 5.5.5.

The result of the purification of Trx-Fam163a from fresh soluble fraction of cell lysate is shown in Fig. 3.16.A. The spin column was loaded with diluted soluble fraction of cell lysate and there was only a little Trx-Fam163a detected in the flow through, indicating good binding between his-tagged fusion protein and its ligand. A number of contaminant proteins above 30 kDa had been removed already by 3 wash steps. The majority of Trx-Fam163a was found in the first elution fraction and pure Trx-Fam163a could be achieved close to homogeneity in the second and third fractions (lanes 7 and 8). The weak protein bands less than 30 kDa were initially supposed to be non-specifically bound contaminants.

3 Experiments

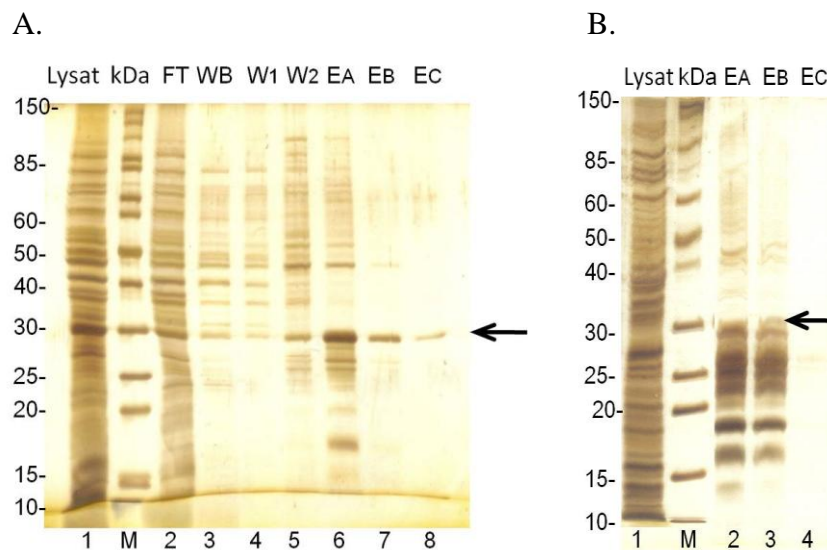


Fig. 3.16 Purification of Trx-Fam163a from fresh (A) and at room temperature overnight incubated (B) soluble fraction of cell lysate via Vivaspure MCMini presented using 12% SDS-PAGE with silver staining. The soluble fractions of cell lysate (lane 1) and from the following steps of IMAC (lanes 2-8 in A and lanes 2-4 in B) are shown. The arrow indicates Trx-Fam163a. Lysat: soluble fraction of cell lysate before purification; FT, flow through; WB: wash fraction with binding buffer; W1, wash fraction with wash buffer 1; W2, wash fraction with wash buffer 2; EA, first elution fraction; EB, second elution fraction; EC: third elution fraction; M, protein marker (Fermentas SM0661).

3.2.3.2.2 Degradation of Trx-Fam163a

The purification of Trx-Fam163a was also performed after soluble fraction of cell lysate was incubated overnight at room temperature as shown in Fig. 3.16.B. It was noticed that, there was no Trx-Fam163a detected in primary cell lysate after incubation and the protein bands under 30 kDa became intensively visible in elution fractions, especially between 25 and 30 kDa as well as at 18 and 20 kDa. It was hypothesized that, the soluble Trx-Fam163a might be sensitive to bacterial proteases, resulting in unexpected degradation.

The effect of temperature with time on stability of Trx-Fam163a in soluble fraction of cell lysates was studied. The degradation of Trx-Fam163a in the soluble fraction from expression at 26 °C for 6 h at different temperatures (4 °C, 20 °C and 37 °C) was tested for 3 days as shown in Fig. 3.17. Temperature plays an important role in degradation of Trx-Fam163a. The higher the

3 Experiments

temperature was, the more quickly would the protein be degraded. In comparison to the initial sample, after only 1 day, more than 98% Trx-Fam163a was not identifiable at 20 °C while the intensity of bands at 27 and 28 kDa increased. Insoluble protein aggregate formed at 37 °C on the first day and a completely disappearance of Trx-Fam163a band was detected. It was observed from lanes 2-4, degradation has been postponed as a consequence of low temperature at 4 °C and that still about 40% Trx-Fam163a could be detected on the first day which was further reduced in the following 2 days of incubation. Like the 20 °C, after only one day, a particularly marked decrease of band intensity at 30 kDa and an increase of protein concentration at 20, 27 and 28 kDa could be observed.

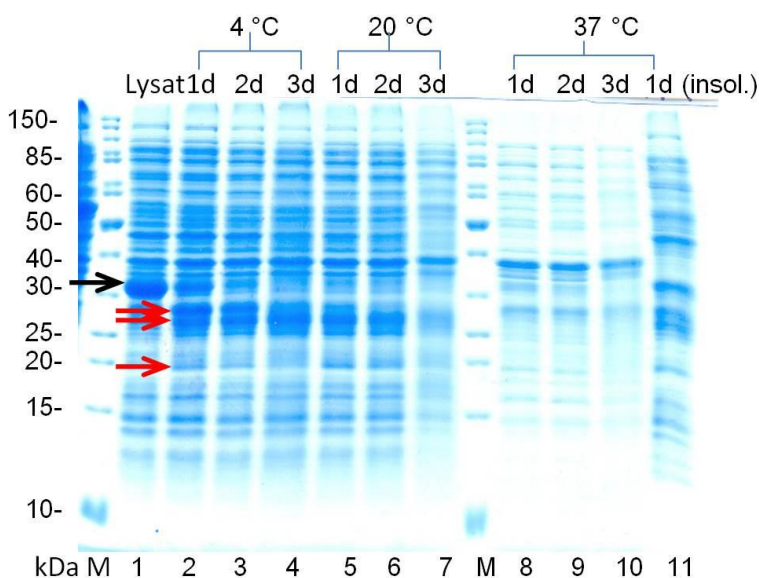


Fig. 3.17 Time course of degradation of Trx-Fam163a in soluble fraction of cell lysate at different temperatures in 3 days presented using 12% SDS-PAGE with blue silver staining. Lane 1, fresh soluble fraction of cell lysate from expression at 26 °C for 6 h; lanes 2-4, incubated at 4 °C; lanes 5-7, incubated at 18 °C; lanes 8-10, incubated at 37 °C; lane 11, insoluble fraction of cell lysate after incubation at 37 °C for 1 day. The black arrow indicates Trx-Fam163a and the red arrows indicate the degradation products. Lysat: fresh soluble fraction of cell lysate; insol.: insoluble; d, day; M, protein marker (Fermentas SM0661).

Identification of degradation products

Since the proteins at 18, 20, 27 and 28 kDa were detected in elution fractions of IMAC, these

3 Experiments

proteins were assumed to be fragments with 6×his tag of degraded Trx-Fam163a. For identification of Trx-Fam163a degradation products, a WB was performed and the protocol is seen in Appendix 5.5.3. The fresh soluble fraction of cell lysate from expression at 26 °C for 6 h in LB medium and the fraction which incubated at 4 °C for 1 day were applied to WB, respectively. After gel electrophoresis and transfer to a PVDF membrane, his-tagged proteins were detected by the specific mouse monoclonal antibody against 6×his tag and the secondary antibody peroxidase-conjugated anti-mouse IgG.

Fig. 3.18 shows the result of the WB. Based on these results, the degradation of Trx-Fam163a was found to have already occurred as it was expressed at 26 °C for 6 h. The fusion protein was cleaved into above mentioned small fragments less than 30 kDa. The detected proteins also took the 6×his tag, whose intensity increased significantly after incubation for 1 day and that was the reason for their strong affinity to Vivaspure MCM*ini*. Moreover, the fresh soluble fraction of cell lysate from Trx-Fam163a expression at 26 °C for 3 h was tested by WB and it was found that, degradation of Trx-Fam163a occurred even as it expressed at this temperature for 3 h (data not shown).

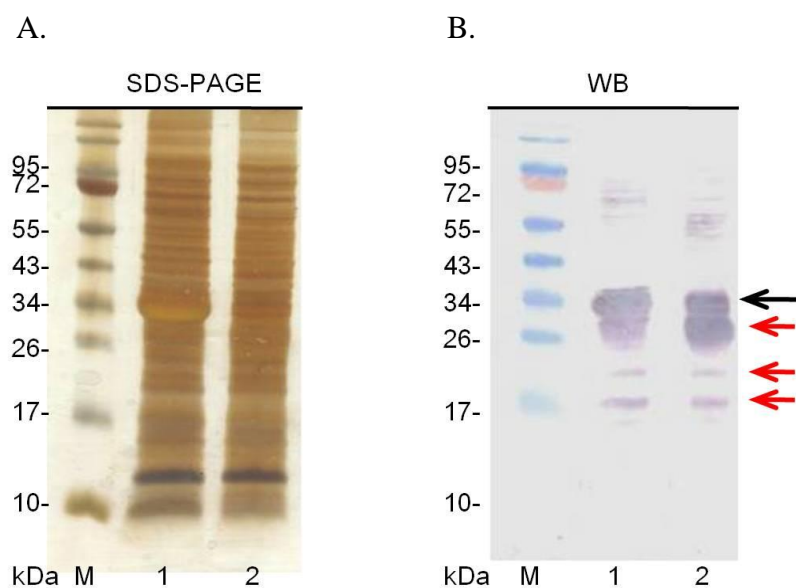


Fig. 3.18 Identification of Trx-Fam163a degradation fragments. A. SDS-PAGE analysis (12% with silver staining) of fresh soluble fraction of cell lysate from expression at 26 °C for 6 h (lane 1) and incubated at 4 °C for 1 day (lane 2). B. WB of fractions in A with anti-his antibody. The black arrow indicates Trx-Fam163a and the red arrows indicate the degradation fragments. M, protein marker (Fermentas SM0671).

3 Experiments

Effect of protease inhibitors

Taking account of the possible negative effects of the ingredients in *BugBusterTM Protein Extraction Reagent* in the degradation of Trx-Fam163a, this treatment was replaced by sonication for cell disruption. Moreover, to increase the stability of proteins and reduce the proteolytic degradation of proteins, protease inhibitors were added to cell lysate. Ethylenediaminetetraacetic acid (EDTA) was used to inactivate the metalloproteases and phenylmethanesulfonylfluoride (PMSF) was used as serine protease inhibitor. The commercial *Protease Inhibitor Cocktail* was also employed for this study, which is a mixture of protease inhibitor with a broad specificity for the inhibition of serine, cysteine, aspartic, thermolysin-like protease, and aminopeptidase.

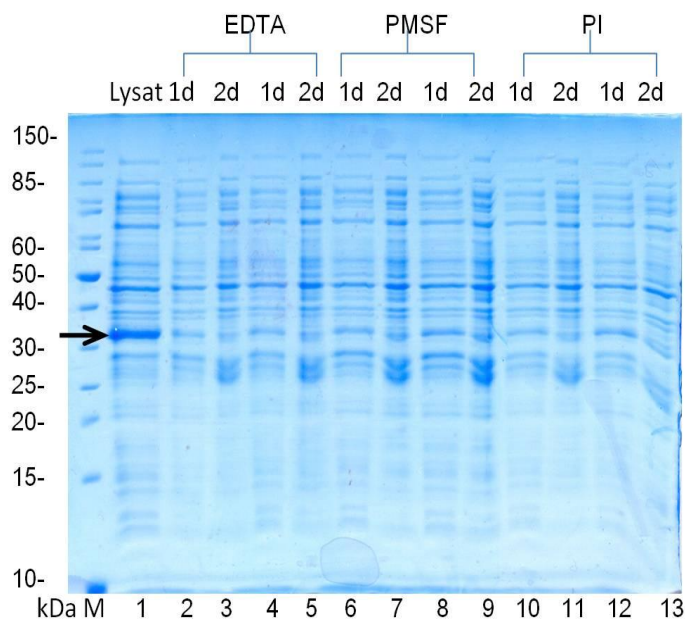


Fig. 3.19 Stability of Trx-Fam163a in diluted soluble fraction of cell lysate after incubation at 4 °C for 2 days with different protease inhibitors presented using 12% SDS-PAGE with blue silver staining. Lanes 1, fresh soluble fraction of cell lysate; lanes 2-5, incubated with 10 or 20 mM EDTA; lanes 6-9, incubated with 1 or 2 mM PMSF; lanes 10-13, incubated with *Protease Inhibitor Cocktail*. The black arrow indicates Trx-Fam163a. M, protein marker (Fermentas SM0661).

10 mM EDTA and 1 mM PMSF, as well as *Protease Inhibitor Cocktail* were added to protein suspension prior to sonication and the protocol is described in Appendix 5.5.11. Their effects

3 Experiments

were investigated after the fresh soluble fraction of cell lysate was incubated at 4 °C for 2 days and the results are shown in Fig. 3.19. No protease inhibitors used showed inhibitory effect on the degradation of Trx-Fam163a because noticeable reduction of Trx-Fam163a band intensity was detected in all fractions on the first day. Moreover, the result remained the same when the concentration of inhibitors was increased 2-fold. This might demonstrate that the enzymes which were capable of degrading the fusion protein do not belong to the protease family mentioned above.

Analysis of the stability of purified Trx-Fam163a

The stability of Trx-Fam163a was also studied as a purified preparation. The second elution fraction of Trx-Fam163a purification from the soluble fraction of cell lysate with Vivaspure *Mini*, in which Trx-Fam163a seemed very pure, was incubated at 4 °C for 3 days of which the SDS-PAGE is shown in Fig. 3.20. The band of Trx-Fam163a in the soluble fraction of cell lysate at 4 °C decreased in intensity as shown on the SDS-PAGE (Fig. 3.17, lanes 1 to 4), while the band had almost constant intensity throughout the incubation period. It was evident that the enzyme responsible for the cleavage of Trx-Fam163a must be associated with the bacterial intracellular proteases in *E. coli*.

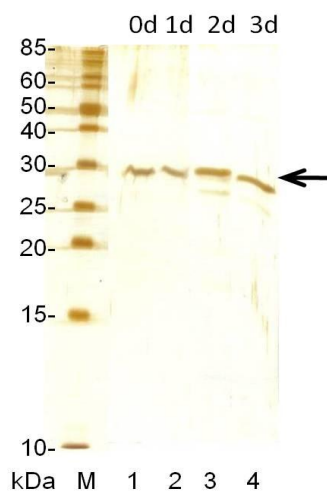


Fig. 3.20 Time course of the stability of by Vivaspure MCM*ini* purified Trx-Fam163a after incubation at 4 °C for 3 days presented using 12% SDS-PAGE with silver staining. Lanes 1-4, incubated for 0, 1, 2 and 3 days, respectively. The black arrow indicates Trx-Fam163a. d, day; M, protein marker (Fermentas SM0661).

3 Experiments

3.2.3.2.3 Upscaling of immobilized metal ion affinity chromatography

The recombinant *E. coli* cells containing Trx-Fam163a grown at 26 °C for 3 h were chosen as starting material for purification at laboratory scale via FPLC. After treatment with *BugBuster™ Protein Extraction Reagent*, the soluble fraction of cell lysate was applied to an IDA-75 membrane preloaded with Ni²⁺ immediately, because degradation of the fusion protein must be kept at a minimum. In order to remove protein contaminants as much as possible, wash buffers with varying NaCl concentrations (0-500 mM) were tested. Elution was carried out and optimized not only in respect to imidazole concentration (0-400 mM) but also as to elution strategy (stepwise or gradient). The chromatogram of optimized Trx-Fam163a purification is shown in Fig. 3.21 and the chosen fractions were analyzed by SDS-PAGE with silver staining as shown in Fig. 3.22.

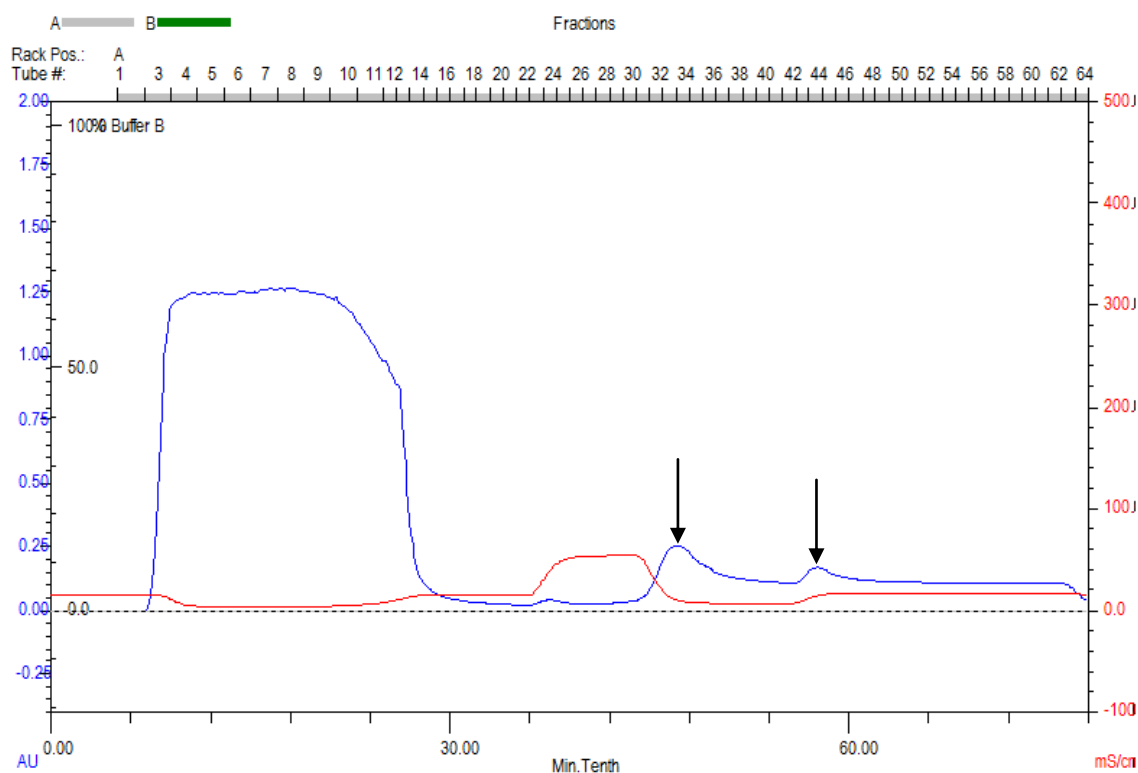


Fig. 3.21 Chromatogram of IMAC-purification of Trx-Fam163a from the soluble fraction of cell lysate. The UV-absorption (AU) and conductivity (mS/cm²) dependent on time were shown. The arrows indicate the elution peaks of Trx-Fam163a.

3 Experiments

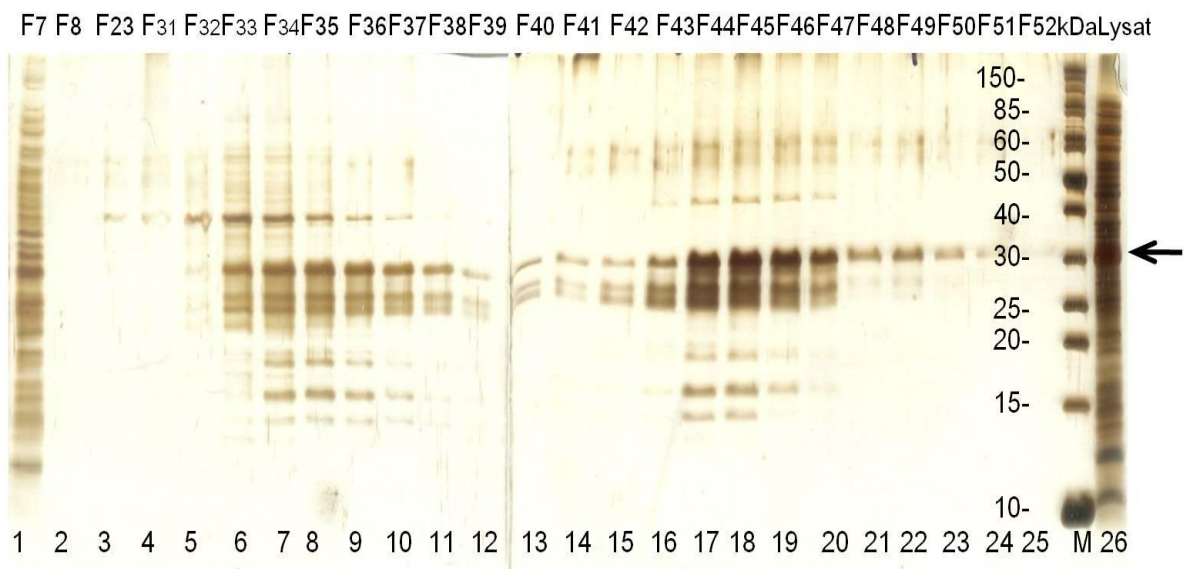


Fig. 3.22 IMAC-purification of Trx-Fam163a from the soluble fraction of cell lysate presented using 12% SDS-PAGE with silver staining. The black arrow indicates Trx-Fam163a. Lysat: soluble fraction of cell lysate; F, fraction; M, protein marker (Fermentas SM0661).

Although the fresh soluble cell lysate was used as the initial sample for purification it was always difficult to separate Trx-Fam163a from the partially degraded products also with the 6×his tag. A small part of contaminated protein at about 40 kDa could be removed using buffer containing 500 mM NaCl. A pre-elution was performed with only 100 mM imidazole and the second elution was done using 300 mM imidazole. The FPLC protocol is seen Appendix 5.5.7.3 "Purification of Trx-Fam163a". Trx-Fam163a was detected in both elution peaks, along with its degradation products. Compared to the first peak, the UV-value was lower in second peak, where the concentration of eluted Trx-Fam163a was higher. In the posterior part of the elution, relatively pure Trx-Fam163a was detected (Fr. 47-51). These fractions were pooled and dialyzed against 50 mM Tris-HCl, pH 7.0 for the following cleavage of fusion protein.

3.2.3.3 Cleavage of Trx-Fam163a

The cleavage of by ultrafiltration using *Vivaspin* concentrated Trx-Fam163a was performed at different temperatures (4 °C, 15 °C and 30 °C) and in buffers with different ratios of GSH/GSSG (20:1, 10:1, 5:1, 2:1 and 1:5). *AcTEV*TM-protease was employed for the cleavage of fusion

3 Experiments

protein again.

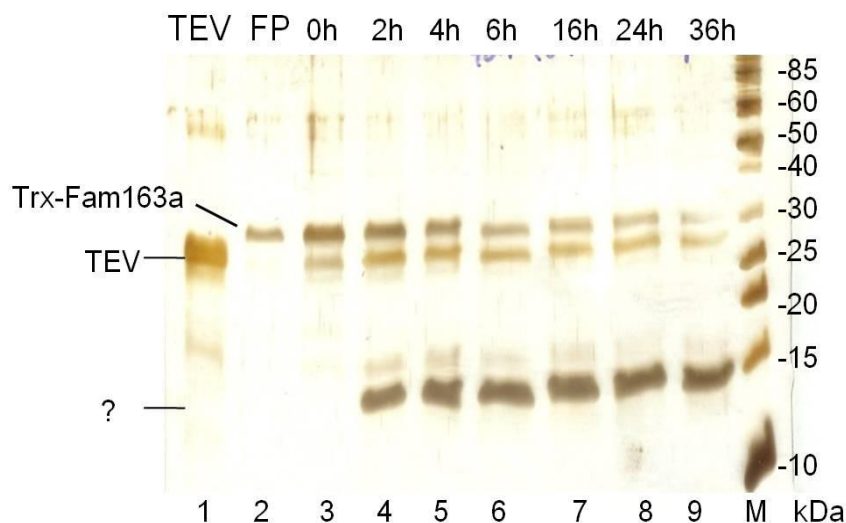


Fig. 3.22 Time course of Trx-Fam163a cleavage with *AcTEVTM*-protease at 4 °C with GSH/GSSG in ratio of 5:1 presented using 12% SDS-PAGE with silver staining. Lane 1, *AcTEVTM*-protease; lane 2, purified Trx-Fam163a; lane 3, 3-fold concentrated fusion protein; lanes 4-9, the samples 2, 4, 6, 16, 24 and 36 h after addition of *AcTEVTM*-protease. FP, fusion protein; M, protein marker (Fermentas SM0661).

Fig. 3.22 shows the result of Trx-Fam163a cleavage at 4°C for 36 h in buffer with GSH/GSSG in the ratio of 5:1 detected by SDS-PAGE with silver staining. The TEV-protease and concentrated fusion protein were located in lanes 1 and 2 with 27 and 30 kDa, respectively. It could be observed that, the concentration of fusion protein and TEV decreased over the course of time. Already after 2 h incubation of *AcTEVTM*-protease and fusion protein a single new band at about 15 kDa was detected and in the following 34 h its intensity seemed to increase very slowly. The released Fam163a without signal sequence has an expected size of 14.8 kDa which is comparable to its fusion partner Trx of 14.5 kDa. So the single band was assumed to be composed of the overlapping two proteins which was further identified by mass spectrometry (MS) described below.

Moreover, in the first 4 h an unknown protein detected at about 17 kDa had been noticeable which has been identified by WB as cleavage product of Trx-Fam163a with 6×his tag (data not shown). It seemed that, this 17 kDa protein came from nonspecific Trx-Fam163a cleavage and

3 Experiments

it was further digested into Trx and a smaller fragment, because it disappeared toward the end of protease assay. Additionally, the band intensity of this 17 kDa protein changed in the presence of different ratios of GSH/GSSG. For example, this protein was found in the least amount when cleavage was performed at 4 °C for 4 h in buffer with GSH/GSSG 2:1 (data not shown).

The degree of cleavage was temperature dependent and an acceleration of cleavage at 15 °C and 30 °C was also observed. In the concentrate (lane 3) the protein with an identical size to TEV-protease was a degradation product of fusion protein and its possible cleavage product with expected size at about 12 kDa was not detected at 4 °C but identified at 15 °C or 30 °C during the tested time (data not shown).

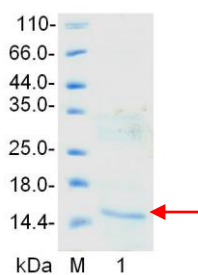
Identification of Fam163a via mass spectrometry

The identification of the band at about 15 kDa via MS was kindly supported by Mr. Manfred Nimtz (Helmholtz-Center for Infection Research, Braunschweig). The proteins were cleaved with trypsin and the generated peptides were investigated by determination of their molecular masses. The experimentally obtained masses were compared with theoretical peptide masses of proteins stored in databases using the peptide mass fingerprint search program Mascot.

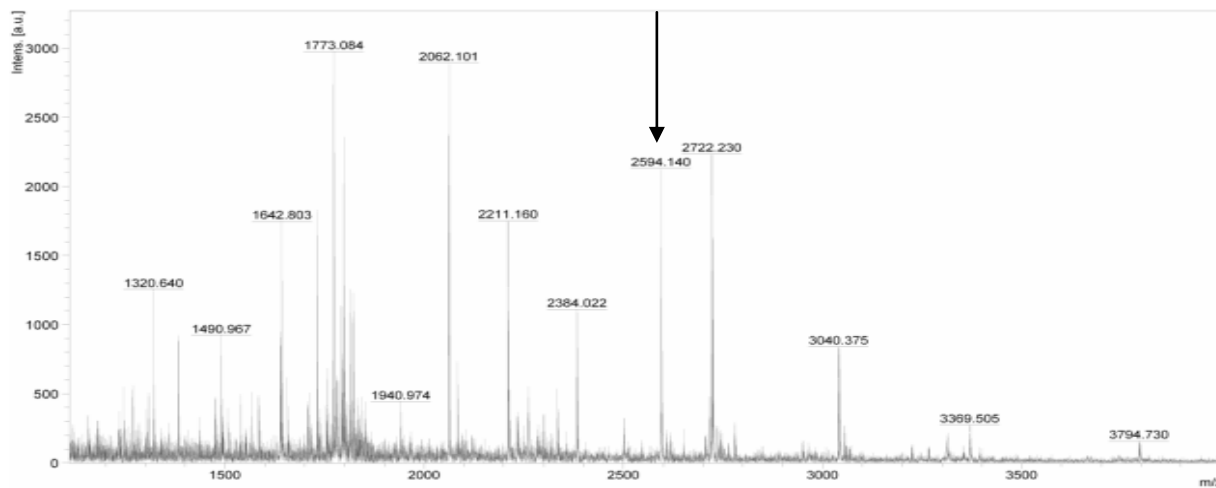
The cleavage products of Trx-Fam163a were analyzed by SDS-PAGE with blue silver staining as shown in Fig. 3.23.A and the corresponding spectrum of the band at 15 kDa derived from gel is shown in Fig. 3.23.B. The peptides of Trx and Fam163a were detected. The mass peaks at 1490.97 and 2062.10 matched Trx while mass peaks at 1642.79, 2594.13, 3040.36 and 2722.22 matched the component of Fam163a. And the Mascot analysis of spectrum showed the similarity with Trx from *E. coli* (score 76) and Fam163a (score 58). The non-specific mass peaks (for example, at 1773.08) may correspond to contaminants, like keratin or autolysis products of trypsin. The sequence of peptide matching mass peak at 2594.13 was further analyzed by tandem mass spectrometry (MS/MS) as shown in Fig. 3.23.C. and this method provided a high level of confidence of identification of Fam163a with increased the score of 150 by Mascot.

3 Experiments

A.



B.



C.

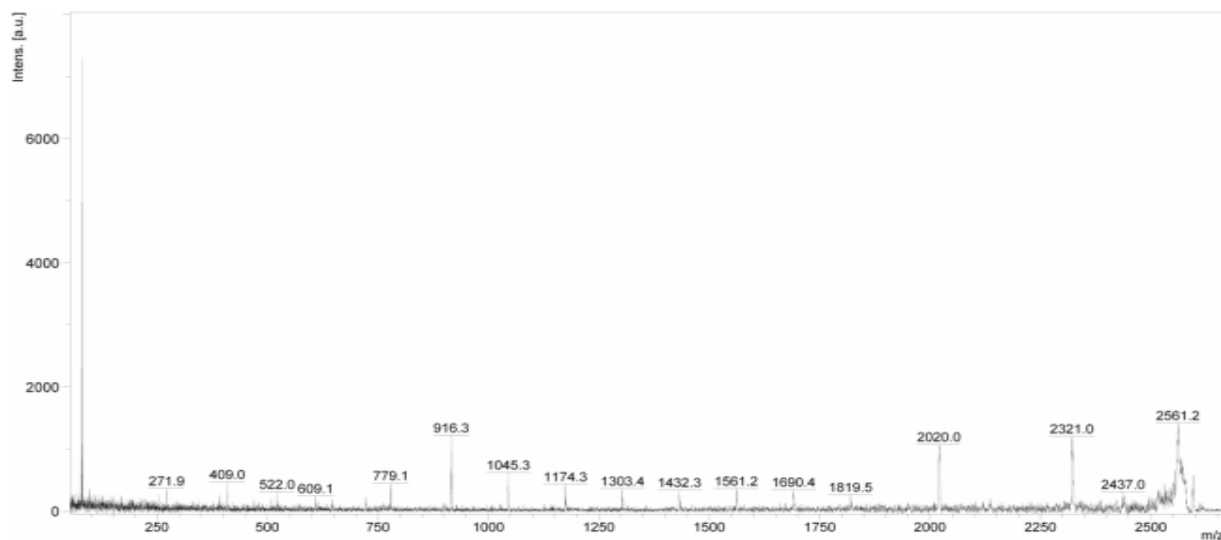


Fig. 3.23 Identification of the 15 kDa band derived from gel by MS and MS/MS data analysis. A. Cleavage products of Trx-Fam163a presented using 15% SDS-PAGE with blue silver staining. The red arrow indicated protein band was selected for MS. M, protein marker (Thermo, 26610). B. The corresponding spectrum of the protein band at 15 kDa. C. The corresponding MS/MS spectrum of peptide matching peak masse at 2594.13 shown in B. The intensity (a u) and the mass-to-charge values (m/z) are shown.

3 Experiments

3.2.3.4 Purification of Fam163a

3.2.3.4.1 Immobilized metal ion affinity chromatography

Subsequently, the released Fam163a must be separated from the protein mixture containing also incompletely digested fusion protein, TEV-protease and the released Trx. Fam163a without his tag was expected to be detected in flow through by passing second IMAC. The isolation of Fam163a in analytical scale was performed via Vivaspure *MCMini* and used buffers for binding, wash and elution remained the same as described in 3.2.3.2.1.

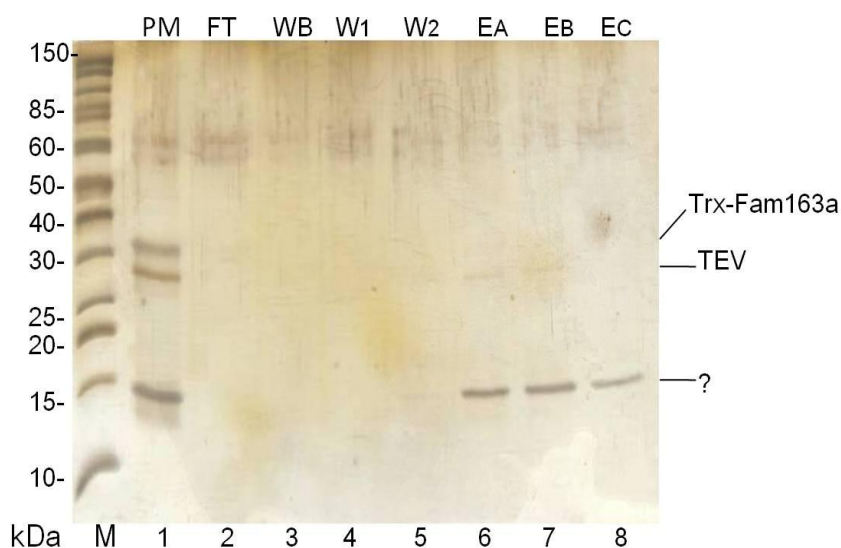


Fig. 2.24 Purification of Fam163a from Trx-Fam163a cleavage products via Vivaspure *MCMini* presented using 12% SDS-PAGE with silver staining. The protein mixture after cleavage of fusion protein at 15 °C for 8 h ((lane 1), the fractions from following steps of IMAC (lanes 2-8) are shown. PM: protein mixture after cleavage of Trx-Fam163a; FT, fraction of flow through; WB, wash fraction with binding buffer; W1, wash fraction with wash buffer 1; W2, wash fraction with wash buffer 2; EA, first elution fraction; EB, second elution fraction; EC: third elution fraction; M, protein marker (Fermentas SM0661).

The result of the purification as shown in Fig. 2.24 was different to expectations. No protein was detected in the flow though. Elution with 250 mM imidazole was repeated three times and the incompletely digested fusion protein and TEV-protease were detected mainly in the first elution fraction and the protein bands at about 15 kDa were found in all three elution fractions.

3 Experiments

The reason for the absence of Fam163a in the flow through was investigated. It is reported that naturally occurring proteins, which are rich in histidine, aspartic acid or glutamic acid, exhibit high affinity to IMAC resins like his-tagged proteins (132). According to this statement, Fam163a containing 8 glutamic acids at N-terminus in a series was assumed to bind IMAC ligand and subsequently eluted along with other his-tagged proteins.

In addition, purification of Fam163a using stepwise elution was also performed and the bound proteins were eluted stepwise with 100, 150, 200 and 250 mM imidazole. Fam163a was expected to be separated from other his-tagged proteins using different imidazole concentrations. The protocol and results of purification are presented in Appendix 5.5.5. Subsequently, the first fractions for each imidazole concentration were concentrated using trichloroacetic acid (TCA) precipitation (see Appendix 5.5.13) and loaded on the gel using blue silver staining and the bands at 15 kDa derived from gel were analyzed via MS. However, the identities of the three bands were confirmed as Trx (data not shown).

3.2.3.4.2 Immunoprecipitation

Immunoprecipitation is a useful method for isolating protein of interest from cellular extracts using specific antibodies. In the present work, purification of released Fam163a using immunoprecipitation was attempted. It is theoretically possible to pull the his-tagged members out of Trx-Fam163a cleavage products mixture with an anti-his antibody and Fam163a as the single protein without 6×his tag remains in the flow through.

The purification of Fam163a was performed using anti-his tag beads with a spin column provided in commercial *His tagged Protein PURIFICATION KIT*. The cleavage products of Trx-Fam163a were incubated with the anti-his tag beads overnight at 4 °C. After centrifuging the flow through (supernatant) was retained. The elution of his-tagged proteins from the beads for control was achieved by addition of a competitive 6×his peptide. The protocol is seen in Appendix 5.5.12.1 and the result of purification is shown in Fig. 3.25.

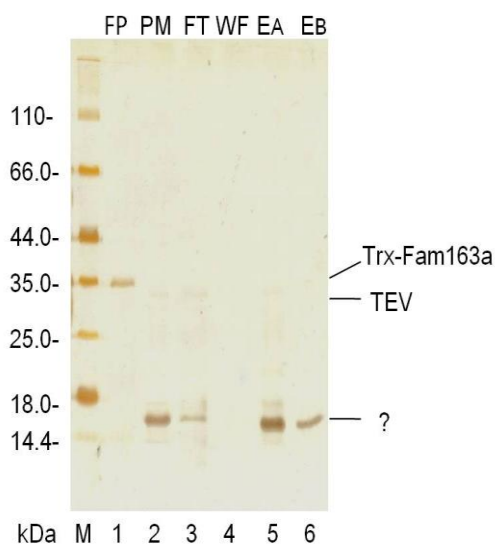


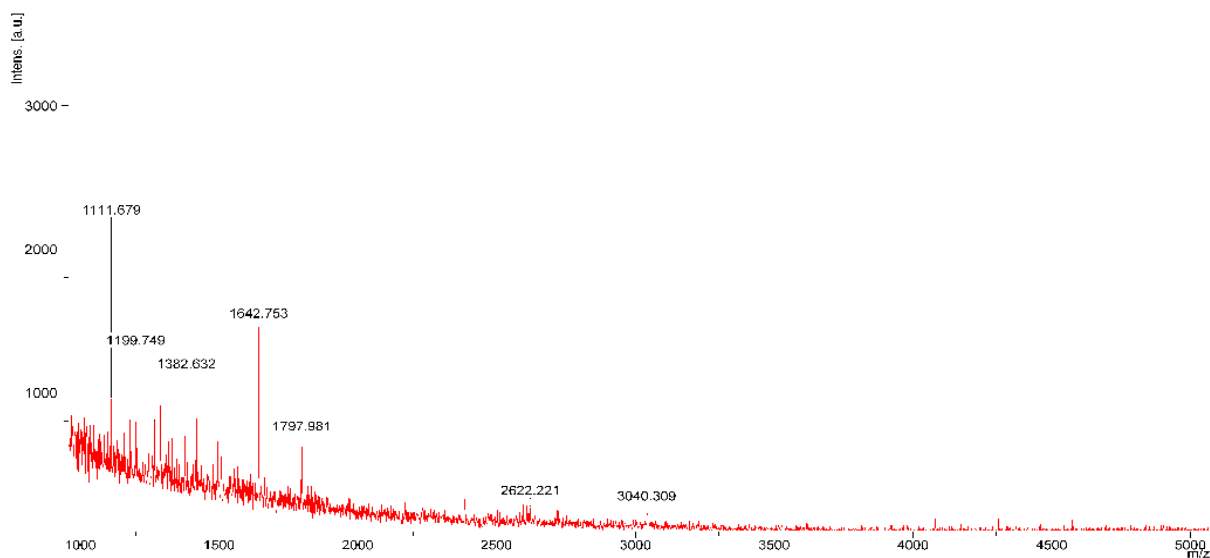
Fig. 3.25 Isolation of Fam163a from Trx-Fam163a cleavage products using anti-his tag beads presented using 12% SDS-PAGE with silver staining. The purified Trx-Fam163a (lane 1), Trx-Fam163a after cleavage at 4°C for 36 h (lane 2) and the fractions from following steps of immunoprecipitation (lanes 3-6) are shown. FP, fusion protein; FT, flow through; WF: wash fraction; EA: first elution fraction; EB: second elution fraction; M, protein marker (Thermo, 26610).

The cleavage products of Trx-Fam163a were present in lane 2, where the fusion protein was so completely digested that Trx-Fam163a did not leave any trace behind and only the thick band at about 15 kDa and weak band at 27 kDa matching TEV-protease were detected. This 15 kDa band was also detected in fractions of flow through and elution respectively, but the band intensity in elution was much more than in flow through.

The bands at 15 kDa detected in flow through and elution fraction were analyzed by MS and the corresponding spectrums are shown in Fig. 3.26. The protein in the elution fraction was identified as Trx while in the flow through fraction the identity of Fam163a was confirmed. Subsequently, the MS/MS analysis of the peptides 1001.64 and 1642.74 indicated their extensive homology of Trx (Mascot score 37) and Fam163a (Mascot score 53), respectively (data not shown).

3 Experiments

A.



B.

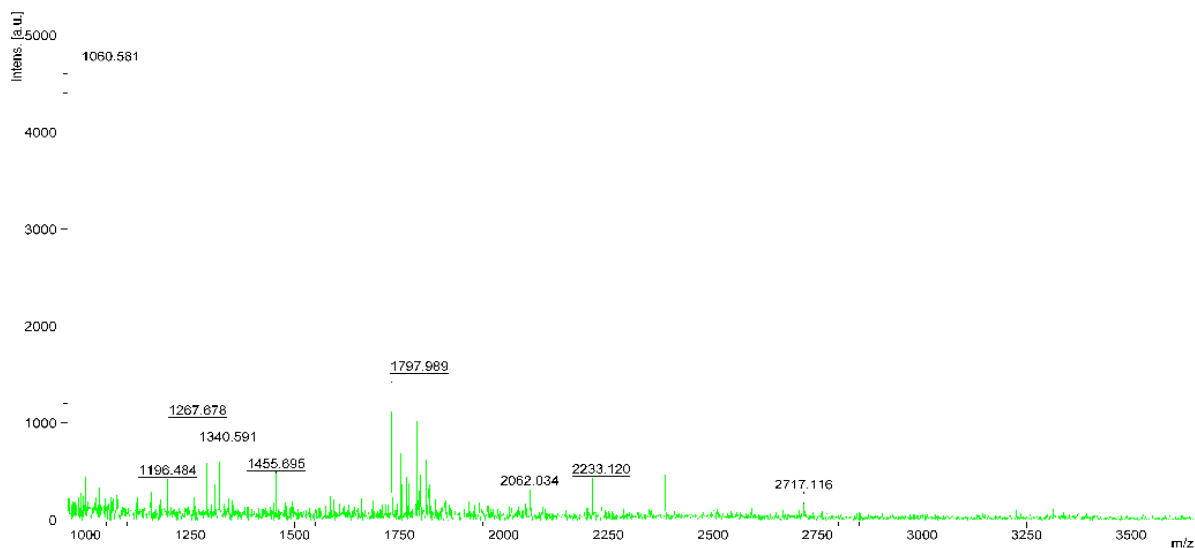


Fig. 3.26 Identification of the 15 kDa band derived from gel by MS data analysis. A. The corresponding spectrum of the protein band from the flow through; B. Spectrum of the protein band from first elution fraction. The intensity (a u) and the mass-to-charge values (m/z) are shown.

Additionally, using the immunoprecipitation complex with anti-his antibody solution and protein G sepharose beads was employed for Fam163a purification. The complex was further incubated with digested products of Trx-Fam163a. The expectation was that, the his-tagged proteins would bind the antibody and also pelleted and subsequently eluted by the addition of

3 Experiments

the elution buffer whereas Fam163a would be detected in the flow through or wash fraction. Contrary to expectations, this method resulted in the unsuccessful separation of Fam163a from other his-tagged proteins. The protocol and result are seen in Appendix 5.5.6.1. The binding capacity of protein G to the antibody differed from product instructions described and an increase of protein G employed did not improve the result (data not shown).

3.2.3.5 Test of biological activity

In this study, the bioactivity of purified Fam163a and Trx-Fam163a were tested via scratch assay. The work was done cooperatively with Dr. Marc Reboll (Department of Cardiology and Angiology, Hanover Medical School). Scratch assay is an easy and well-developed method to measure cell migration *in vitro*. The basic steps involve creating a scratch in a cell monolayer and capturing the images at the beginning and at regular intervals during cell migration to close the scratch (133). The migration of cells toward the wounds is expressed as percentage of wound closure:

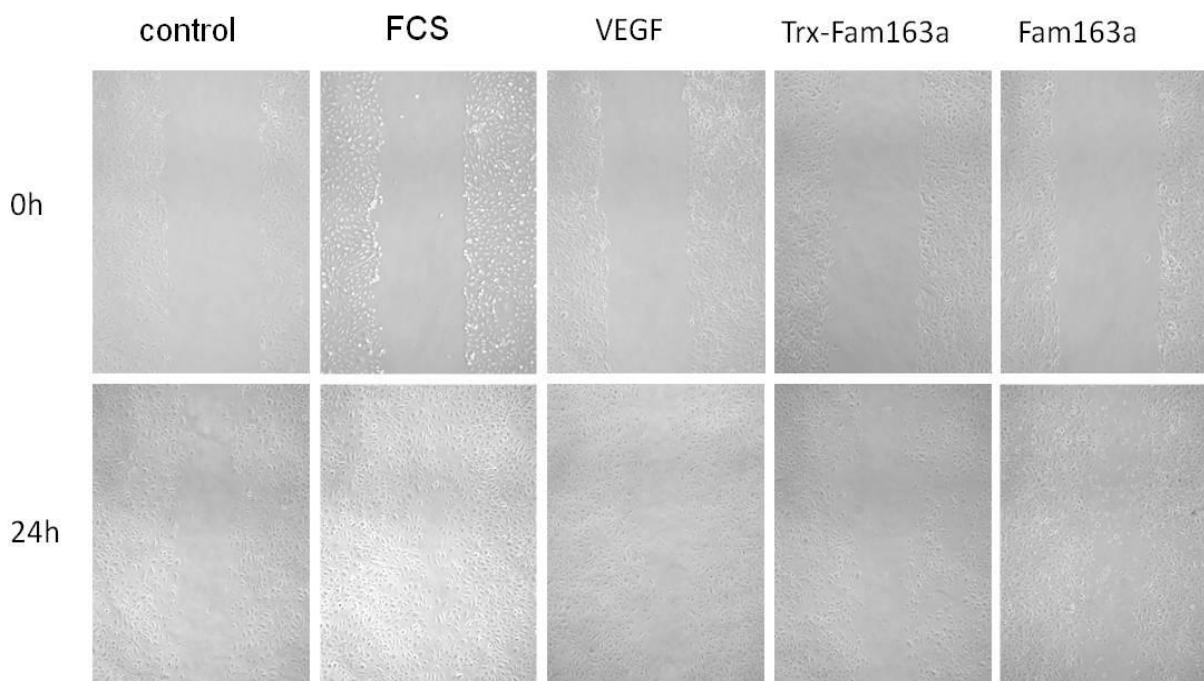
$$(\%) \text{ of wound closure} = [(A_{t=0h} - A_{t=\Delta h}) / A_{t=0h}] \times 100 (\%),$$

where $A_{t=0h}$ is the area of wound measured immediately after scratching and $A_{t=\Delta h}$ is the area of wound measured at interval (134).

The monolayer of HCAEC was removed with pipette tips and the recovery of denuded area monolayer due to cell migration stimulated by purified Trx-Fam163a and Fam163a was observed separately at 0 h and 24 h. The cells without any stimulation were used as negative control and the cells growing in full medium with 15% foetal calf serum (FCS) and simulated with VEGF were used as positive controls. The photomicrographs of wounded HCAEC at 0 h and 24 h are presented in Fig. 3.27.A.

3 Experiments

A.



B.

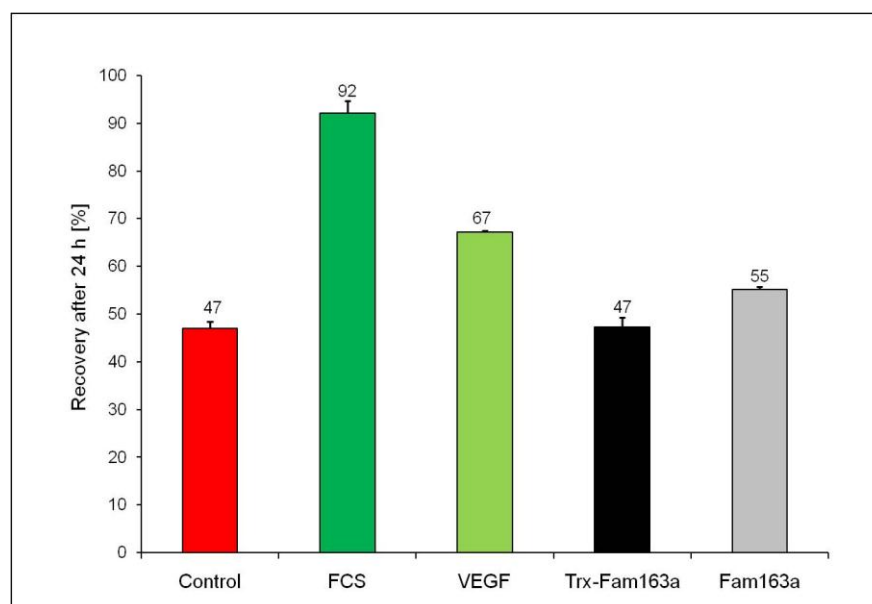


Fig. 3.27 Comparative efficacy of purified Fam163a, Trx-Fam163a and VEGF (each with 100 ng/mL) in scratch assay. A. Photomicrographs of wounded HCAEC before and after 24 h treatment with VEGF and purified Fam163a, Trx-Fam163a or grew in 15% FCS. The cells without any cytokine treatment were used as negative control. B. The effects of different samples on HCAEC migration were potted as a percentage of wound closure.

3 Experiments

The effects of different samples on HCAEC migration are recorded as a percentage of wound closure which is shown in Fig. 3.27.B. After 24 h incubation, the cells in full medium and stimulated by VEGF migrated toward the scratch with recovery of 92% and 67%, respectively. Compared with the two positive controls, the cells stimulated by purified Fam163a migrated slower to close the scratch with recovery of 55%. But the recovery stimulated by Trx-Fam163a was the same as the negative control with 47%, indicating less or no bioactivity of the fusion protein.

Positive stimulation of proliferation by Trx-Fam163a had been observed previously (data not shown). However, Fam163a with and without Trx fusion demonstrated different stimulation effects in the scratch assay. It possibly indicates there was a difference in folding between the fusion protein and that cleaved from Trx. The test of angiogenic activities of Fam163a with respect to other aspects will be performed later and so the results are still expected.

3.2.3.6 Summary

In the present work, a process of production and purification of Fam163a was developed and the flow chart is presented in Fig. 3.28. The production of soluble Fam163a in *E. coli* BL21(DE3) was achieved and the formation of inclusion bodies had been prevented by the production of a fusion protein with the solubility tag Trx. The overexpression of Trx-Fam163a was detected at 37 °C and 26 °C in LB medium.

The stability of Trx-Fam163a produced in the soluble fraction of cell lysate was investigated and the degradation of Trx-Fam163a was observed when the soluble cell lysate was incubated at different temperatures (4 °C, 18 °C and 37 °C) for 3 days. At 4 °C Trx-Fam163a was gradually degraded, while at 37 °C the degradation was very fast. Moreover, it was found that the fusion protein was degraded immediately as it was expressed, even 3 h after IPTG induction. Fam163a was degraded by a proteolytic cleavage into several smaller fragments which were detected by anti-his antibody. Purified Trx-Fam163a was incubated for comparison but no degradation was observed. Therefore, it was believed that the bacterial proteases were involved in the degradation of Trx-Fam163a. The three tested inhibitors had no effect on the degradation of

fusion protein.

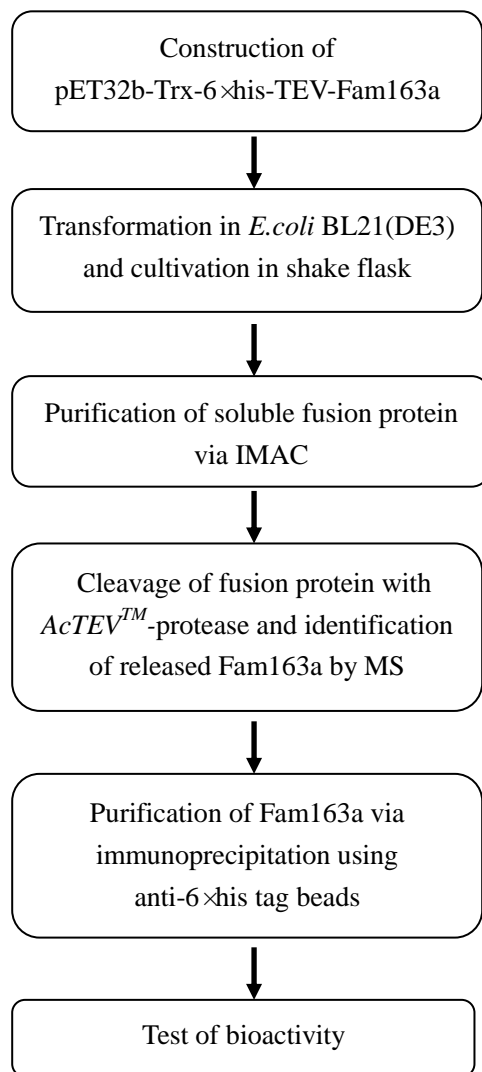


Fig. 3.28 The flow chart of Fam163a production process.

The fusion protein was purified via IMAC. Following this, the Trx-Fam163a elution fractions free of degradation products were pooled for further cleavage and this led to a large loss of fusion protein. After removal of imidazole in the protein solution, Trx-Fam163a was digested with TEV-protease and the released Fam163a and Trx were detected as overlapping bands at about 15 kDa whose identities were confirmed by MS.

Contrary to expectations, Fam163a could not be purified from the protein mixture after cleavage via second IMAC and detected as the single protein in flow through, probably due to

3 Experiments

eight glutamic acids at the N-terminal which showed the same affinity to bind to the column of IMAC. Additionally, the stepwise elution with imidazole did not help to separate Fam163a from Trx.

Subsequently, the isolation of Fam163a at analytical scale was successfully done by immunoprecipitation with anti-his tag beads where Fam163a was detected in flow through with extensive homology confirmed by MS, while immunoprecipitation using protein G and anti-6xhis antibody solution did not work. Finally, based on the result of the scratch assay the purified Fam163a was confirmed to be biologically active.

3.2.4 Production of murine hematopoietic signal peptide-containing secreted 1

3.2.4.1 Expression of Trx-mHSS1

After the plasmid pET32b-Trx-6×his-TEV-mHSS1 was transformed in *E. coli* BL(DE3), the cultivation of the recombinant *E. coli* was performed separately in LB medium at 18 °C, 26 °C and 37 °C. The expression of fusion protein was induced by the addition of 0.25 mM IPTG. Moreover, instead of IPTG induction Trx-mHSS1 synthesis in *E. coli* was also attempted using autoinduction medium, which has been reported to significantly improve the cell density and solubility of expressed Auto27-243-GST compared with cultures in LB medium (135). The carbon substrate consists of glucose, glycerol and lactose in the simple-to-prepare defined autoinduction broth (S-DAB) medium and expression of the T7 polymerase is automatically induced in late log-phase growth due to the depletion of carbon sources other than lactose (136). Finally, the production of Trx-mHSS1 using the two methods was compared with each other.

3.2.4.1.1 IPTG-induction

Cultivation in LB medium at 26 °C

At first, Trx-mHSS1 was produced in LB medium at 26 °C. The cells were collected at 1, 3, 5, 7 and 9 h after IPTG induction and disrupted by sonication. The production of soluble and insoluble Trx-Fam163a was analyzed by SDS-PAGE and the result is shown in Fig.3.29.

3 Experiments

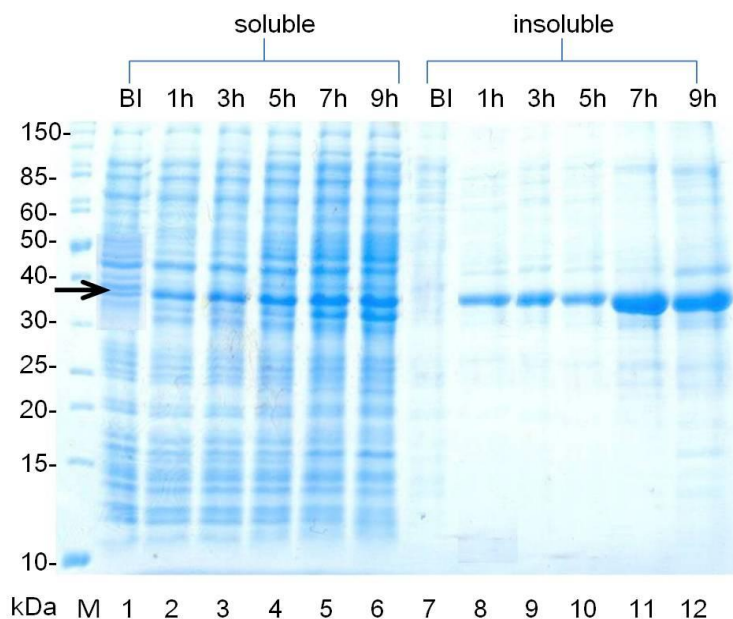


Fig. 3.29 Time course of Trx-mHSS1 production in LB medium at 26 °C and presented using 12% SDS-PAGE with blue silver staining. The soluble (lane 1) and insoluble (lane 7) fractions before induction; soluble (lanes 2-6) and insoluble fractions (lanes 8-12) 1, 3, 5, 7 and 9 h after induction, respectively. The black arrow indicates Trx-mHSS1. BI, before induction; M, protein marker (Fermentas SM0661).

After just 1 h after induction by IPTG, in both soluble and insoluble fractions of cell lysate a band was visualized at about 40 kDa which was homologous with the expected size of expressed Trx-mHSS1. There was an increase in yield of protein in soluble and insoluble fractions up until 7 h. Further induction for 2 h resulted in concentration decrease of this protein in insoluble fraction only, while it remained constant in the soluble fraction.

Subsequently, it was necessary to identify the expressed fusion protein in the soluble and also insoluble the fractions of cell lysate by WB. The used antibodies were the same as identification of Trx-Fam163a degradation products described in 3.2.3.2.2 and results of SDS-PAGE and WB are shown in Fig. 3.30.

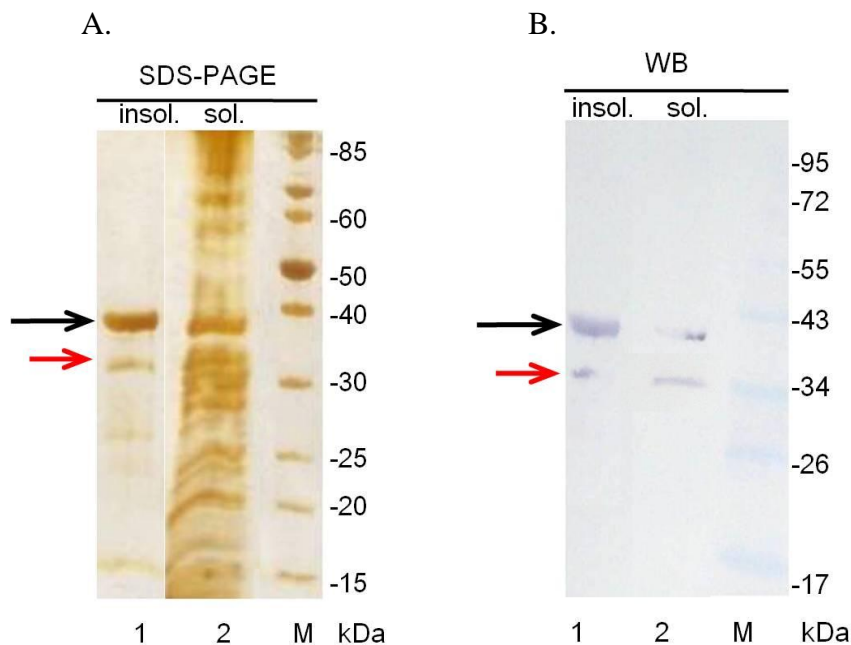


Fig. 3.30 Identification of Trx-mHSS1. A. SDS-PAGE analysis (12% with silver staining) of diluted soluble and insoluble cell lysate 7 h after induction at 26 °C. B. WB of fractions in A with anti-his antibody. The black and red arrows indicate Trx-mHSS1 and protein at 32 kDa, respectively. Sol., soluble cell lysate; insol., insoluble cell lysate; M (A), protein marker (Fermentas SM0661); M (B), protein marker (Fermentas SM0671).

The proteins with anti-his antibody detected in both soluble and insoluble fractions of cell lysate migrated separately as bands of about 39.5 and 32 kDa. The first one matched the theoretical mass of expressed Trx-mHSS1. Based on Fig. 3.29, the protein at 32 kDa was produced only after induction and it was thought to be a degraded fragment of Trx-mHSS1.

Cultivation at 18 °C and 37 °C

The production of Trx-mHSS1 in LB-medium was performed at 18°C and 37°C and the SDS-PAGE analysis of optimal soluble Trx-HSS1 expression at both temperatures (18°C for 16 h, 37°C for 4 h) is shown in Fig. 3.31.

3 Experiments

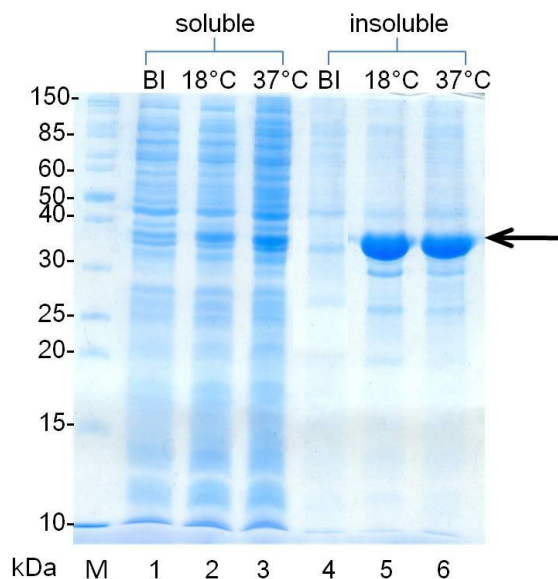


Fig. 3.31 Production of Trx-mHSS1 in LB medium at 18 °C and at 37 °C presented using 12% SDS-PAGE with blue silver staining. The soluble (lane 1) and insoluble (lane 4) fractions before induction; soluble (lane 2) and insoluble (lane 5) fractions after 16 h induction at 18 °C; soluble (lane 3) and insoluble (lane 6) fractions after 4 h induction at 37 °C. The black arrow indicates Trx-mHSS1. BI, before induction; M, protein marker (Fermentas SM0661).

Unlike the expression at 26 °C, the production of Trx-mHSS1 at 18 °C was seen only in the insoluble fraction until 4 h after induction with IPTG (data not shown). Induction at 18 °C for long time had only a slight effect on the solubility of Trx-mHSS1 and even after 16 h only a faint band of fusion protein could be detected in the soluble fraction. By contrast, the synthesis of soluble and insoluble Trx- mHSS1 at 37 °C began 2 h after IPTG induction and after 4 h a reduction of band intensity of expressed soluble Trx-mHSS1 could be observed (gels not shown). At this time, the concentration of produced soluble Trx-mHSS1 was higher than that produced at 18 °C for 16 h.

In conclusion, the production of soluble Trx-mHSS1 could be detected both at 26°C and 37°C. Contrary to expectations, production at a lower temperature (18°C) did not help to improve the solubility of expressed Trx-mHSS1. To achieve more soluble expressed target protein, 26°C was considered as the most suitable cultivation temperature.

3.2.4.1.2 Autoinduction

The defined non-inducing broth (DNB) as preculture of recombinant *E. coli* containing Trx-mHSS1 was used to inoculate the main culture S-DAB medium giving a starting OD₆₀₀ of 0.02. Then the cultivation using autoinduction medium was carried out at 26°C. The cells were collected at 0, 9, 13, 17, 21 and 24 h and disrupted by sonication. Fig. 3.31 shows the time course of soluble Trx-mHSS1 production in S-DAB medium.

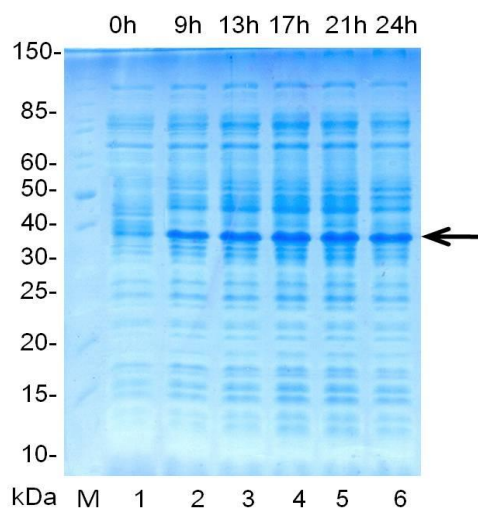


Fig. 3.31 Time course of Trx-mHSS1 production in soluble fractions of cell lysate in S-DAB medium at 26 °C presented using 12% SDS-PAGE with blue silver staining. The soluble fractions after 0, 9, 13, 17, 21 and 24 h cultivation of main culture are shown. The arrow indicates Trx-mHSS1. M, protein marker (Fermentas SM0661).

The slow increase in soluble Trx-mHSS1 synthesis could be detected at 17 h, after which a reduction of fusion protein was observed. Moreover, compared to cultivation in LB medium at the same temperature no significant degradation product of Trx-mHSS1 at 32 kDa was detected.

Comparing production of soluble Trx-mHSS1 in LB-and S-DAB media

The production of soluble Trx-mHSS1 was performed separately in LB- and S-DAB media at 26 °C for 24 h. The OD₆₀₀ during the 24 h of both cultures were recorded and the growth curves are presented in Fig. 3.32.

3 Experiments

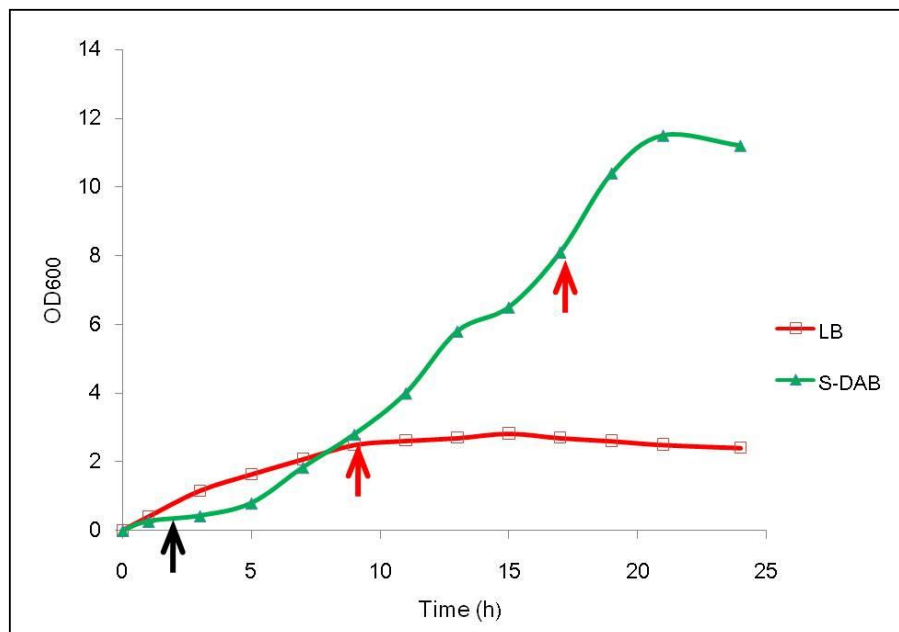


Fig. 3.32 Growth curves of *E. coli* in LB- and S-DAB media at 26 °C for 24 h. The red arrows indicate the optimal harvest times, respectively. The black arrow indicates the time for IPTG induction.

After 9 h (7 h after IPTG induction) the growth rate of *E. coli* in LB medium seemed slow and the OD₆₀₀ remained stable. Compared to the LB medium, the *E. coli* cells grew slowly in S-DAB medium in the first 8 h and OD₆₀₀ increased gradually up to 11.2 over 24 h. 17 h in S-DAB medium and 7 h after IPTG induction in LB medium, where the expressed soluble Trx-mHSS1 accounted for the largest share of total soluble proteins, were considered the optimal harvest times. At these time points, OD₆₀₀ in S-DAB medium reached 7.9 corresponding to 2.92 g/L dry cell mass (DCM), which was much higher than in LB medium with 2.5 and 0.93 g/L DCM.

Moreover, the concentration of total proteins in the soluble cell lysate was measured by Bradford assay and the calculation of soluble Trx-mHSS1 concentration was performed using band densitometric analysis. Table. 3.1 shows an overview of soluble Trx-mHSS1 production in LB-and in S-DAB media at 26 °C for 24 h.

3 Experiments

Table. 3.1 Overview of soluble Trx-mHSS1 production in LB-and in S-DAB media at 26 °C for 24 h.

	LB	S-DAB
Optimal harvest time (h)	9 (7 after induction)	17
OD ₆₀₀ at optimal harvest time	2.5	7.9
DCM (g L ⁻¹)*	0.93	2.92
Concentration of total soluble protein (mg L ⁻¹)	93	243
Concentration of soluble Trx-mHSS1 (mg L ⁻¹)	29.8	82.3
Soluble Trx-mHSS1 in relation to total soluble protein (%)	32	34
Soluble Trx-mHSS1 in relation to DCM (mg g ⁻¹)	32.1	28.2

*calculation according to statement in (135)

The share of soluble Trx-mHSS1 in the total soluble protein from LB-medium and S-DAB medium was comparable, with 32% and 34% respectively. But the proportion of fusion protein amount and dry cell mass for LB-medium with 32.1 mg g⁻¹ was higher than for S-DAB medium with 28.2 mg g⁻¹. So in the following experiments all the samples arose from cultivation in LB medium at 26 °C.

3.2.4.2 Purification of Trx-mHSS1

3.2.4.2.1 Purification of soluble Trx-mHSS1

The purification of soluble Trx-mHSS1 at analytical scale was previously performed via Vivawell 8-*Strips* with membrane adsorber as the matrix. The membranes were preloaded with four metal ions (Co²⁺, Cu²⁺, Ni²⁺ and Zn²⁺), respectively. After loading the same amount of soluble fraction of cell lysate by centrifugation, the non-bound proteins could be detected in flow through. Co²⁺ showed the strongest binding affinity for the protein of interest compared to the other three metal ions. Additionally, binding buffers of different pH were optimized and a buffer with pH 6.5 had been determined as the most suitable parameter (data not shown).

3 Experiments

Subsequently, the membrane was washed with two wash buffers to remove non-tagged proteins. Finally, the elution of Trx-mHSS1 was done twice with 250 mM imidazole in binding buffer. The protocol is seen in Appendix 5.5.6.

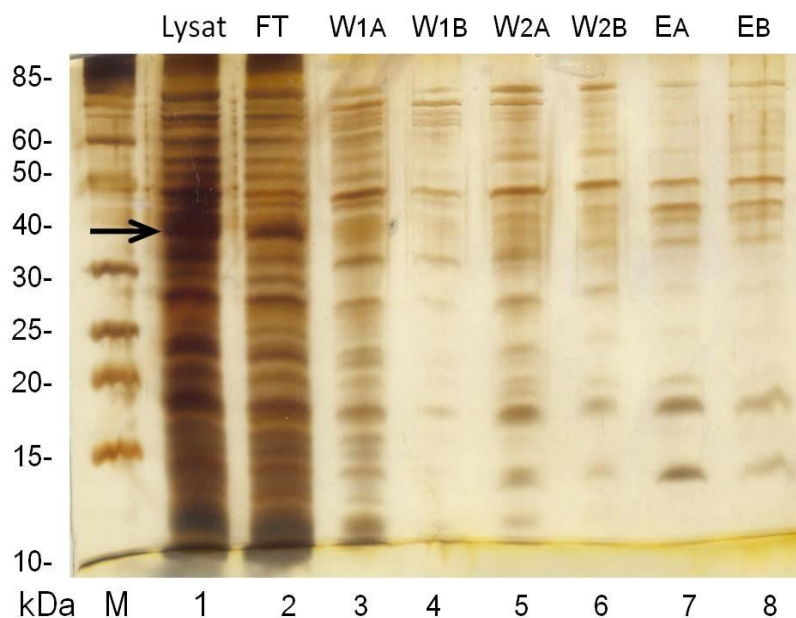


Fig. 3.33 Purification of Trx-mHSS1 from the soluble fraction of cell lysate via Vivawell 8-Strips presented using 12% SDS-PAGE with silver staining. The soluble cell lysate (lane 1) and the fractions from following IMAC steps (anes 2-8) are shown. Lysat: soluble cell lysate before purification; FT, fraction of flow through; W1A, first wash fraction with wash buffer 1; W1B, second wash fraction with wash buffer 1; W2A, first wash fraction with wash buffer 2; W2B, second wash fraction with wash buffer 2; EA, first elution fraction; EB, second elution fraction; M, protein marker (Fermentas SM0661).

Fig. 3.33 shows the result of soluble Trx-mHSS1 purification. Although Co^{2+} and the binding buffer with pH 6.5 were employed for protein binding, more than 80% of the soluble fusion protein was detected in the flow through. This indicated that the great part of soluble Trx-mHSS1 as initial material for purification was lost. It was assumed that, the location of 6×his in the middle of fusion protein was not easily accessible for binding the metal ion when Trx-mHSS1 is in its native form.

Moreover, only a little Trx-mHSS1 was eluted, along with proteins at 13, 17, 32 and 47 kDa. Based on the result of WB, these proteins except for at 32 kDa did not refer to degradation

3 Experiments

products of the fusion protein taking the 6×his tag, and that they might be binding nonspecifically to the membrane. In conclusion, due to low yield and poor purity further Trx-mHSS1 purification from soluble cell lysate was not continued.

3.2.4.2.2 Purification of Trx-mHSS1 from inclusion bodies

Since it seemed difficult to purify Trx-mHSS1 from soluble cell lysate, the alternative idea of Trx-mHSS1 isolation from inclusion bodies was developed. Quantification of Trx-mHSS1 concentration in inclusion bodies was carried out by densitometry and the insoluble Trx-mHSS1 was evaluated as 84% of the total fusion proteins and it could contain sufficient amounts of material for purification.

IMAC under denaturing conditions with subsequent refolding

At first, bioactive Trx-mHSS1 was expected to be achieved by purification from inclusion bodies under denaturing conditions and subsequent renaturation *in vitro*. The inclusion bodies of fusion protein were washed and solubilized previously. Then the protein sample was applied to the IDA-75 membrane connected to FPLC, preloaded with Co^{2+} and equilibrated with binding buffer. After the membrane adsorber was washed with buffer without NaCl and followed with buffer containing 300 mM NaCl, the bound protein was eluted with 250 mM imidazole. The FPLC protocol is described in Appendix 5.5.7.3 "Purification of Trx-mHSS1 under denaturing conditions". In Fig. 3.34 is presented the chromatogram of the purification and Fig. 3.35 shows the SDS-PAGE analysis with silver staining of the selected fractions.

3 Experiments

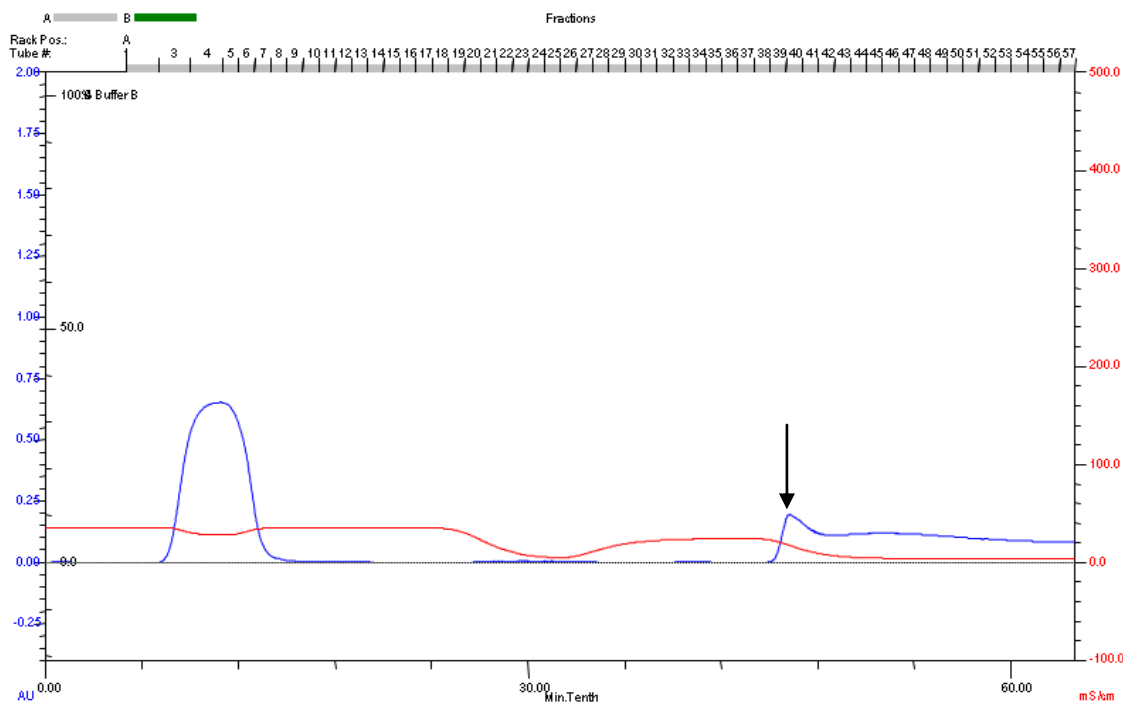


Fig. 3.34 Chromatogram of IMAC-purification of Trx-mHSS1 from solubilized inclusion bodies. The UV-absorption (AU) and conductivity (mS/cm^2) dependent on time are shown. The arrow indicates the elution peak of Trx-mHSS1.



Fig. 3.35 IMAC-purification of Trx-mHSS1 from solubilized inclusion bodies presented using 12% SDS-PAGE with silver staining. SI: solubilized inclusion bodies before purification; F, fraction; M, protein marker (Fermentas SM0661).

3 Experiments

It can be seen that, there was no Trx-mHSS1 detected in the flow through (Fr. 4) indicating good binding between solubilized Trx-mHSS1 and its ligand. The elution with 250 mM imidazole was successful. The degraded protein at 32 kDa was also present in the first three fractions of elution, but from Fr. 42 the protein seemed to be pure. After the eluted Trx-mHSS1 (Fr. 40-48) were collected, the concentration was determined and then adjusted to 100 $\mu\text{g/mL}$. Subsequently, they were refolded *in vitro* by dialysis against 50 mM Tris-HCl, pH 7.5 at 4 $^{\circ}\text{C}$ for 2 days. The buffer was refreshed at least two times.

Combination of refolding and IMAC

Alternatively, Trx-mHSS1 was also refolded *in vitro* on membrane absorbers combined with IMAC. The solubilized inclusion bodies were diluted 1:2 with binding buffer and the diluted protein solution was loaded onto the IDA-75 membrane equilibrated with binding buffer. After loading the sample, the membrane adsorber was washed with 40 mL refolding buffer containing 10 mM GSH, 1 mM GSSG and a descending gradient of urea at a flow rate of 0.5 mL min^{-1} . The target protein was finally eluted by refolding buffer containing 1 M urea and 250 mM imidazole which was subsequently removed by dialysis against 50 mM Tris-HCl, pH 7.5 at 4 $^{\circ}\text{C}$ for 8 h. The FPLC protocol is seen in Appendix 5.5.7.3 "Purification of Trx-mHSS1, combination of refolding and IMAC". The chromatogram of IMAC-purification combined with refolding is presented in Fig. 3.36 and Fig. 3.37 shows the SDS-PAGE analysis with silver staining of the chosen fractions.

3 Experiments

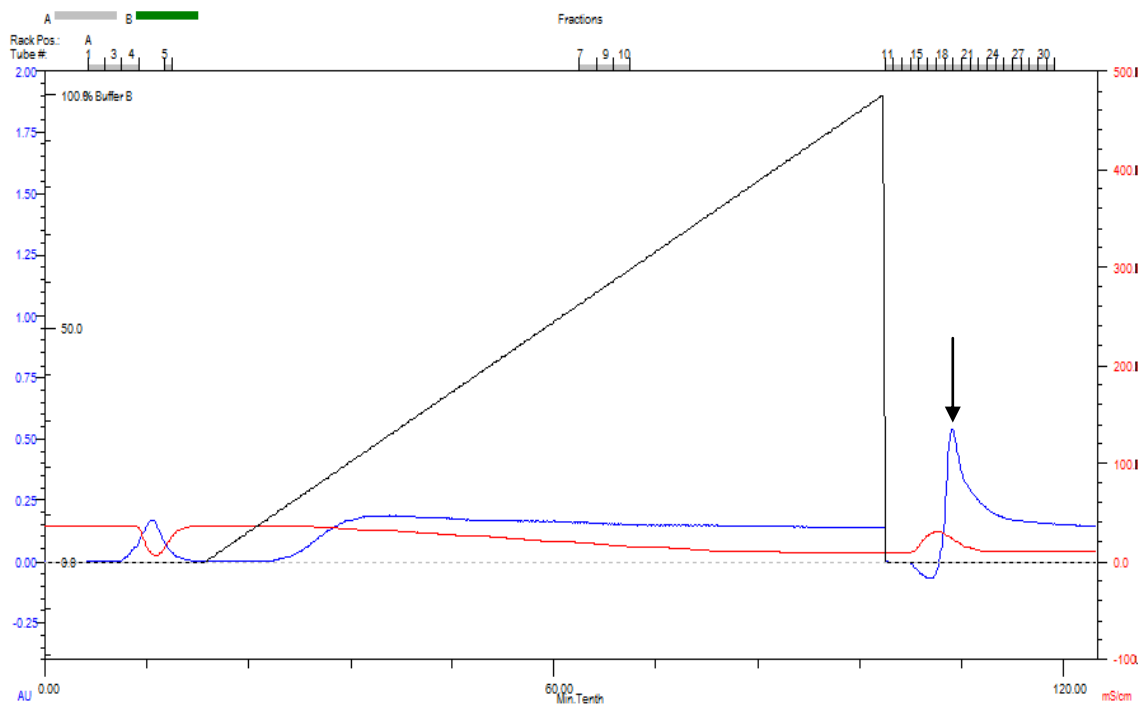


Fig. 3.36 Chromatogram of IMAC-purification and refolding of Trx-mHSS1 from solubilized inclusion bodies. The UV-absorption (AU) and conductivity (mS/cm^2) dependent on time were shown. The arrow indicates the elution peak of Trx-mHSS1 and the black line marks the refolding buffer gradient.

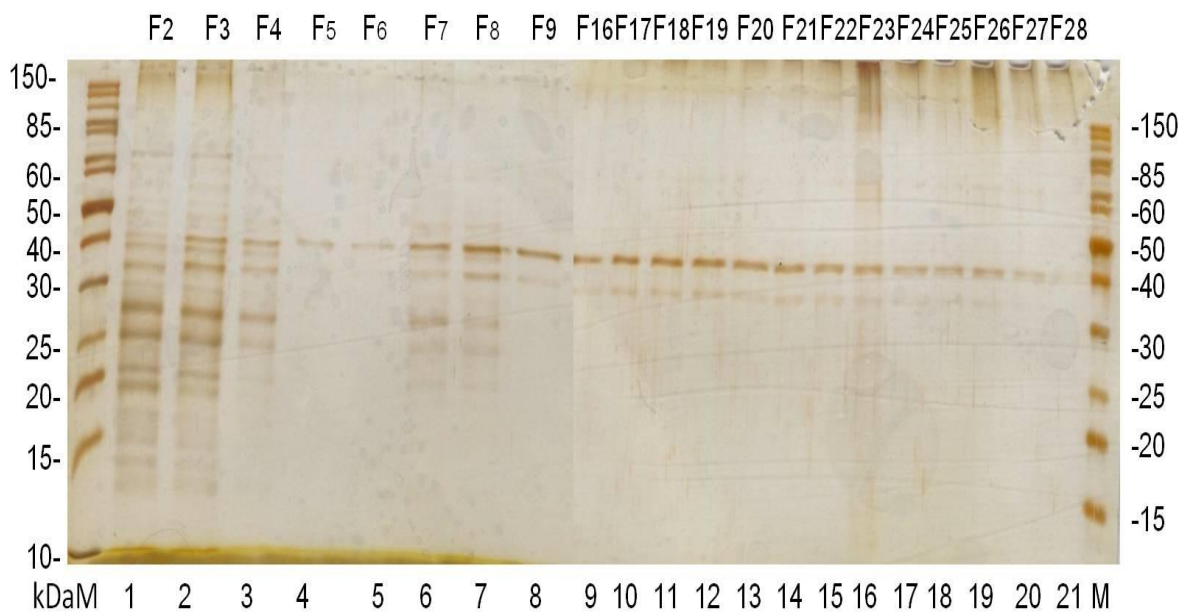


Fig. 3.37 Combination of Trx-mHSS1 refolding and IMAC-purification from solubilized inclusion bodies presented using 12% SDS-PAGE with silver staining. F, fraction; M, protein marker (Fermentas SM0661).

3 Experiments

The contaminating proteins such as at 25 and 28 kDa were washed away with refolding buffer but Trx-mHSS1 was also detected in the flow through fractions of refolding buffer (Fr. 7- 9). It was supposed that, these proteins were removed from the membrane absorber with GSH/GSSG. Trx-HSS1 could be seen in the peak of elution, together with its degraded fragment migrating at 32 kDa with low intensity.

However, the yield of Trx-mHSS1 refolding via IMAC depends on the initial protein concentration of loaded sample. In this study, protein samples with different initial concentrations were applied to purification to investigate the effect on renaturation of fusion protein. As shown in Fig. 3.38, the amount of pooled Trx-mHSS1 increased when initial protein concentration from was raised from 0-333 $\mu\text{g}/\text{mL}$ (loading volume always 3 mL and corresponding protein content 0-1 mg). When the protein concentration exceeded 333 $\mu\text{g}/\text{mL}$, a rapid reduction of eluted Trx-mHSS1 was observed. It seemed that, in the presence of denaturant the loaded denatured protein could absorb to the top of the membrane and there was a greater chance for denatured fusion protein to form aggregates. When the initial protein concentration was too high, the degree of aggregation would be increased greatly. So the solubilized inclusion bodies must be diluted to a lower concentration to give rise to properly refolded protein. On the other hand, the aggregation of unfolded Trx-mHSS1 or its folding intermediate was minimized when the denaturant urea was gradually removed from the membrane adsorber in the presence of glutathione redox components, which promotes correct formation of disulfide bonds.

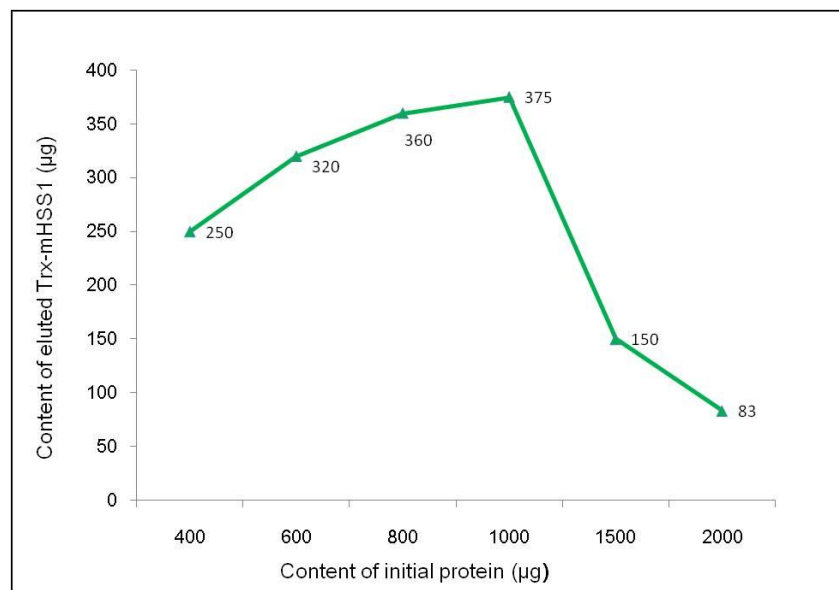


Fig. 3.38 Effects of initial protein content on eluted Trx-mHSS1 amount from membrane absorber IDA-75.

Comparing refolding pattern via dialysis and chromatography

When comparing refolding of Trx-mHSS1 via dialysis with via chromatography, the advantages were easily recognized. When the purification was combined with refolding, the whole process could be finished in a few hours and a large amount buffer for dialysis could be saved. However, the purification of Trx-mHSS1 with subsequent refolding by dialysis could be performed with a high initial concentration whereas refolding via chromatography must be done with only a low initial concentration. When the eluate was concentrated prior to cleavage, the protein at 32 kDa that also eluted was noticeable. This result prompted the use of renatured Trx-mHSS1 via dialysis for all subsequent work.

3.2.4.3 Cleavage of Trx-mHSS1

*AcTEV*TM-protease was employed for the cleavage of Trx-mHSS1 and the cleavage of fusion protein was performed at 10 °C for 16 h as shown in Fig. 3.39.A.

3 Experiments

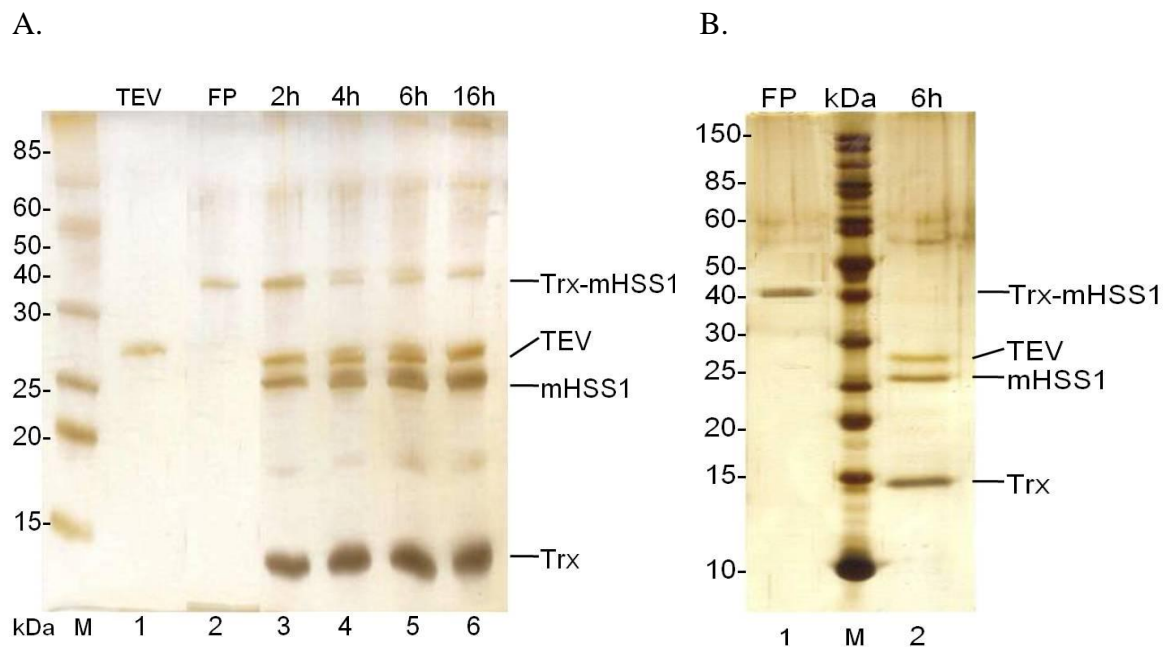


Fig. 3.39 A. Time course of Trx-mHSS1 cleavage with *AcTEVTM*-protease at 10 °C for 16 h presented using 12% SDS-PAGE with silver staining. Lane 1, *AcTEVTM*-protease; lane 2, purified Trx-mHSS1; lanes 3-6, the samples at 2, 4, 6 and 16 h after incubation of protease. B. Cleavage of Trx-mHSS1 with *AcTEVTM*-protease at 23 °C for 6 h presented using 15% SDS-PAGE with silver staining. FP, fusion protein; M, protein marker (Fermentas SM0661).

The cleavage seemed to be efficient and the following protein bands could be seen after 2 h incubation of fusion protein with TEV-protease: the released mHSS1 at 24.5 kDa and Trx at 14.5 kDa, the incompletely digested fusion protein at 39.5 kDa, as well as TEV-protease at 27 kDa whose concentration was very stable during the whole cleavage process. Over time the band intensity of Trx-mHSS1 became weaker whereas the released mHSS1 enhanced.

It was also observed that, Trx-mHSS1 cleavage was also influenced by temperature. A relatively high temperature improved the degree of cleavage of fusion protein. For example, there was no identified fusion protein on the gel even by silver staining when cleavage was performed at 23 °C for 6 h as shown in Fig. 3.39.B, indicating complete digestion of the fusion protein.

A WB analysis with polyclonal HSS1 antibody was performed to confirm the identity of released mHSS1. Thereby solubilized cell pellet and the purified Trx-mHSS1 from IMAC, as

3 Experiments

well as the digested product at 10 °C for 16 h and 23 °C for 6 h was analyzed by SDS-PAGE with silver staining and then transferred to the membrane. With the help of conjugated goat-anti-rabbit as secondary antibody mHSS1 could be detected.

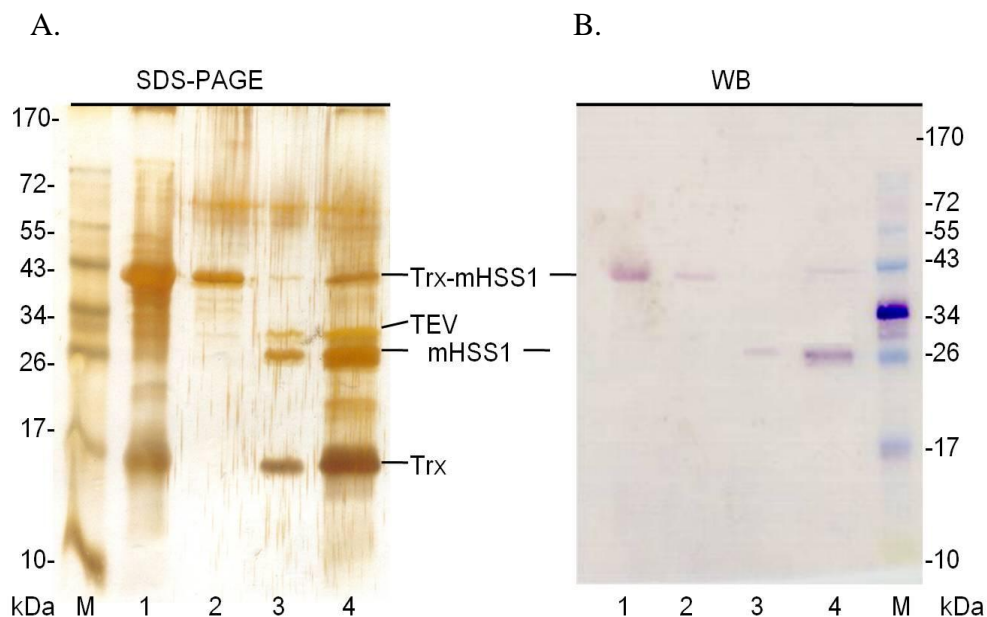


Fig. 3.40 Identification of Trx-mHSS1. A. SDS-PAGE analysis (12% with silver staining) of samples during purification process. B. WB of fractions in A. 1, solubilized cell pellet; 2, purified Trx-mHSS1 from IMAC; 3, digested product of Trx-mHSS1 at 10 °C for 16 h; 4, cleavage products of Trx-mHSS1 at 23 °C for 6 h; M, protein marker (Fermentas SM0671).

Fig.3.40.A shows the SDS-PAGE of different samples and the results of the related WB can be seen in Fig. 3.40.B. mHSS1 in fusion protein in the cell pellet and eluate from IMAC was detected (lanes 1 and 2). Contrary to expectations, there was no identified band at 32 kDa. The reason for this is unknown, probably because of the sensitivity of the polyclonal antibody. In lane 3 only the released intact mHSS1 at 24.5 kDa was specifically detected, neither TEV-protease nor Trx. In lane 4 except for mHSS1, the incompletely digested Trx-mHSS1 was also detected.

3 Experiments

3.2.4.4 Purification of mHSS1

3.2.4.4.1 Screening with Vivawell 8-strips

The released mHSS1 must be separated from the protein mixture containing TEV-protease and released Trx and possibly incompletely digested fusion protein. Within these proteins mHSS1 is the single protein which does not have 6×his and expected to be isolated via second IMAC and detected in the flow through. The Vivawell 8-strips was employed for screening of mHSS1 purification again due to the simplicity and the protocol is described in Appendix 5.5.6.

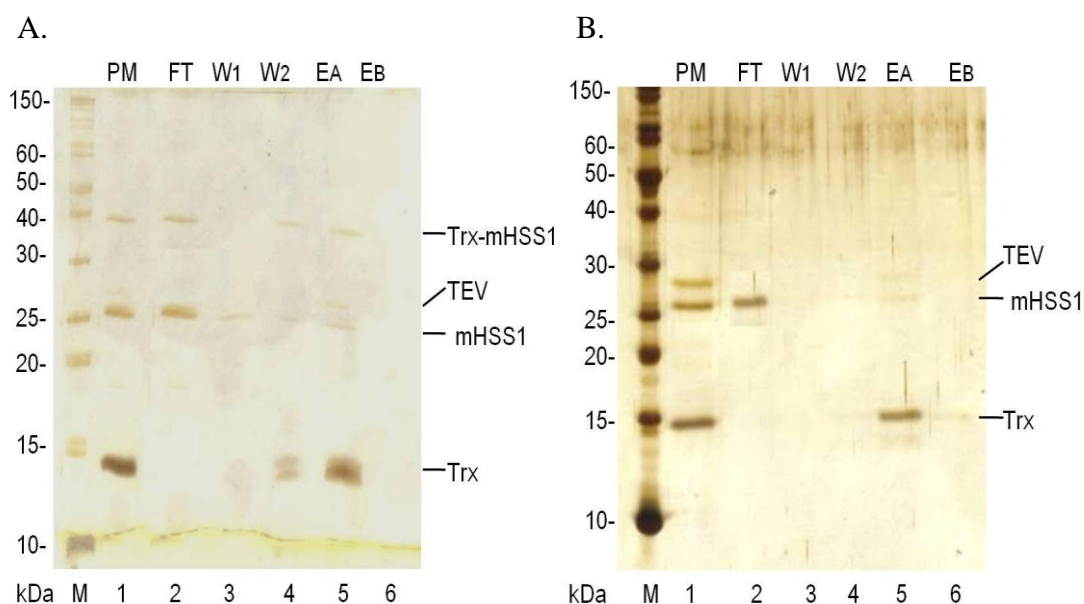


Fig. 3.41 Purification of mHSS1 from cleavage products of Trx-mHSS1 at 10 °C for 16 h (A) at 23 °C for 6 h (B) via Vivawell 8-Strips presented using 12% SDS-PAGE with silver staining. The soluble cell lysate (lane 1) and the fractions from following IMAC steps (lanes 2-6) are shown. PM: protein mixture after cleavage of Trx-mHSS1; FT, fraction of flow through; W1, wash fraction with wash buffer 1; W2, wash fraction with wash buffer 2; EA, first elution fraction; EB, second elution fraction; M, protein marker (Fermentas SM0661).

Fig. 3.41.A shows the result of screening of isolation of mHSS1 from the protein mixture after cleavage of Trx-mHSS1 at 10 °C for 16 h where the three proteins mentioned above were present. A successful purification of released mHSS1 was not achieved via second IMAC, because not only mHSS1 but also the incompletely digested fusion protein was detected in the flow through, which indicated a weak binding between the 6×his tag of Trx-mHSS1 and its

3 Experiments

ligand. However, this result was in accordance with the assumption described in 3.2.4.2.1 and when Trx-mHSS1 is present in its native conformation, it is difficult to access the 6×his tag which is probably hidden in fusion protein. The Trx and TEV-protease seemed to be tightly bound to the membrane and eluted mainly with 250 mM imidazole. A part of released mHSS1 was found in elution fractions probably because of non-specific interactions with the membrane adsorber.

In contrast, pure mHSS1 was obtained when mHSS1 was isolated from the protein mixture after cleavage of the fusion protein at 23 °C for 6 h was performed as shown in Fig.3.41.B. The fusion protein was completely digested into mHSS1 and Trx, which was detected in the flow through and the second elution fraction.

3.2.4.4.2 Upscaling of immobilized metal ion affinity chromatography

The scale-up purification of released mHSS1 via IMAC was performed and an IDA-75 membrane connected to FPLC system was once again employed. The membrane adsorber was equilibrated with binding buffer and subsequently loaded with digestion products of the fusion protein at 23 °C for 6 h. After flow through of mHSS1 and washing the membrane, Trx and TEV-protease were further eluted with buffer containing 250 mM imidazole for control.

In Fig. 3.42 and Fig. 3.43 the chromatogram and SDS-PAGE analysis of chosen fractions with silver staining are shown. Similarly to the screening via Vivawell 8-strips, the released mHSS1 without 6×his tag did not bind to the membrane adsorber and it was detected in the flow through after sample loading. The purity of purified mHSS1 was assumed to be more than 95% via SDS-PAGE analysis with silver staining. The TEV-protease and Trx with 6×his tag were detected in the first three fractions, as well as an unknown protein at about 13 kDa, which was thought to be a smaller fragment of Trx. Moreover, by determination of mHSS1 and Trx concentration by Bradford assay, mHSS1 was found to be only 32% of the fusion protein.

3 Experiments

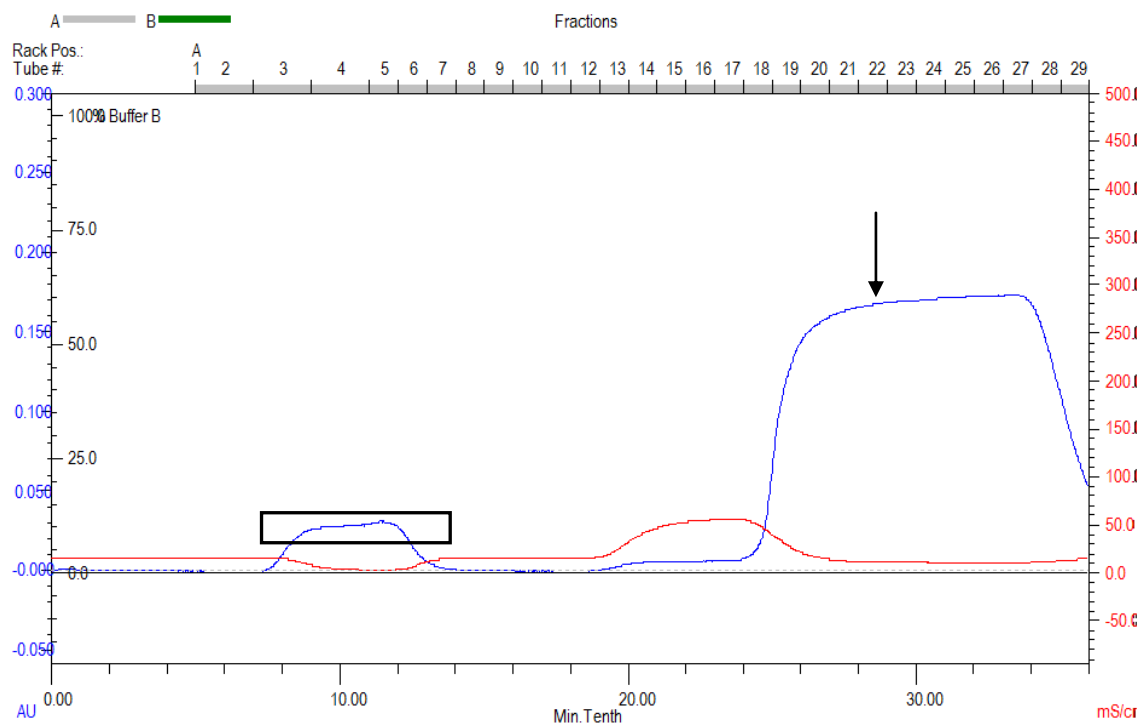


Fig. 3.42 Chromatogram of IMAC-purification of mHSS1 from cleavage products of Trx-mHSS1 at 23 °C for 6 h. The UV-absorption (AU) and conductivity (mS/cm^2) dependent on time were shown. The arrow indicates the elution peak of his-tagged proteins and the black line marks the flow through fractions.

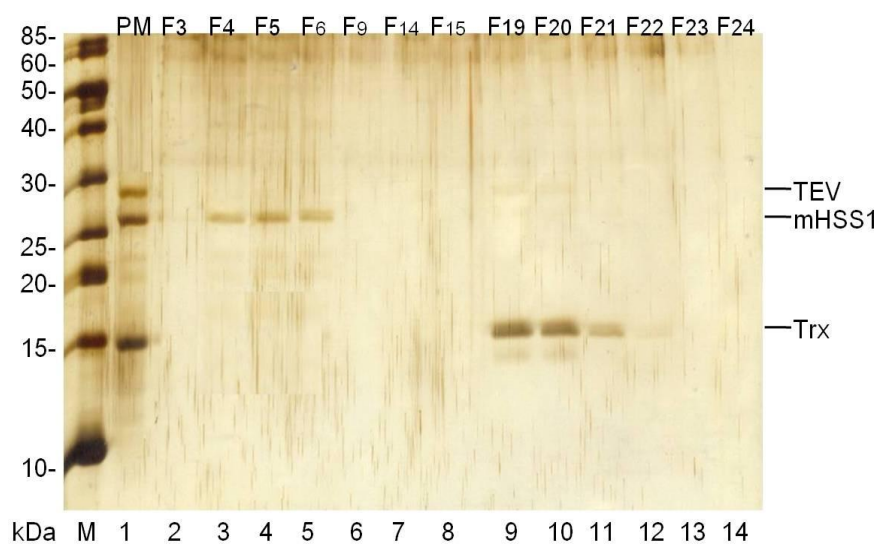


Fig. 3.43 IMAC-purification of mHSS1 from cleavage products of Trx-mHSS1 at 23 °C for 6 h presented using 12% SDS-PAGE with silver staining. PM: protein mixture after cleavage of Trx-mHSS1; F, fraction; M, protein marker (Fermentas SM0661).

3.2.4.5 Size exclusion-HPLC

Size exclusion-HPLC was carried out in order to determine the presence of related impurities like aggregates and different conformational forms of the purified mHSS1. The system set-up and chromatography conditions are described in Appendix 5.5.14.

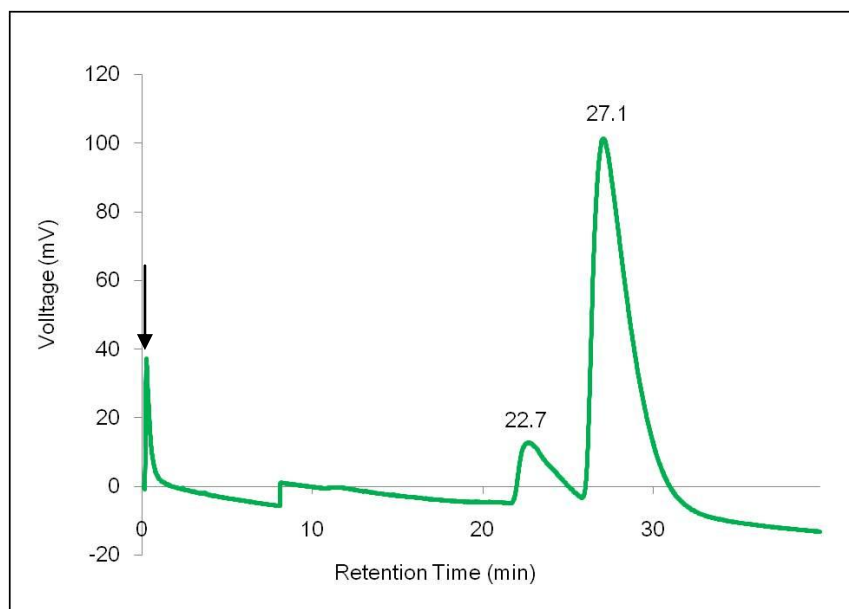


Fig. 3.44 Size exclusion-HPLC profile of purified mHSS1 preparation. The arrow indicates the buffer peak.

The size exclusion-HPLC profile of purified mHSS1 preparation is presented in Fig. 3.44. There are two peaks in the chromatogram from SE-HPLC and the retention times of peaks 1 and 2 were 22.7 min and 27.1 min, respectively. Peak 1 was smaller than peak 2, but the protein molecular weight in peak 1 was higher than in peak 2. The results of the SDS-PAGE analysis show that the subunit molecular weight of the two protein fractions was the same. Moreover, the identities of the two proteins were confirmed by WB using anti-HSS1 antibody as shown in Fig. 3.45. Since the protein in peak 1 eluted through the column more quickly than peak 2, it was thought to be the aggregated mHSS1 with incorrect folding. When the areas of both peaks were compared, mHSS1 in peak 2 held 67.4%. The mHSS1 in peak 2 was used in the following activity test.

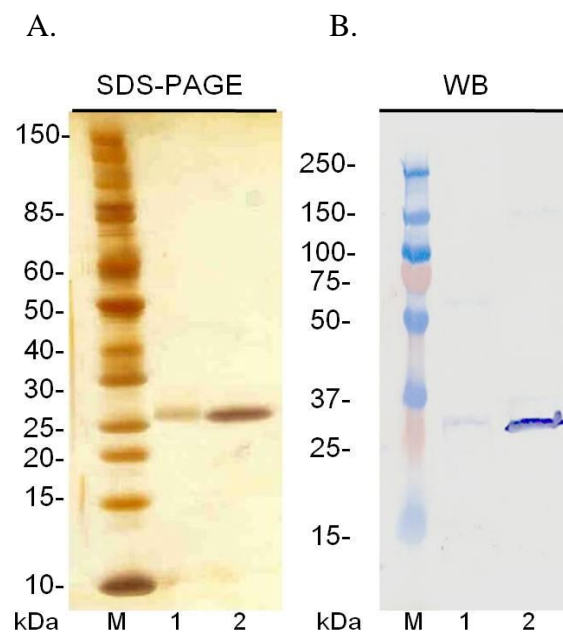


Fig. 3.45 Identification of proteins peaks from size exclusion-HPLC. A. SDS-PAGE analysis (12% with silver staining) of peaks. B. WB analysis (20%) of fractions in both peaks . Lane 1, protein in peak 1; lane 2, protein in peak 2. M (A), protein marker (Fermentas SM0661); M (B), protein marker (Bio-Rad, 161-0374).

3.2.4.6 Test of biological activity

The hHSS1 expressed in HEK cells displayed pro-angiogenic activity of HCAEC as described in 2.1.4. The biological activity of mHSS1 produced in recombinant *E. coli* was tested by Dr. Mortimer Korf-Klingebliel (Department of Cardiology and Angiology, Hanover Medical School). The cells were incubated with purified mHSS1 or fusion protein Trx-mHSS1 alone, or the two proteins in combination. The cells treated without any cytokines were used as negative control while cells grown with 15% FCS or stimulated with VEGF were used as positive control, which are well known to promote pro-angiogenesis.

3 Experiments

3.2.4.6.1 Proliferation

The proliferation of HCAEC was evaluated based on cultivation in a microtiter plate. HCAEC were grown in 96-well plates with 15% FCS and prior to the proliferation assay the cells were starved for 4 h in medium containing 0.5% FCS. Three samples were added to the wells of microtiter plate and the cells were cultured for a further 24 h. Bromodeoxyuridine (BrdU) is a synthetic nucleoside that is an analogue of thymidine which can be incorporated into the newly synthesized DNA of replicating cells during S phase of the cell cycle (137). The amount of incorporated BrdU in the cells can be detected with the help of antibodies and quantified using a spectrophotometer.

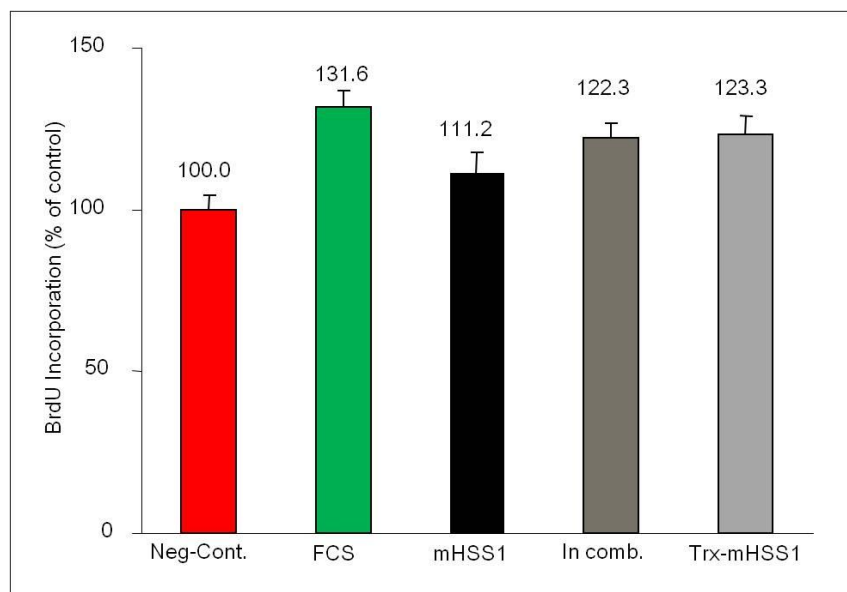


Fig. 3.46 Comparative efficiency of 15% FCS and various purified samples (each with 100 ng/mL) in HCAEC proliferation as % of the negative control. The cells without any cytokine treatment were used as negative control. In comb.: mHSS1 and Trx-mHSS1 in combination; Neg-Cont.: negative control.

The effects of the various samples on HCAEC proliferation are presented in Fig. 3.46. The culture without a supplement of any cytokines had its rate of BrdU incorporation defined as 100%. So that in other samples the rates were evaluated as a % of this control. The full medium with 15% FCS resulted in a large effect on endothelial cell proliferation and was recorded as 132% at the end of the test. The proliferation of cells treated with the three samples was

3 Experiments

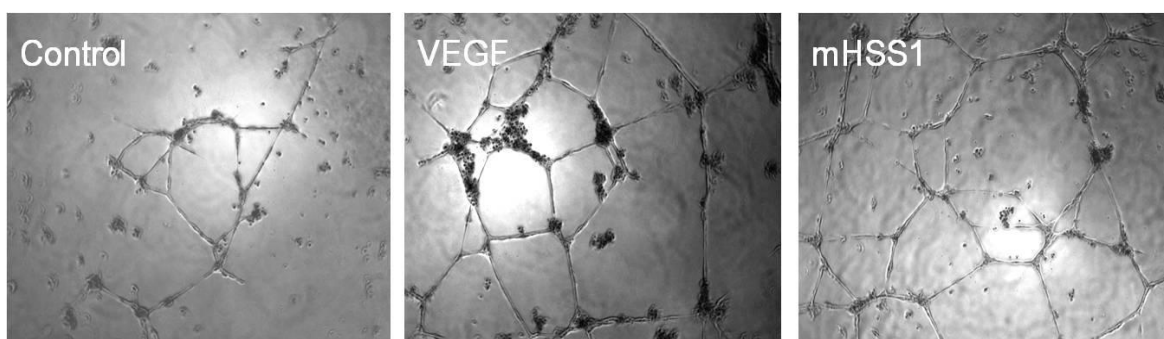
observed. Compared with the negative control, the purified mHSS1 alone did not stimulate cell proliferation very significantly and its efficiency was only 111%. Notably, the proliferation achieved with Trx-mHSS1 and mHSS1 in combination was comparable to the effect with fusion protein alone, 122% and 123% respectively.

3.2.4.6.2 Tube formation

The biological activity of purified mHSS1 was confirmed by tube formation where the *in vitro* formation of capillary-like tubes by endothelial cells based on matrix gel can be measured. It is a powerful *in vitro* method to screen for various factors that promote or inhibit angiogenesis (138).

Endothelial cell tube formation was assayed in a 24-well plate coated with growth factor reduced matrix gel. The HCAEC were supplemented with 0.5% FCS in the presence of VEGF or purified mHSS1 and incubated at 37 °C for 16 h. Microscopic pictures were taken at the end of the experiment as shown in Fig. 3.47.A. The pictures were analyzed based on various parameters, such as the number of tubes, the tube length and branching points.

A.



3 Experiments

B.

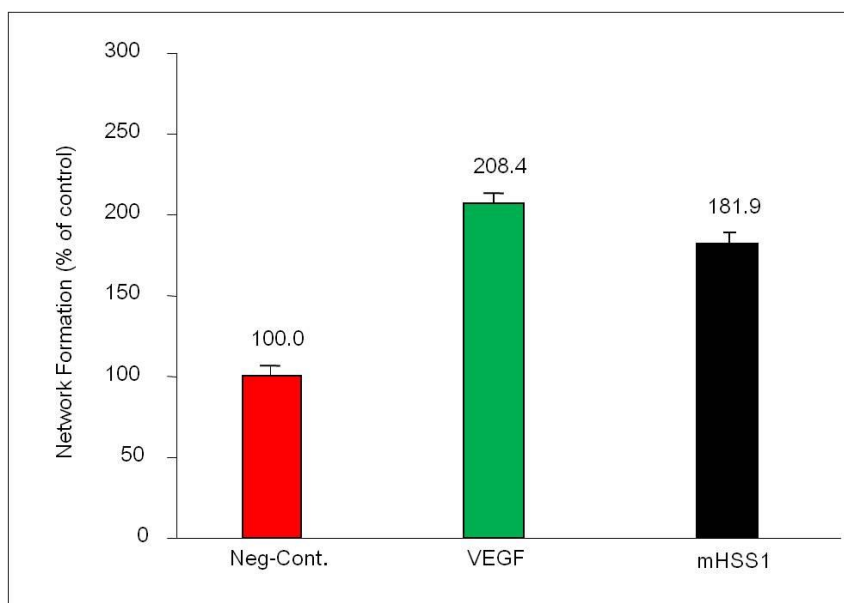


Fig. 3.47 Comparative efficacy of VEGF and purified mHSS1 (each with 100 ng/mL) in the tube formation assay. A, graphical depiction of tube formation after treatment with VEGF and purified mHSS1 at 37 °C for 16 h and the cells without any cytokine treatment were used as negative control. B, evaluation of the network formation as % of the negative control. Neg-Cont.: negative control.

Fig. 3.47.B shows that the network formation in the negative control was recorded as 100% and VEGF was sufficient to support endothelial morphogenesis in this 3D model of angiogenesis with 208 % efficiency of control. It was observed that HCAEC formed branching networks when stimulated with purified mHSS1 with 182 % of the control.

3.2.4.6.3 Mouse aortic ring assay

It was demonstrated that mouse or rat aorta rings reproducibly generate microvessel outgrowths in fibrin or collagen gels, and provide a sensitive assay for the study of angiogenesis in a chemically defined environment (139). In this present work, this assay was performed in growth factor reduced matrix gel in 24-well plates and the cells were cultured for up to 2 weeks in a medium with 1% FCS and incubated with mHSS1. A negative control was stimulated with unconditioned serum-free medium. Cellular outgrowth was assessed by phase contrast

3 Experiments

microscopy and expressed as the number of vessels and branching, as well as their maximal length.

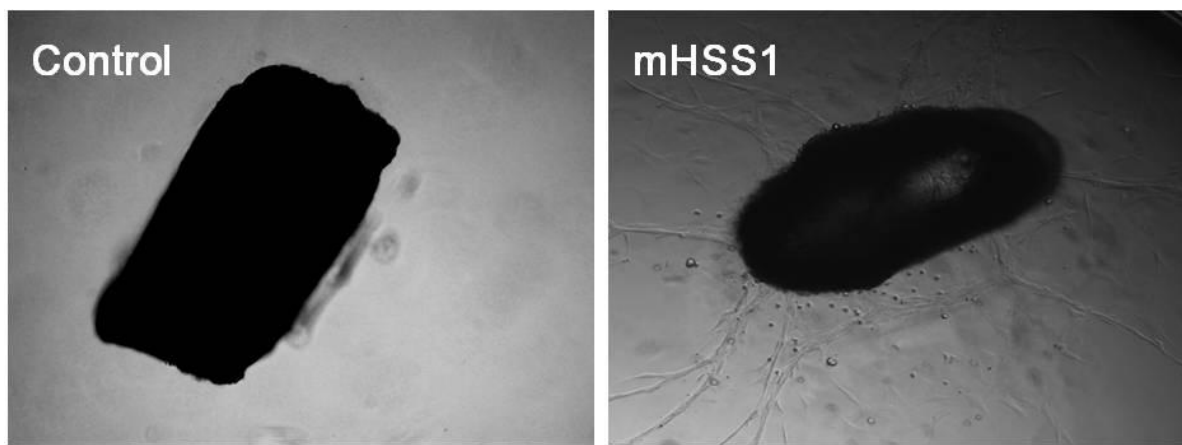


Fig. 3.48 Photomicrographs of microvessel outgrowth from the mouse aorta treated with purified mHSS1 (100 ng/mL). The mouse aorta without cytokine treatment was used as control.

Fig. 3.48 shows the photomicrographs at the end of test. In the negative control, the serum-free medium failed to support angiogenesis from mouse explants. In the tested culture in the presence of serum and stimulated with mHSS1, only isolated and dispersed fibroblast-like cells migrated into the gel within the early phase. Subsequently, microvessel outgrowth arose from the edges of the parental vessels and the initial linear sprouting of endothelial cells progressively branched, anastomosed and formed a microvascular network.

3.2.4.6.4 Scratch assay

In this study, the monolayer of HCAEC was removed with pipette tips. The effect of mHSS1 on HCAEC migration was observed and the cells stimulated with VEGF were used as a positive control, while the cells without any cytokine treatment were used as negative control. The photomicrographs of wounded HCAEC before and after treatment at 6, 9 and 18 h are presented in Fig. 3.49.A. The recovery of the wound stimulated by different samples over 18 h was plotted as a percentage which is shown in Fig. 3.49.B.

3 Experiments

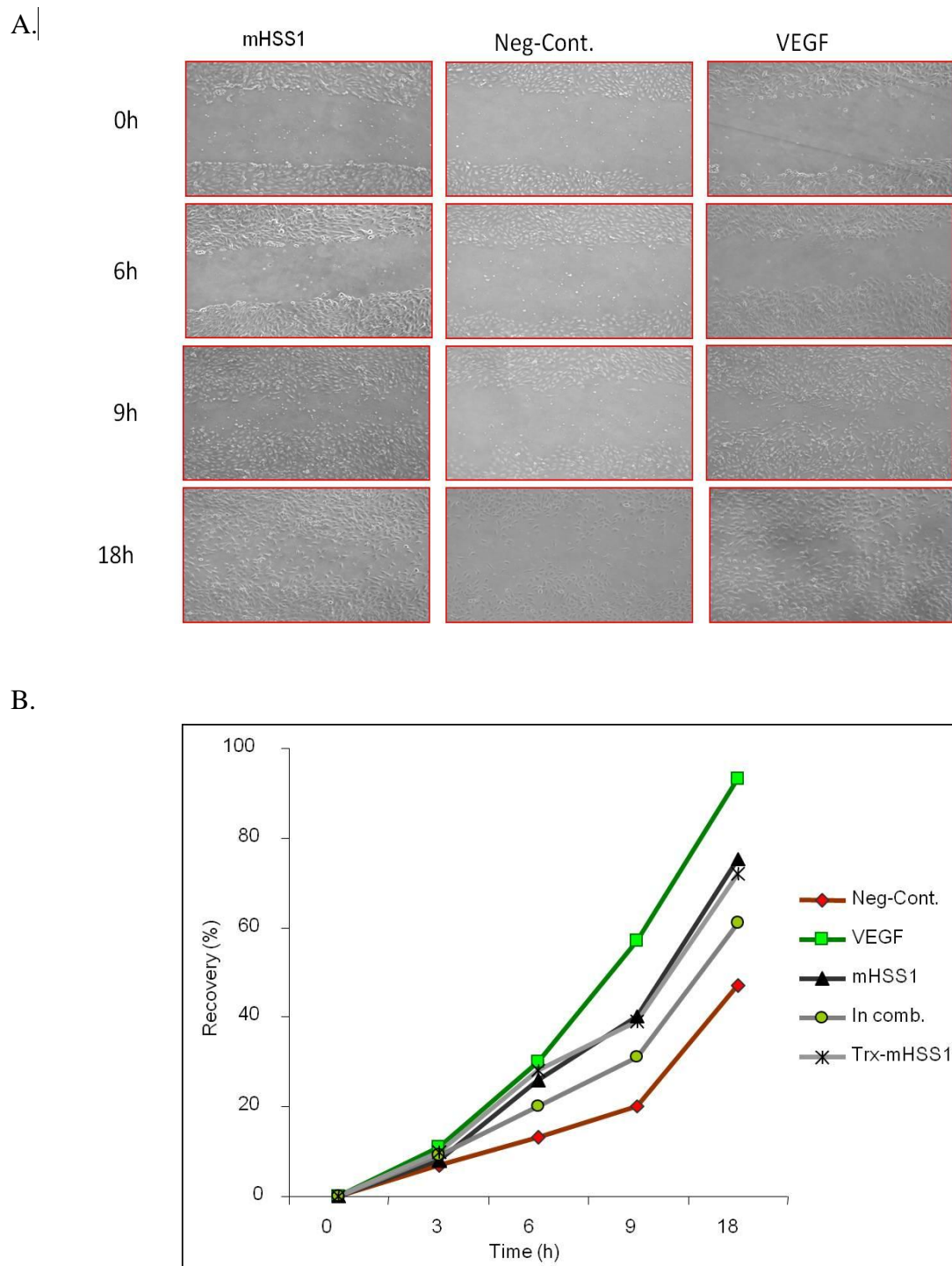


Fig. 3.49 Comparative efficacy of VEGF and purified proteins (each with 100 ng/mL) in the scratch assay. A. photomicrographs of wounded HCAEC before and after treatment with VEGF and purified mHSS1 at 6, 9 and 18 h. The cells without any cytokine treatment were used as negative control. B. Effects of different samples on HCAEC migration were plotted as a percentage of wound closure. In comb.: mHSS1 and Trx-mHSS1 in combination; Neg-Cont.: negative control.

3 Experiments

The positive control VEGF showed significant migration of the cells toward the scratch and after 18 h, the recovery was more than 90%. The HCAEC responded typically to the actions of the tested three samples. During the whole period, the cells stimulated with mHSS1 migrated almost at the same rate as the cells treated with Trx-mHSS1 at the leading edge of the scratch and the percentage of wound closure at end of the test was recorded as 74% and 72%, respectively. In contrast, for the cells treated with mHSS1 and Trx-mHSS1 in combination the recovery was only 60%.

3.2.4.7 Summary

In the present work, a process of production and purification of mHSS1 was developed and the flow chart is presented in Fig. 3.50.

The mHSS1 cDNA was fused with Trx and inserted into plasmid pET32b and then transformed into *E. coli* BL21(DE3). Production of soluble Trx-mHSS1 could be detected after cultivation in LB medium at 26 °C, but its concentration was still low compared to overexpressed inclusion bodies. The solubility of produced Trx-mHSS1 was not improved by a change of cultivation temperature. Moreover, soluble Trx-mHSS1 could be produced in S-DAB medium instead of IPTG induction, however its yield was less than in LB medium.

Due to the 6×his tag not being exposed to its ligand in its conformation and nonspecific binding of contaminants, the soluble cell lysate was replaced by inclusion bodies as initial material for the purification of Trx-mHSS1 via IMAC. The renaturation of purified Trx-mHSS1 was achieved by dialysis against refolding buffers. Alternatively, refolding of Trx-mHSS1 was performed on a membrane adsorber combined with IMAC. Although this could be done only with very low initial protein concentrations, it might offer an attractive approach for purification of other proteins in the future.

It was necessary to perform the cleavage of Trx-mHSS1 at a relatively high temperature, so that the fusion protein would be completely digested into mHSS1 and Trx, which were separated

3 Experiments

from each other in the subsequent IMAC. In this case, the overall yield of mHSS1 from a 1 L bacterial culture (cultivation in shake flask) was 12.6 mg.

The biological activities of the purified proteins were tested successfully and not only pure mHSS1 but also fusion protein could promote pro-angiogenesis, as could the two proteins in combination.

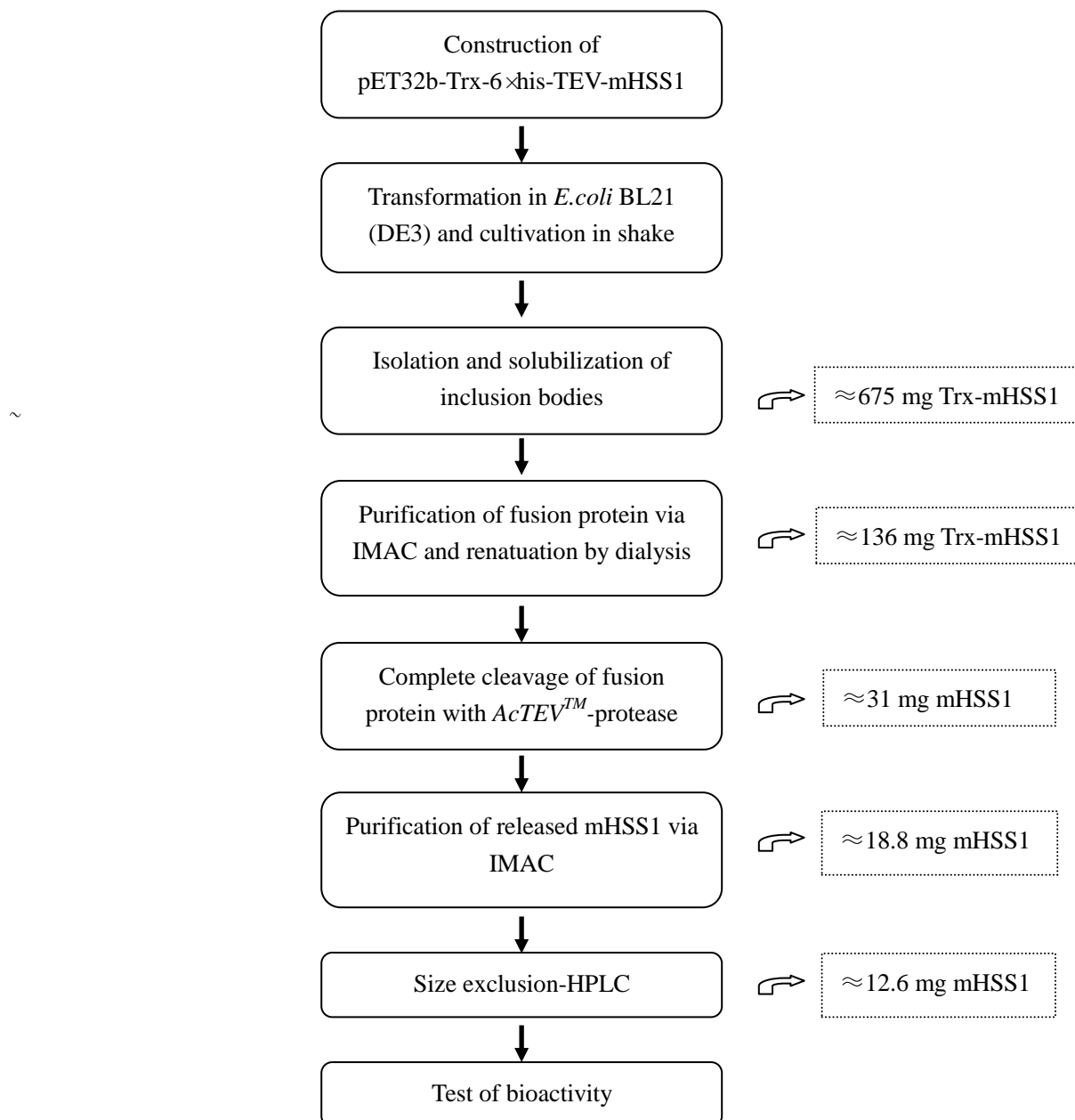


Fig. 3.50 The flow chart of the mHSS1 production process. The specified protein amount refers to a 1 L culture from cultivation in shake flask.

4. SUMMARY AND OUTLOOK

Cytokines are small cell signaling proteins which can regulate the proliferation and differentiation of cells and they also have critical importance in the restoration of damaged tissues or organs. However, some cytokines may have a negative effect on cells and in some cases they are associated with diseases and tumors. Therefore, characterization of cytokines has received more and more attention from the research community. Due to various applications, cytokines are needed with increasing quantity. Generally, although the produced cytokines from eukaryotic cells are bioactive, the production amounts are limited through this medium.

In the present work, the production and purification of four cytokines in recombinant *E. coli* was developed and optimized. In the first part of the work, the optimized production and purification of 16-kDa hPRL was described thought to be the major cause of PPCM. After a 2-step chromatographic purification by anion exchange membrane-and size exclusion chromatography followed by removal of endotoxins, the apoptotic activity of purified 16-kDa hPRL on NRCM via the activation of NF- κ B signaling was confirmed. Moreover, the 16-kDa hPRL injected mice exhibited left ventricular dilatation. In the future, the production of 16-kDa hPRL based on this developed protocol can be scaled up. For example, the production scale can be transferred from 500 mL shake flask to 2 L bioreactor.

In the second part, a new process for production and purification of hActivin A, mHSS1 and Fam163a was developed. Activin A has a prominent role in the area of haematopoiesis, while hHSS1 and FAM163A have exhibited pro-angiogenetic activities. In order to have soluble production of these three cytokines, they were fused with N-terminal Trx and expressed as fusion proteins.

The fusion with Trx did not improve solubility of hActivin β A at all and Trx-hActivin β A was expressed entirely as inclusion bodies. However, Trx-Fam163a could be detected only in the soluble fraction of cell lysate. For mHSS1, the amount of soluble fusion protein was low compared with insoluble part.

For purification of hActivin A, work was only completed until cleavage of soluble Trx-hActivin

4 Summary and outlook

β A. The renaturation of Trx-hActivin β A by dialysis was performed prior to purification of the fusion protein via IMAC. The released hActivin β A from the cleavage of fusion protein was found to be insoluble which indicated the innative conformation of released target protein. It seems extremely difficult to determine the proper refolding conditions for Activin A which possesses 9 intramolecular and intermolecular disulfide bonds. Mason AJ *et. al* examined the relationship between the efficiency of secretory expression of Activin A by use of animal cells and the structure of an expression vector. They reported that besides the region for the amino acids sequence of Activin A, a pro-sequence region is essential for refolding (79). This report suggests that in future work a new construct of Trx-hActivin β A with the pro-sequence should be created, where the solubility of the target protein can be improved.

Although the Trx fusion was effective in increasing soluble Fam163a production, it was difficult to purify the protein. So far, purified Fam163a is only available at the analytical scale. At first, degradation resulted in a low yield of intact fusion protein which was sensitive to the bacterial proteases and digested into several smaller fragments during expression. Trx-Fam163a was purified via IMAC, together with its digestion products. In order to avoid too many contaminants being present after the subsequent cleavage, the fusion protein could only be pooled from small quantities. In the second purification step, the released Fam163a from the fusion protein could be only achieved using immunoprecipitation with anti-his tag beads. Finally, Fam163a demonstrated the bioactivity to close the scratch on a monolayer of HCAEC whereas Trx-Fam163a had less effect.

Currently, the production of Fam163a is limited by the application of anti-his tag beads and its disadvantages are well recognized, including cost and scale. As described in 3.2.3.4.1, 8 glutamic acids in a series at the N-terminus of Fam163a were assumed to bind the IMAC ligand with the same affinity like 6 \times his tag. A new construct of fusion protein in the absence of 6 \times his tag could be created to solve this problem. Instead of the 6 \times his tag, the fusion protein is expected to combine IMAC with its own 8 glutamic acids and a TEV-protease recognition-site can be replaced with another protease without a 6 \times his tag. Moreover, it is necessary to investigate a better method to prevent Fam163a degradation.

4 Summary and outlook

The low affinity of the 6×his tag in soluble Trx-mHSS1 for its ligand created significant difficulties during purification. So instead, the solubilized inclusion bodies containing the fusion protein were applied to IMAC. Refolding of Trx-mHSS1 was achieved with dialysis *in vitro*. Alternatively, renaturation of the fusion protein could be combined with IMAC. After complete cleavage of Trx-mHSS1 at a higher temperature, the released mHSS1 could be obtained in the second purification via IMAC. Finally, with or without Trx fusion, the refolded mHSS1 was biologically active and stimulated proliferation, migration of HCAEC and tube formation and induced cell spouting in a mouse aortic ring assay.

In the future, the production of Trx-mHSS1 based on this developed protocol will be scaled up, as it exhibited similar bioactivity to mHSS1. In addition, new constructs can be created. Instead of between Trx and mHSS1, the 6×his tag can be placed at the N-terminus of Trx, where it may make it more accessible for binding in native state. Moreover, a new construct of mHSS1 without Trx fusion can be made. This “naked” mHSS1 with 6×his tag can be expressed alone and renatured after purification, saving the work of cleavage. Furthermore, it would make sense to compare its expression’s solubility and efficiency for refolding to fusion with Trx. Dr. Mortimer Korf-Klingebiel has attempted to make this new plasmid and it was often observed that mHSS1 was unstable and its sequence would change suddenly. Strangely, a gene which was confirmed by sequencing before was found have been replaced by a new gene in the subsequent purification of the plasmid. However, in most cases, the genes were found to have been deleted.

In addition, from the feedback of Dr. Mortimer Korf-Klingebiel, when the cells were treated with endotoxin-containing Trx-mHSS1, an expression of chemokine C-X-C motif ligand 1 (CXCL1) could be detected. CXCL1 is a well-known pro-inflammatory cytokine and its expression can be induced by endotoxins. By contrast, the endotoxin-free Trx-mHSS1 exhibited no stimulation. It seems that, it is enough to stimulate the cells with very low endotoxin levels. So removal of endotoxins in purified mHSS1 and Trx-mHSS1 is a necessity.

Besides the optimization of the production of mHSS1 and Fam163a, the future work may involve the production of other cytokines, which have been also isolated from bone marrow

4 Summary and outlook

cells and exhibit pro-angiogenic activity. For example, interleukin-25, this cytokine from *E. coli* culture is already commercially available (Thermo Fisher Scientific, Karlsruhe). It is also possible to express the protein with Trx fusion in recombinant *E. coli* and that the purified protein can be compared with the commercial interleukin-25, which can be used as a standard in tests.

5. APPENDIX

5.1 Materials

5.1.1 Chemicals

Reagent	Manufacturer, location
acetic acid	AppliChem GmbH, Darmstadt
acrylamide/bisacrylamide (37.5:1)	Carl Roth GmbH& Co, Karlsruhe
agar	Carl Roth GmbH& Co, Karlsruhe
AgCl	Carl Roth GmbH& Co, Karlsruhe
ampicillin	Fluka Chemie AG, Seelze
APS	Sigma Aldrich Chemie GmbH, Steinheim
β -Mercaptoethanol	Fluka Chemie AG, Seelze
bromophenol blue	Fluka Chemie AG, Seelze
BSA	Sigma Aldrich Chemie GmbH, Steinheim
CH ₃ COONa	Fluka Chemie AG, Seelze
citric acid	Fluka Chemie AG, Seelze
CoCl ₂ 6H ₂ O	Fluka Chemie AG, Seelze
Coomassie brilliant blue G250	Fluka Chemie AG, Seelze
Coomassie brilliant blue R250	Fluka Chemie AG, Seelze
CuCl ₂ 2H ₂ O	Fluka Chemie AG, Seelze
DTT	Fluka Chemie AG, Seelze
EDTA	Fluka Chemie AG, Seelze
ethanolamine	Fluka Chemie AG, Seelze
Fe (III) Citrate	Sigma Aldrich Chemie GmbH, Steinheim
formaldehyde	Fluka Chemie AG, Seelze
glucose	Carl Roth GmbH& Co, Karlsruhe
glycine	Carl Roth GmbH& Co, Karlsruhe
GSH	Sigma Aldrich Chemie GmbH, Steinheim
GSSG	Sigma Aldrich Chemie GmbH, Steinheim
H ₃ BO ₃	Sigma Aldrich Chemie GmbH, Steinheim
imidazole	Sigma Aldrich Chemie GmbH, Steinheim
F ₃ Fe(CN) ₆	Fluka Chemie AG, Seelze
K ₂ HPO ₄	Fluka Chemie AG, Seelze
KH ₂ PO ₄	Fluka Chemie AG, Seelze
lactose	Carl Roth GmbH& Co, Karlsruhe
methanol	Carl Roth GmbH& Co, Karlsruhe
MgSO ₄ 7H ₂ O	Fluka Chemie AG, Seelze

5 Appendix

MnCl ₂ · 4H ₂ O	Fluka Chemie AG, Seelze
NaAc	Fluka Chemie AG, Seelze
Na ₂ S ₂ O ₃	Fluka Chemie AG, Seelze
Na ₂ CO ₃	Carl Roth GmbH & Co, Karlsruhe
Na ₂ MoO ₄ · 2H ₂ O	Merck KGaA, Darmstadt
NaCl	Merck KGaA, Darmstadt
NaH ₂ PO ₄	Fluka Chemie AG, Seelze
NaN ₃	Fluka Chemie AG, Seelze
NaOH	Sigma Aldrich Chemie GmbH, Steinheim
(NH ₄) ₂ HPO ₄	AppliChem GmbH, Darmstadt
(NH ₄) ₂ SO ₄	Amersham Biosciences, Piscataway, USA
NH ₄ HCO ₃	Fluka Chemie AG, Seelze
NiSO ₄ · 7H ₂ O	Fluka Chemie AG, Seelze
phosphoric acid	Sigma Aldrich Chemie GmbH, Steinheim
PMSF	Sigma Aldrich Chemie GmbH, Steinheim
potassium hexacyanoferrate (III)	Fluka Chemie AG, Seelze
SDS	Sigma Aldrich Chemie GmbH, Steinheim
TCA	Sigma Aldrich Chemie GmbH, Steinheim
TEMED	Carl Roth GmbH & Co, Karlsruhe
TDCA/Na	Sigma Aldrich Chemie GmbH, Steinheim
Titriplex III	Fluka Chemie AG, Seelze
Tris	Sigma Aldrich Chemie GmbH, Steinheim
Tris-base	Amersham Biosciences, Piscataway, USA
Tris-HCl	Carl Roth GmbH & Co, Karlsruhe
Triton X-100	Merck KGaA, Darmstadt
trypone	Fluka Chemie AG, Seelze
Tween 20	Serva Elektrophoresis GmbH, Heidelberg
urea	Carl Roth GmbH & Co, Karlsruhe
yeast extract	Carl Roth GmbH & Co, Karlsruhe
Zn(CH ₃ COO) ₂ · 2H ₂ O	Carl Roth GmbH & Co, Karlsruhe
ZnSO ₄ · 7H ₂ O	Fluka Chemie AG, Seelze

5.1.2 Consumable materials

Material	Types, manufacturer and location
Centrifugal concentrator	Vivaspin® 2, Sartorius Stedim Biotech GmbH, Göttingen
Falcon tubes	15 and 50 mL, Sarstedt AG & Co. KG, Nuembrecht
Fiber pads	Bio-Rad Laboratories GmbH, Munich
Shake flasks	100 and 500 mL, VWR international GmbH, Darmstadt
Syringes	1, 5 and 10 mL, B.Braun Biotech, Melsungen
Syringe filters 0.2 µm	Sartorius Stedim Biotech GmbH, Göttingen

5 Appendix

PVDF membrane

Bio-Rad Laboratories GmbH, Munich

Pipette tips

Sarstedt AG & Co. KG, Nuembrecht

5.1.3 Enzymes

Benzonase (Cat. No 70746-4), Novagen, Darmstadt

*AcTEV*TM-protease (Cat. No 12575-015), Invitrogen, Darmstadt

Lysozyme (Cat.62971), Sigma Aldrich Chemie GmbH, Steinheim

5.1.4 Antibodies

WB for identification of Trx-mHSS1 and degradation fragments of Trx-Fam163a

Primary antibody:

Mouse monoclonal anti-6×his antibody (GE Healthcare, Freiburg)

Secondary antibody:

Goat anti-mouse secondary antibody conjugated to peroxidase (Bio-Rad Laboratories GmbH, Munich)

WB for identification of mHSS1

Primary antibody:

Rabbit polyclonal anti-C19orf63 (mHSS1) antibody (N-term) (Abgent, San Diego, USA)

Secondary antibody:

Goat anti-rabbit secondary antibody conjugated to peroxidase (Bio-Rad Laboratories GmbH, Munich)

Immunoprecipitation using protein G

Mouse monoclonal anti-6×his antibody (GE Healthcare, Freiburg)

5.1.5 Molecular weight markers

PageRulerTM unstained protein ladder, SM 0661 (Fermentas, St. Leon-Rot)

PageRulerTM prestained protein ladder, SM 0671 (Fermentas, St. Leon-Rot)

Unstained protein molecular marker, 26610 (Thermo Scientific, Bremen))

Prestained protein molecular marker, 161-0374 (Bio-Rad Laboratories GmbH, Munich)

5 Appendix

5.1.6 Columns and membrane adsorbers

Column:

SEC: Proteema100Å (Polymer Standards Service, Mainz)

Membrane adsorber:

IMAC: Sartobind IDA-75 (Sartorius Stedim Biotech GmbH, Göttingen)

AEC: Sartobind Q75 (Sartorius Stedim Biotech GmbH, Göttingen)

Spin column:

Vivaspure MCMini (Sartorius Stedim Biotech GmbH, Göttingen)

8-Strips:

Vivawell 8-Strips, 15 layers (Sartorius Stedim Biotech GmbH, Göttingen)

5.2 Equipments

Equipment	Types, manufacturer and location
Autoclave	Systec V-150, Systec GmbH, Wettengel
Electrophoresis chamber	Mini Protean Tetra Cell, Bio-Rad Laboratories GmbH, Munich
FPLC	BioLogic AVR7-3, Bio-Rad Laboratories Inc., Munich
Incubator	CertomatR HK, B.Braun Biotech, Melsungen
pH-electrode	Checker® Hanna Instruments Ltd, Leight on Buzzard, UK
Pipettes	Research®, Eppendorf AG, Hamburg
Shaker	MTS 4, IKA Werke GmbH, Staufen
Ultrasonic probe	Labsonic M, Sartorius Stedim Biotech GmbH, Göttingen
Spectrophotometer	Multiskan, Thermolabsystems GmbH, Langenselbold
Thermocentrifuge	Megafug1.0RS, Heraeus Holding GmbH, Hanau
Thermocentrifuge	Fresco 17, Heraeus Holding GmbH, Hanau
Thermomixer	Compact, Eppendorf AG, Hamburg
Vortex mixer	VM-300, NeoLab Migge GmbH, Heidelberg
Western blot system	Criterion Blotter, Bio-Rad, Laboratories GmbH, Munich

5.3 Bacterial strain

The strain *E. coli* BL21(DE3) (Novagen, Darmstadt) was employed as the competent cells for production of 16-kDa hPRL, hActivin A, Fam163a and mHSS1. The transformation of the four

5 Appendix

expression vectors are performed individually.

5.4 Expression vectors

PT7L-16-kDa hPRL

The vector PT7L-16-kDa hPRL was provided from Prof. Denise Hilfiker-Kleiner (Department of Molecular Cardiology and Angiology, Hanover Medical School). It contains cDNA of 16-kDa hPRL (40) which is under the control of an IPTG inducible T7 promoter and ampicillin resistance.

pET32b-Trx-6×his-TEV-TP

The expression vector pET32b-Trx-6×his-TEV-TP is used for the production of hActivin A, Fam163a and mHSS1. TP stands for the three cytokines. With a Lac-operator the protein expression can be induced by IPTG and the expression vector contains an additional gene of ampicillin-resistance as the selection marker. The vector map is shown in Fig. 5.1.

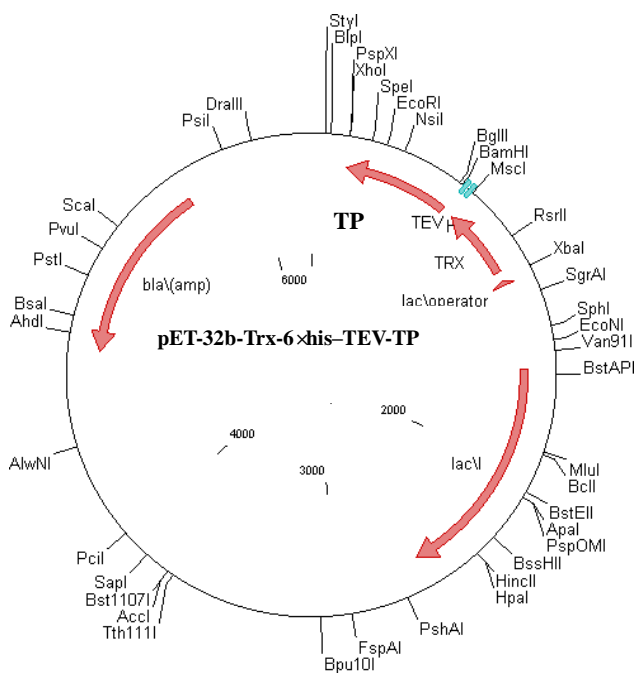


Fig. 5.1 Vector map of pET32b-Trx-6×his-TEV-TP. TP, target protein (hActivin β A, Fam163a or mHSS1).

5 Appendix

The sequences of bases encoding Trx-6×his-TEV and the corresponding amino acids as one-letter-code are presented. The coding areas for 6×his tag and TEV-protease recognition sequences are separately marked by a blue and red background. The cDNA of hActivin βA was amplified by Dr. Axel Schambach (Institute of Experimental Hematology, Hanover Medical School). The mHSS1 and Fam163a genes were amplified by Dr. Mortimer Korf-Klingebiel (Department of Cardiology and Angiology, Hanover Medical School). The cDNA- and amino acids sequences of hActivin βA, Fam163a and mHSS1 are also given below, respectively.

Trx-6×his-TEV:

atgagcgataaaattattcacctgactgacgacagttttgacacggatgtactcaaagcggacggggcgatcctcg
 tcgatttctgggcagagtgggtgcggtccgtgcaaaatgatcgccccgattctggatgaaatcgctgacgaatatca
 gggcaactgaccgttgcaaaactgaacatcgatcaaaacctggcactgcgccgaaatatggcatccgtggtatc
 ccgactctgctgctgttcaaaaacgggtgaagtggcggcaaccaaagtgggtgactgtctaaaggtcagttgaaag
 agttcctcgacgctaacctggccggttctggttctggccatatgcaccatcatcatcatcattcttctggtgagaa
 tctttattttcagggatcc

MSDKIIHLTDDSFDTDVLKADGAILVDFWAEWCGPCKMIAPILDEIADEYQGKLTVAKL
 NIDQNPGTAPKYGIRGIPTLLLKNGEVAATKVGALS KGLKEFLDANLAGSGSGHMH
 HHHHHSSGENLYFOGS

hActivin βA:

cttgagtgatggcaaggtcaacatctgctgtaagaaacagttctttgtcagtttcaaggacatcggctggaat
 gactggatcattgctccctctggctatcatgccaactactgcgagggtgagtgcccagccatatagcaggcacgt
 ccgggtcctcactgtccttccactcaacagtcacaccactaccgcatgcggggccatagcccccttgccaacct
 caaatcgtgctgtgtgcccaccaagctgagaccatgtccatgttgtactatgatgatggtcaaaacatcatcaaa
 aaggacattcagaacatgatcgtggaggagtgtgggtgctcatag

GLECDGKVNICCKKQFFVSFKDIGWNDWIIAPSGYHANYCEGECPSHIAGTSGSSLSFH
 STVINHYRMRGHSPFANLKS CCVPTKLRPMSMLYDDGQNIKKDIQNMIVEECGCS

Fam163a:

cagtattactgctgcaagaagggcacagatggcgaggatgctgaggaggaagaggaagaggaggaacacggccttt
 ccatccatccccgagtccccgcctgcaatgcctgcagctcccacgtcctggacggcagaggcggcctggcacctct
 caccagegagtcctgcagccagccgtgtgggggtggccagccactgtaccacttgcctccccttaccgcacccccctt
 tacatacggacagctgacatggtgcccacgggggtggaggcgagaggctctccttgcacctacacactacaaag

5 Appendix

aggggggaaccccatccctcaagttggcagcaccacagaattaccgggtgacctggccaagttctgggcatgaggc
cttcaactaatccaagggtatttagtaccgatgta^{taa}

**QYYCCKKGTGDGEDAEEEEEEHGLSIHPRVPACNACSSHVLDGRGGLAPLTSESCSQ
PCGVASHCTTCSFYRTPFYIRTADMVPNGGGGERLSFATHYKEGGTPSLKLAAPQNY
VTWPSSGHEAFTNPRAISTDV**

mHSS1:

ggctgccgggcccgggactggtgcgcgaggggctggggcggaaggtcgagagggcgaggcctgtggcacggtggggc
tgctgctggagcactcatttgagatcgatgacagtgccaaacttccggaagcggggctcactgctctggaaccagca
ggatggtaccttgtccctgtcacagcggcagctcagcaggaggagcggggccgactccgggatgtggcagccctg
aatggcctgtaccgggtccggatccaaggcgaccggggccctggatggcctggaagctggtggctatgtctcct
ccttgtccctgctgctcctggtggagtcgcacctgtcggaccagctgacctgcacgtggatgtggccggcaa
cgtggtgggctgtcgggtgacgcacccccggggctgccggggccatgaggtggaggacgtggacctggagctg
ttcaacacctcggtgcagctgcagccgccaccacagcccccaggccctgagacggcgcccttcattgagcgctgg
agatggaacaggcccagaaggccaagaacccccaggagcagaagtccttcttccgcaatactggcacatcctcct
ggggggggccggtgttgctcacagccctgctcctgctgcgccagggcccgcgccaccgccacaggaggcc^{tga}

**SGCRVGASARGTGADGREAEKGTVALLEHSFELGDGANFQKRGLLLWNQQ
DGTLSATQRQLSEEERGLRDVAVNLYRVRVPRRPGTLDSEAGGHVSSFVPAC
SLVESHLSDQLTLHVDVAGNVVGLSVVYPGGCRGSEVEDEDLELFNtSVQLRS
TAPGPETAAFIERLEMEQAQKAKNPQEQKSFFAKYWHLILGGAVLLTALRPAAG
PAPAPTEA**

5.5 Methods

5.5.1 Working with recombinant *E. coli* strains

5.5.1.1 Media compositions

LB: 10 g tryptone; 5 g yeast extract; 10 g NaCl; 1000 mL dd H₂O

TB: solution 1: 12 g tryptone; 24 g yeast extract; 4 mL glycerol; 900 mL dd H₂O

solution 2: 2.31 g KH₂PO₄; 12.54 g K₂HPO₄; 100 mL dd H₂O

Antibiotic: ampicillin stock solution (25mg/mL)

5 Appendix

DNB and S-DAB (135):

Groups	Components	S-DAB (mL)	DNB (mL)
Magnesium*	0.586 g/L MgSO ₄ · 7H ₂ O	20	20
Carbon source*	2.94 g/L glucose	250	
	11.07 g/L glycerol		
	7.6 g/L lactose		
	10.91 g/L glucose		50
Trace**	2.1 mg/L Na ₂ MoO ₄ · 2H ₂ O	0.2	0.2
Elenments**	2.5 mg/L CoCl ₂ · 6H ₂ O	0.5	0.5
	15 mg/L MnCl ₂ · 4H ₂ O		
	1.5 mg/L CuCl ₂ · 2H ₂ O		
	3 mg/L H ₃ BO ₃		
	33.8 mg/L Zn(CH ₃ COO) ₂ · 2H ₂ O		
	14.1 mg/L Titriplex III		
Nitrogen*	4 g/L (NH ₄) ₂ HPO ₄	20	20
Phososphate and other salts*	13.3 g/L KH ₂ PO ₄	100	100
	1.55 g/L Citric acid	20	20
	0.10 g/L Fe (III) Citrate	20	20
pH (6.8) adjusting*	5 M NaOH	13.5	13.5
Solvent*	ddH ₂ O	556.5	756.5

*autoclave

**sterilize by filtration

5.5.1.2 Transformation

8 μL plasmid (16-kDa hPRL: 55 $\mu\text{g } \mu\text{L}^{-1}$; hActivinA: 214 $\mu\text{g } \mu\text{L}^{-1}$; Fam163a: 179 $\mu\text{g } \mu\text{L}^{-1}$; mHSS1: 203 $\mu\text{g } \mu\text{L}^{-1}$) is added to 10 μL competent cells and the mixture is placed immediately on ice and incubated for 5 min. The cells are then heated for 2 min at 42 °C and incubated on ice for 2 min. Then, 250 μL LB medium is added to the cells and the mixture is incubated at 37 °C for 1h. Finally, the cell suspension is spread onto a LB agar plate with ampicillin (75 $\mu\text{g}/\text{mL}$) for selection and incubated overnight at 37 °C.

5.5.1.3 Cultivation of *E. coli* and expression of recombinant proteins

LB-and TB media

A pre-culture is prepared by transferring an isolated single colony from the agar plate into 20 mL of LB-and TB media with ampicillin (60 μ L from stock solution). After incubation overnight at 130 rpm and 30 $^{\circ}$ C, the main culture of 100 mL medium with ampicillin (300 μ L from stock solution) is inoculated with 2 mL pre-culture. The bacteria are cultivated at 37 $^{\circ}$ C and the expression of recombinant protein is induced by the addition of IPTG until OD₆₀₀ reaches 0.6-0.8 (LB medium) or 1.5-2.0 (TB medium).

S-DAB medium

The preculture with 20 mL LB medium with ampicillin (60 μ L from stock solution) is shaken at 37 $^{\circ}$ C for 4-6 h until OD₆₀₀ reaches 1.0. Subsequently, DNB medium is inoculated with LB medium pre-culture to give a starting OD₆₀₀ of 0.02. The DNB medium preculture is shaken at 37 $^{\circ}$ C for 6-7 h until OD₆₀₀ is between 1.5 and 2.0, then it is used to inoculate the main S-DAB culture to give a starting OD₆₀₀ of 0.02.

Cell harvest

After expression, the cells are transferred to 50 mL falcon tubes (2 mL Eppendorf tubes for smaller amounts) which are subsequently centrifuged at 4000 g for 20 min. The supernatants are decanted and the cell pellets are frozen at -20 $^{\circ}$ C or applied directly to the proceeding step.

5.5.1.4 Cell lysis

The cell pellets are disrupted by sonication or lysed directly with a treatment of *Bugbuster*TM *Protein Extraction Reagent* (Novagen, Darmstadt). For detection of the expression of the target proteins, the OD₆₀₀ is always adjusted to 10.

Cell lysis by sonication

The cell pellets are resuspended in lysis buffer and the cell suspension is sonicated three times

5 Appendix

on ice for 1-2 min with 30 sec breaks.

Lysis buffer 50 mM Tris, pH 8.0
 0.1% (v/v) Triton X-100
 1 mM PMSF
 5 U benzonase
 2 mM MgCl₂

Cell lysis with *Bugbuster*TM Protein Extraction Reagent

The cell pellet is resuspended in *Bugbuster*TM Protein Extraction Reagent. 100 U lysozyme and 2.5 U Benzonase per 1 mL *Bugbuster*TM are added to the suspension in order to improve the protein extraction efficiency. Then the cell suspension is incubated for 20 min at room temperature.

Separation of soluble and insoluble cell components

After cell lysis, the soluble proteins are separated from insoluble proteins and cell debris by centrifugation of cell lysate at 4 °C and 17000 g for 45 min. Then the supernatants and pellets are collected. For the detection of expressed insoluble target proteins, the pellets are resuspended in lysis buffer with an OD₆₀₀ of 10.

5.5.1.5 Washing and solubilization of cell pellets

The pellets are resuspended in wash buffer and incubated at room temperature for 10 min. After centrifuging the suspension at 4 °C and 17000 g for 20 min, the pellets are collected. Subsequently, the washed inclusion bodies are suspended in solubilization buffer and incubated whilst being constantly shaken overnight at room temperature for complete solubilization.

Wash buffer for all the inclusion bodies:

50 mM Tris, pH 7.5
25 mM EDTA
0.5 M NaCl
1 M urea
0.1% (v/v) Triton X-100

5 Appendix

Solubilization buffer for inclusion bodies of 16-kDa hPRL:

20 mM ethanolamine, pH 9.0
8 M urea
1% (v/v) β -mercaptonethanol

Solubilization buffer for inclusion bodies of hActivin β A and mHSS1:

50 mM Tris-HCl, pH 8.0
8 M urea
0.5 M DTT

5.5.2 Electrophoresis and staining

5.5.2.1 Native PAGE

Gel preparation

The gels are prepared as shown in Table. 5.1.

Table. 5.1 Recipe for Native-PAGE gel (2X).

Components	Stacking gel	Separating gel (12%)
Acrylamide/Bisacrylamide-solution (37.5:1)	1 mL	2.625 mL
1.5 M Tris-HCl, pH 8.8	--	4.225 mL
0.5 M Tris-HCl, pH 6.8	2.5 mL	--
ddH ₂ O	6.4 mL	3.475 mL
25% APS	15 μ L	15 μ L
TEMED	10 μ L	10 μ L

Sample preparation

The samples are mixed 1:1 with loading buffer.

Loading buffer: 2 mL 1M Tris-HCl, pH 6.8; 2 mL (55% ig (v/v)) glycerol; 4 mL 1% (m/v) solution of bromophenol blue; 5.4 mL ddH₂O

Gel running

After running at 100 V for 30 min, the voltage is shifted to 200 V and the gels run for a further 45 min.

Running buffer 25 mM Tris-base; 192 mM glycine; pH 8.3

5 Appendix

5.5.2.2 SDS-PAGE**Gel preparation**

The gels are prepared as shown in Table. 5.2.

Table. 5.2 Recipe for SDS-PAGE gel (2X).

Components	Stacking gel		Separating gel	
	(6%)	(12%)	(15%)	(20%)
Acrylamide/bisacrylamide (37.5:1)	0.75 mL	3 mL	4 mL	5 mL
1.5 M Tris-HCl, pH 8.8		2.8 mL	2.8 mL	2.8 mL
0.5 M Tris-HCl, pH 6.8	630 μ L			
SDS (1%)	300 μ L	1 mL	1 mL	1 mL
ddH ₂ O	3.77 mL	3.2 mL	2.2 mL	1.2 mL
25% APS	10 μ L	20 μ L	20 μ L	20 μ L
TEMED	10 μ L	20 μ L	20 μ L	20 μ L

Sample preparation

The samples are 1:1 mixed with LaemmLi-buffer, then heated at 95 °C for 5 min.

SDS-sample-buffer: 20 mM Tris-HCl; 2 mM EDTA; 5 % SDS (w/v); 0.02 % (w/v) bromophenol blue; pH 6.8

LaemmLi-buffer: 80 % (v/v) SDS-sample-buffer; 10 % (v/v) glycerol (55% ig (v/v)); 10 % (v/v) β -mercaptoethanol

Gel running

After running at 100 V for 30 min the voltage is shifted to 200 V and the gels run for a further 45 min.

SDS-running buffer (1x TGS): 25 mM Tris-base; 192 mM glycine; 0.1 % SDS (w/v); pH 8.3

5 Appendix

5.5.2.3 Staining

All operations are performed on a shaker.

Coomassie staining

The protocol is listed below:

1. Stain the gel in the stain solution for at least 45 min, until the gel is a uniform blue color.
2. Destain the gel in the destain solution for 1 - 2 h.

Stain solution: 0.25% (m/v) Coomassie brilliant blue R250; 10% (v/v) acetic acid; 40% (v/v) methanol; 50% (v/v) ddH₂O

Destain solution: 10% (v/v) acetic acid; 40% (v/v) methanol; 50% (v/v) ddH₂O

Blue silver staining

The protocol is listed below:

1. Wash the gel with ddH₂O for 5 min, repeat 3 times.
2. Stain the gel in the stain solution for 2 - 4 h.
3. Destain the gel with ddH₂O for at least 30 min until a clear background is reached.

Stain solution: 0.12% (m/v) Coomassie brilliant blue G250; 10% (v/v) phosphoric acid; 10% (m/v) (NH₄)₂SO₄; 20% (v/v) methanol; 80% (v/v) ddH₂O

Silver staining

The protocol is listed below:

1. Lay the gel in silver-destain-fix solution for at least 30 min.
2. Wash gel shortly with ddH₂O for 2 times.
3. Lay the gel in Farmer's reducer for 2.5 min.
4. Wash gel with ddH₂O for 5 min. Repeat the wash step until the gel is colorless.
5. Lay the gel in 0.1% (m/v) silver solution for 30 min. then discard the solution.
6. Wash gel with ddH₂O for 2 times for 30 sec.
7. Rinse gel with 2.5% (v/v) Na₂CO₃ solution.
8. Lay the gel in 100 mL 2.5% (v/v) Na₂CO₃ solution with 400 µL formaldehyde. Wait until yellow-brown bands appear.
9. Lay the gel in 5% acetic acid for 10 min to stop the stain.

5 Appendix

Silver-destain-fix solution: 80 mL acetic acid; 400 mL ethanol; 400 mL H₂O

Farmers reducer: 0.1% (m/v) Na₂S₂O₃; 0.1% (m/v) potassium hexacyanoferrate (III)

5.5.3 Western Blot

Transfer

The operation procedures are listed below:

1. Wash the PVDF membrane with methanol for a few sec.
2. Soak the gel and the PVDF membrane in transfer buffer for a minimum of 15 min to remove salts and detergents.
3. Saturate two fibred pads in transfer buffer.
4. Assemble on the black side of a cassette in the following order:
 - 1 fiber pad
 - 1 SDS gel
 - 1 PVDF membrane
 - 1 fiber pad
5. Insert the cassette into the electrode module. Be sure to check the direction so that the transfer is from the gel to the membrane.
6. Place a stirrer and a Bio-Ice cooling unit (stored at -20 °C) in the buffer tank. Place the electrode module in the buffer tank.
7. Fill the tank with transfer buffer. Place the buffer tank on a magnetic stir plate and stir at medium speed.
8. Attach electrodes and electrophoresis at 100 V for 50 min.

Detection

The operation procedures are listed below:

1. Block the membrane in block buffer for 1h with shaking.
2. Remove the block buffer. Add the primary antibody to the block buffer (anti-6×his 1:5000; anti-mHSS1 1:1500) and incubate the blots for 1h with shaking.
3. Wash 3 times; each time 5 min with block buffer at room temperature.
4. Add the second antibody to the TBST (1:3000) buffer and incubate for 1 h at room temperature with shaking.

5 Appendix

5. Wash 3 times; each time 5 min with TBST buffer and then 2 times with TBS at room temperature.

6. Wash the blot with AP -buffer for 5 min.

7. Shake the membrane with Color-Development-Reagent from *AP conjugate substrat kit* (Bio-Rad Laboratories GmbH, Munich) and wait about 5 min for bands to appear.

Transfer buffer: 25 mM Tris; 192 mM glycine; 10% (v/v) methanol; pH 8.3

TBS: 25 mM Tris; 150 mM NaCl; pH 7.4

TBST: 25 mM Tris; 150 mM NaCl; 0.5% (v/v) Tween 20; pH 7.4

Block buffer: 25 mM Tris; 150 mM NaCl; 2% (w/v) BSA; 0.5% (v/v) Tween 20; pH 7.4

AP -buffer: 100 mM Tris-HCl; 100 mM NaCl; 5 mM MgCl₂; pH 9.0

5.5.4 Determination of protein concentration

5.5.4.1 Bradford assay

For this assay, standard BSA solutions (1000 $\mu\text{g mL}^{-1}$, 750 $\mu\text{g mL}^{-1}$, 500 $\mu\text{g mL}^{-1}$, 250 $\mu\text{g mL}^{-1}$, 200 $\mu\text{g mL}^{-1}$, 100 $\mu\text{g mL}^{-1}$, 50 $\mu\text{g mL}^{-1}$) were prepared. 10 μL of samples and standards are added to a 96-well plate, then 300 μL Bradford reagent was added. After incubation of the plate at 37 °C for 10 min, the absorbance at 595 nm is measured using a SkanIt software (Thermo Fisher Scientific, Karlsruhe). Finally, a linear regression of measured absorbance of standard BSA can be made and using this equation the concentration of the protein sample is calculated.

Bradford reagent: dissolve 100 mg of Coomassie brilliant blue G250 in 50 mL of 95% ethanol. The solution is then mixed with 100 mL of 85% phosphoric acid and made up to 1 L with ddH₂O. The reagent should be filtered through filter paper and then stored in an amber bottle at room temperature.

5.5.4.2 Densitometric analysis

For concentration determination of a target protein in a mixture, densitometric analysis of a stained gel is performed using *Gel-Pro Analyzer 6.0* software. (Media, Cybernetics, Marlow, UK). A series of standard BSA with different concentrations (1000 $\mu\text{g mL}^{-1}$, 750 $\mu\text{g mL}^{-1}$, 500

5 Appendix

($\mu\text{g mL}^{-1}$, $250 \mu\text{g mL}^{-1}$, $100 \mu\text{g mL}^{-1}$) and samples are loaded onto the SDS-gel, which is subsequently stained with Coomassie or blue silver solution. The color intensities of standard BSA are used to create a calibration, by which the concentration of the target protein can be calculated.

5.5.5 Purification using Vivapure MCMini

The Vivapure MCMini incorporates pre-packed Ni^{2+} -IDA agarose resin plugs in ready-to-use spin columns and the protein mixture can be separated by rapid centrifugation. The employed volume of buffer or solution is always 650 μL .

Purification of Trx-Fam163a

Step	Buffer or Solution	Components	Centrifugation	Repeat
1	Binding Buffer	50 mM sodium phosphate, pH 7.4; 200 mM NaCl	1800 g, 1 min	2X
2	Protein Solution		650 g, 5 min	1X
3	Binding Buffer	50 mM sodium phosphate, pH 7.4; 200 mM NaCl	1800 g, 1 min	1X
5	Wash Buffer 1	50 mM sodium phosphate, pH 7.4;	500 g, 2 min	1X
6	Wash Buffer 2	50 mM sodium phosphate, pH 7.4; 50 mM imidazole	500 g, 2 min	1X
7	Elution Buffer	50 mM sodium phosphate, pH 7.4; 200 mM NaCl; 250 mM imidazole	500 g, 3 min	3X

Purification of Fam163a

The protocol is the same as above.

Purification of Fam163a using imidazole stepwise elution

The other steps are as above. Except that the bound proteins are eluted stepwise with 100, 150, 200 and 250 mM imidazole and each elution step is repeated 3 times. The eluates were subjected to SDS-PAGE with silver-staining as shown in Fig. 5.2.

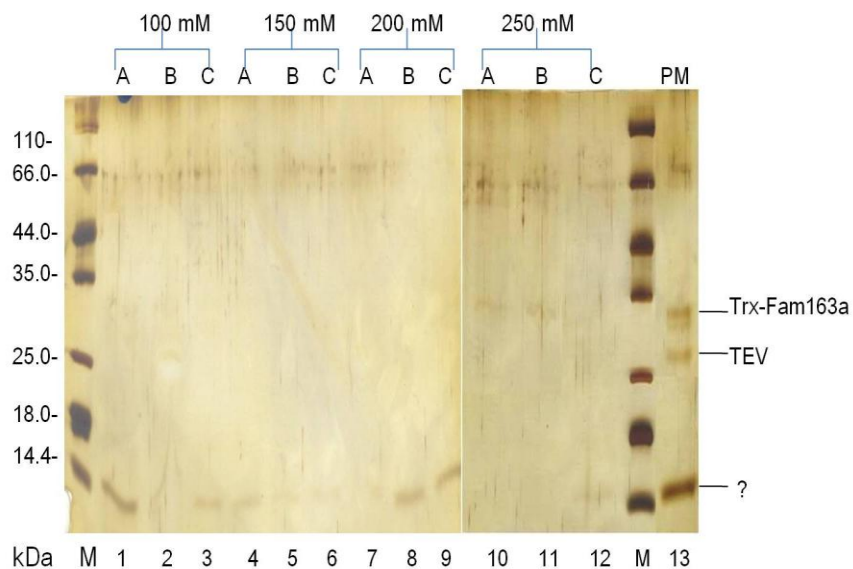


Fig. 5.2 Purification of Fam163a from Trx-Fam163a cleavage products using imidazole stepwise elution presented using 12% SDS-PAGE with silver staining. Lanes 1-12, elution with 100, 150, 200 and 250 mM imidazole, respectively; lane 13, Trx-Fam163a after cleavage at 4 °C for 12 h. A, first elution fraction; B, second elution fraction; C, third elution fraction; PM, protein mixture. M, protein marker (Thermo, 26610).

The incompletely cleaved fusion protein was detected mainly in elution fraction with 250 mM imidazole. This protein band at 15 kDa was detected in the elution fractions with 100, 150, 200 mM imidazole and the band intensities seemed to decrease slowly in the repeated three fractions eluted with the above mentioned three imidazole concentrations. It may indicate three protein peaks during elution.

5.5.6 Purification using Vivawell 8-strips

A 96-well-plate with a hole frame is combined with the 8 units of Vivawell 8-strips, which are located close to one another. For each step 300 μ L buffer or solution is always loaded on the membrane and subsequently centrifuged. ZnSO_4 , NiSO_4 , CuSO_4 and CoCl_2 (0.5 M in equilibration buffer) are used for the screening of metal ions.

5 Appendix

Purification of soluble Trx-mHSS1

Step	Buffer or solution	Components	Centrifugation	Repeat
1	Equilibration buffer	100 mM NaAc; 500 mM NaCl; pH 4.5	1200 g, 1 min	2
2	Metal solution	0.5 M ZnSO ₄ in equilibration buffer	1200 g, 1 min	1
3	Binding buffer	50 mM NaH ₂ PO ₄ ; 500 mM NaCl; pH 8.0	1200 g, 1 min	2
4	Protein solution		600 g, 3 min	1
5	Wash buffer 1	50 mM Tris-HCl, pH 8.0	1200 g, 1 min	2
6	Wash buffer 2	50 mM Tris-HCl; 100 mM imidazole; pH 8.0	1200 g, 1 min	2
7	Elution buffer	50 mM Tris-HCl; 250 mM imidazole; 200 mM NaCl; pH 8.0	1200 g, 1 min	2

Purification of mHSS1

The steps and buffers used remain the same as above, except that each wash step is repeated only once.

5.5.7 Purification using FPLC**5.5.7.1 Anion exchange chromatography**

Step		Parameter		Volume (mL)	Flow rate (mL min ⁻¹)
1	Isocratic Flow	A: A-Buffer 1 B: B-Buffer	100% 0%	5	1
2	Load/ Inject Sample	Sample Static Loop	Auto Inject Valve	3	0.5
3	Isocratic Flow	A: A-Buffer 1 B: B-Buffer	100% 0%	5	1
4	Linear Gradient	A: A-Buffer 1 B: B-Buffer	100%-0% 0%-100%	15	1
5	Isocratic Flow	A: A-Buffer 1 B: B-Buffer	100% 0%	5	1
6	End of Protocol				

5 Appendix

A-Buffer 1, binding buffer: 20 mM ethanolamine, pH 9.0

B-Buffer, elution buffer: 20 mM ethanolamine; 1 M NaCl; pH 9.0

Regeneration and storage of Q75

The membrane adsorber Q75 is washed with 20% (v/v) ethanol and stored at 4 °C.

5.5.7.2 Size exclusion chromatography

Step		Parameter		Volume (mL)	Flow rate (mL min ⁻¹)
1	Isocratic Flow	A: A-Buffer 1 B: B-Buffer	100% 0%	5	1
2	Load/ Inject Sample	Sample Static Loop	Auto Inject Valve	1	0.5
3	Isocratic Flow	A: A-Buffer 1 B: B-Buffer	100% 0%	30	0.5
4	End of Protocol				

A-Buffer 1: 50 mM NH₄HCO₃; 100 mM NaCl; pH 7.5

5.5.7.3 Immobilized metal ion affinity chromatography

For IMAC-purification, the membrane adsorber IDA-75 is prepared with in 10 mL equilibration buffer at a flowrate of 1 mL min⁻¹ for its pre-loading with metal ions.

Equilibration buffer: 100 mM NaAc; 500 mM NaCl; pH 4.5

Purification of Trx-hActivin βA

Prior to purification of Trx-hActivin βA refolding is performed.

Refolding buffer 25 mM Tris-HCl, pH 8.0
 1.0 M urea
 5 mM GSH/1 mM GSSG
 50 mM TDCA/Na

10 mL 0.5 M Zn²⁺ is loaded onto the membrane which is subsequently washed with 15 mL

5 Appendix

equilibration buffer. Prior to starting the FPLC program, the membrane is washed with 20 mL loading buffer (A-Buffer 1) until the conductivity reaches its initial value.

Step		Parameter		Volume (mL)	Flow rate (mL min ⁻¹ .)
1	Isocratic Flow	A: A-Buffer 1 B: B-Buffer	100% 0%	5	1
2	Load/ Inject Sample	Sample Static Loop	Auto Inject Valve	10	0.5
3	Isocratic Flow	A: A-Buffer 1 B: B-Buffer	100% 0%	8	1
4	Isocratic Flow	A: A-Buffer 2 B: B-Buffer	100% 0%	8	1
5	Isocratic Flow	A: Buffer 3 B: Buffer	100%	12	1
6	Isocratic Flow	A: Buffer 4 B: Buffer	100%	20	1
7	Isocratic Flow	A: A-Buffer 1 B: B-Buffer	100% 0%	5	1
8	End of Protocol				

A-Buffer 1, binding buffer: 50 mM NaH₂PO₄; 500 mM NaCl; pH 8.0

A-Buffer 2, wash buffer 1: 50 mM Tris-HCl, pH 8.0

A-Buffer 3, wash buffer 2: 50 mM Tris-HCl; 100 mM imidazole; pH 8.0

A-Buffer 4, elution buffer: 50 mM Tris-HCl; 200 mM NaCl; 250 mM imidazole; pH 8.0

Purification of Trx-Fam163a

10 mL 0.5 M Ni²⁺ is loaded onto the membrane adsorber and the FPLC protocol is the same as for the purification of Trx-hActivin βA.

A-Buffer 1, binding buffer: 50 mM sodium phosphate, pH 7.4; 150 mM NaCl

A-Buffer 2, wash buffer 1: 50 mM sodium phosphate, pH 7.4; 500 mM NaCl; 20 mM imidazole

A-Buffer 3, wash buffer 2: 50 mM sodium phosphate, pH 7.4; 50 mM NaCl; 100 mM imidazole

A-Buffer 4, elution buffer: 50 mM sodium phosphate, pH 7.4; 150 mM NaCl; 300 mM imidazole

5 Appendix

Purification of Trx-mHSS1

10 mL 0.5 M Co²⁺ is loaded onto the membrane adsorber and equilibration of the membrane remains the same as described above. At first, the purification of Trx-mHSS1 is performed under denaturing conditions. Alternatively, refolding is combined with IMAC.

Under denaturing conditions

Step		Parameter		Volume (mL)	Flow rate (mL min ⁻¹)
1	Isocratic Flow	A: A-Buffer 1 B: B-Buffer	100% 0%	5	1
2	Load/ Inject Sample	Sample Static Loop	Auto Inject Valve	3	0.5
3	Isocratic Flow	A: A-Buffer 1 B: B-Buffer	100% 0%	8	1
4	Isocratic Flow	A: A-Buffer 2 B: B-Buffer	100% 0%	8	1
5	Isocratic Flow	A: Buffer 3 B: Buffer	100%	12	1
6	Isocratic Flow	A: Buffer 4 B: Buffer	100%	20	1
7	Isocratic Flow	A: A-Buffer 1 B: B-Buffer	100% 0%	5	1
8	End of Protocol				

A-Buffer 1, binding buffer: 50 mM NaH₂PO₄; 6 M urea; 500 mM NaCl; pH 8.0

A-Buffer 2, wash buffer 1: 50 mM Tris-HCl; 6 M urea; pH 8.0

A-Buffer 3, wash buffer2: 50 mM Tris-HCl; 6 M urea; 300 mM NaCl; 25 mM imidazole; pH 8.0

A-Buffer 4: elution buffer: 50 mM Tris-HCl; 6 M urea; 250 mM imidazole; pH 8.0

5 Appendix

Combination of refolding and IMAC

Step		Parameter		Volume (mL)	Flow rate (mL min ⁻¹)
1	Isocratic Flow	A: A-Buffer 1 B: B-Buffer	100% 0%	5	1
2	Load/ Inject Sample	Sample Static Loop	Auto Inject Valve	3	0.5
3	Isocratic Flow	A: A-Buffer 1 B: B-Buffer	100% 0%	8	1
4	Isocratic Flow	A: A-Buffer 1 B: B-Buffer	100%-0% 0%-100%	40	0.5
5	Isocratic Flow	A: Buffer 2 B: B-Buffer	100% 0%	20	1
6	Isocratic Flow	A: A-Buffer 1 B: B-Buffer	100% 0%	5	1
7	End of Protocol				

A-Buffer 1, binding buffer: 50 mM Tris-HCl; 6 M urea; 500 mM NaCl; pH 8.0

B-Buffer, refolding buffer: 50 mM Tris-HCl; 1 M Urea; 10 mM GSH/1 mM GSSG; pH 8.0

A-Buffer 2, elution buffer: 50 mM Tris-HCl; 1 M Urea; 250 mM imidazole; pH 8.0

Purification of mHSS1

10 mL 0.5 M Co²⁺ is loaded onto the membrane adsorber and equilibration of the membrane remains the same as described above.

Step		Parameter		Volume (mL)	Flow rate (mL min ⁻¹)
1	Isocratic Flow	A: A-Buffer 1 B: B-Buffer	100% 0%	5	1
2	Load/ Inject Sample	Sample Static Loop	Auto Inject Valve	3	0.5
3	Isocratic Flow	A: A-Buffer 1 B: B-Buffer	100% 0%	5	1
4	Isocratic Flow	A: A-Buffer 2 B: B-Buffer	100% 0%	5	1
5	Isocratic Flow	A: Buffer 3 B: B-Buffer	100%	10	1
6	End of Protocol				

5 Appendix

A-Buffer 1, binding buffer: 50 mM Tris-HCl; 100 mM NaCl; pH 8.0

A-Buffer 2, wash buffer: 50 mM Tris-HCl, pH 8.0

A-Buffer3: 50 mM Tris-HCl; 100 mM NaCl; 250 mM imidazole; pH 8.0

Regeneration and storage of IDA-75

The membrane adsorber IDA-75 is regenerated by passing 10 mL of equilibration buffer and the metal ions are removed by passing 10 mL 1 M H₂SO₄. After the membrane is washed with at least 20 mL equilibration buffer, it is stored in equilibration buffer with 0.02% NaN₃.

5.5.8 Endotoxin assay and removal of endotoxin

Determination of endotoxins concentration in purified 16-kDa hPRL is carried out using a Endosafe® PTS™ system (Charles River Laboratories Boston, MA, USA) with a cartridge range 0.1-10 EU mL⁻¹ in accordance with the manufacturer's instruction. The reaction kit (EndoTrap® red, Hyglos GmbH, Bernried) is employed for endotoxin removal following the provided protocol.

5.5.9 Dialysis

The dialysis membrane (Spectra/Por®, Rancho Dominguez, CA, USA) is rinsed with distilled water for 1 h and washed under running water for several times prior to use. Then the membrane is filled with protein solution and introduced into the dialysis buffer.

5.5.10 Cleavage of fusion proteins

Prior to cleavage of fusion proteins, the imidazole in the protein solution is removed by dialysis and the protein concentration is determined by Bradford assay. The cleavage is performed at different temperatures and the conditions for cleavage are as follows:

Fusion protein	20 µg
20×TEV buffer (1M Tris-HCl, pH 8.0; 10 mM EDTA)	7.5 µL
0.1 M DTT *(only for Trx-mHSS1)	1.5 µL
<i>AcTEV</i> TM protease (10U)	1.0 µL
ddH ₂ O	to 150 µL

5 Appendix

*For Trx-Activin β A, 0.1 M DTT is replaced by 0.1M GSH/0.02 M GSSG.

For Trx-Fam163a, 0.1 M DTT is replaced by GSH/ GSSG (0.4 M/0.02 mM, 0.2 M/0.02 M, 0.1M/0.02 M, 0.04 M/0.02 M, 0.02 M/0.1 M).

5.5.11 Protease inhibitor

0.5 M EDTA is dissolved in 50 mM Tris, pH 7.5 and added to the cell lysate with a final concentration of 10 or 20 mM. PMSF is prepared in 100% isopropanol and added to the cell lysate with a final concentration of 1 or 2 mM. For the commercial *Protease Inhibitor Cocktail for purification of Histidine-Tagged Proteins* (Sigma-Aldrich Chemie GmbH, Steinheim), 100 or 200 μ L of this inhibitor solution is added to 10 mL cell lysate.

5.5.12 Immunoprecipitation

5.5.12.1 Anti-his tag beads

Modification from protocol provided from *His tagged Protein PURIFICATION KIT* (Medical & biological laboratories, Nagoya, Japan). 20 μ L anti-his tag beads suspension is dispensed into the protein solution after cleavage and the mixture is incubated with gentle end-over-end mixing overnight at 4 °C. After that, the Eppendorf tube is centrifuged at 400 g for 5 min and the flow through (supernatant) is retained. Then the anti-his tag beads are washed twice in 300 μ L wash buffer by pipetting up and down several times and the supernatant is retained. Subsequently, the resuspended anti-his tag beads are transferred in 300 μ L wash buffer to the spin column and 20 μ L elution peptide with his tag solutions are added to the anti-his tag beads. After incubation for 30 min at room temperature and centrifuging for 10 sec the eluate is retained. For the second elution, 20 μ L elution peptide solution is added to the anti-his tag beads. After incubation for 5 min at room temperature and centrifuging for 10 sec the second eluate is retained.

5.5.12.2 Protein G

20 μ L anti-his antibody solution is pipetted onto 50 μ L protein G sepharose beads (Cambiochem).

5 Appendix

EMD chemicals, San Diego, USA) suspension and the mixture is incubated with gentle end-over-end mixing overnight at 4°C. Subsequently, this complex is incubated with 1 mL cleavage products at 4°C for 3 h. After centrifuging the suspension at 400 g for 5 min, the flow through (supernatant) is removed and the beads are washed twice in 300 µL of wash buffer by pipetting up and down several times. Finally, the his-tagged proteins are expected to be eluted from the sepharose beads in elution buffer by pipetting up and down. The fractions from the purification were analyzed by SDS-PAGE and the results are shown in Fig. 5.3.

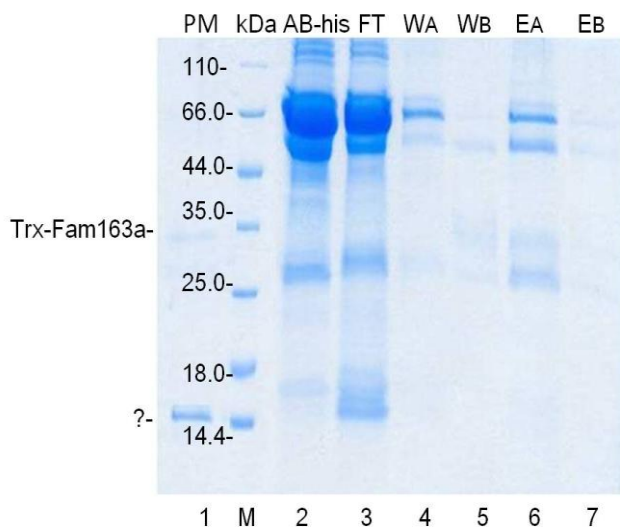


Fig. 5.3 Isolation of Fam163a from Trx-Fam163a cleavage products using protein G sepharose and anti-6×his antibody solution presented using 12% SDS-PAGE with blue silver staining. Trx-Fam163a after cleavage at 4 °C for 12 h (lane 1), anti-6×his antibody (lane 2) and the fractions from following steps of immunoprecipitation (lanes 3-7) are shown. AB-his: anti-6×his antibody; FT, flow through; WA: first wash fraction; WB: second wash fraction; EA: first elution fraction; EB: second elution fraction; M, protein marker (Thermo, 26610).

In Lane 2 are presented the light and heavy chains of anti-his antibody, at about 26 and 52 kDa respectively. Most of the anti-6×his antibody remained unbound with respect to protein G and its bands in the flow through are evident in lane 3. In the elution fraction not only the light and heavy chains of the antibody but also the incompletely digested Trx-Fam163a at 30 kDa with antibody were detected. However, the protein band at 15 kDa could be found only in the flow through and it could be the released Fam163a or Trx which did not bind to the antibody or a combination of the two proteins.

5 Appendix

Wash buffer: 10 mM sodium phosphate, pH 7.0; 150 mM NaCl

Elution buffer: 500 mM acetic acid, pH 3.0 (adjust the pH with 0.005% NH₄OH)

5.5.13 TCA precipitation

100 % (w/v) TCA stored at 4 °C is added to the sample until concentration reaches 20 % (v/v) and after good mix is placed on ice for 1 h. Next, the supernatant is removed after centrifuging at 4 °C and 17000 g for 10 min and the pellet is rinsed with ice cold acid acetone. After centrifuging again, the supernatant is removed and the pellet is air-dried and is subsequently resuspended in buffer for SDS-PAGE.

5. 5.14 Size exclusion-HPLC

The HPLC system is provided with a quaternary pump (L-6200A, Hitachi Europe, Munich), a thermostatted autosampler (Triathion, Spark Holland, AJ Emmen), a column compartment (TSKgel G3000SWXL, 30 cm x 7.8 mm, Sigma Aldrich, Steinheim) and a multiple wavelength ultraviolet detector (L-7400, Hitachi Europe, Munich). SE-HPLC is performed under the following conditions:

Flowrate	0.5 mL min ⁻¹
Temperature	30 °C
Time for analysis	40 min
Wavelength of detector	215 nm
Mobile phase	8.1 mM Na ₂ HPO ₄ ; 1.1 mM K ₂ HPO ₄ ; 400 mM NaCl; pH 7.5

6. REFERENCES

1. Kishimoto T, Taga T and Akira S. (1994) Cytokine signal transduction. *Cell* .76, 253-262.
2. Mackay CR. (2001) Chemokines: immunology's high impact factors. *Nat Immunol.* 2, 95-101.
3. Loppnow H. (2001) Cytokines: Classification, receptors and action mechanisms. *Internist.* 42(1), 13-27.
4. Hanada T and Yoshimura A. (2002) Regulation of cytokine signaling and inflammation. *Cytokine Growth Factor Rev.* 13, 413-421.
5. Taniguchi T. (1995) Cytokine signaling through nonreceptor protein tyrosine kinases. *Science.* 268, 251-255.
6. Lee S and Margolin K. (2011) Review: Cytokines in Cancer Immunotherapy. *Cancers.* 3, 3856-3893.
7. Filshie RJ. (2002) Cytokines in haemopoietic progenitor mobilisation for peripheral blood stem cell transplantation. *Curr Pharm Des.* 8(5), 379-394.
8. Shi Y, Wang R, et al. (1997) Dissociation of cytokine signals for proliferation and apoptosis. *J Immunol.* 159, 5318-5328.
9. Neuman MG, Shear NH, et al. (1998) Role of cytokines in ethanol-induced cytotoxicity in vitro in HepG2 cells. *Gastroenterology.* 115, 157-166.
10. Lacour S, Gautier JC, et al. (2005) Cytokines as potential biomarkers of liver toxicity. *Cancer Biomark.* 1(1), 29-39.
11. Hilfiker-Kleiner D, Sliwa K and Drexler. (2005) HPeripartum cardiomyopathy: recent insights in its pathophysiology. *Trends Cardiovasc Med.* Jul, 18(5), 173-179.
12. Hilfiker-Kleiner D, Kaminski K, et al. (2007) A cathepsin D-cleaved 16 kDa form of prolactin mediates postpartum cardiomyopathy. *Cell.* Feb, 128(3), 589-600.
13. Pan H, Nguyen NQ, et al. (2004) Molecular targeting of antiangiogenic factor 16K hPRL inhibits oxygen-induced retinopathy in mice. *Invest Ophthalmol Vis Sci.* Jul, 45(7), 2413-2419.

6 References

14. Maalouf SW, Talhouk RS and Schanbacher FL. (2010) Inflammatory responses in epithelia: endotoxin-induced IL-6 secretion and iNOS/NO production are differentially regulated in mouse mammary epithelial cells. *J Inflammat.* 7, 85-101.

15. Thompson TB, Woodruff TK, et al. (2003) Structures of an ActRIIB: ActivinA complex reveal a novel binding mode for TGF-beta ligand: receptor interactions. *EMBO J.* 22, 1555-1566.

16. Kingsley DM (1994). The TGF-beta superfamily: new members, new receptors, and new genetic tests of function in different organisms. *Genes & Development.* 8 (2), 133–146.

17. Yu J, Shao LE, et al. (1987) Importance of FSH-releasing protein and inhibin in erythrodifferentiation. *Nature.* 330, 765–767.

18. Okafuji K, Kaku K, et al. (1995) Effects of activin A/erythroid differentiation factor on erythroid and megakaryocytic differentiations of mouse erythroleukemia (Friend) cells: evidence for two distinct modes of cell response. *Exp Hematol.* Mar, 23(3), 210-216.

19. Cornell RA and Kimelman D. (1994) Activin-mediated mesoderm induction requires FGF. *Development.* Feb, 120(2), 453-462.

20. Suzuki K, Kobayashi T, et al. (2010) Activin A induces neuronal differentiation and survival via ALK4 in a SMAD-independent manner in a subpopulation of human neuroblastomas. *Biochem Biophys Res Commun.* Apr, 394(3), 639-645.

21. Leto G. (2010) Activin A and bone metastasis. *J Cell Physiol.* Nov, 225(2), 302-309.

22. Daly R and Hearn MTW. (2005) Expression of heterologous proteins in *Pichia pastoris*: a useful experimental tool in protein engineering and production. *J Mol Recognit.* 18, 119–138

23. Junes-Gill K. (2011) hHSS1: a novel secreted factor and suppressor of glioma growth located at chromosome 19q13.33. *J Neurooncol.* 102(2), 197–211.

24. Vasudevan SA, Shang X, et al. (2009) Neuroblastoma-derived secretory protein is a novel secreted factor overexpressed in neuroblastoma. *Mol Cancer Ther.* 8(8), 2478-2489.

25. Ben-Jonathan N, Mershon JL, et al. (1996) Extrapituitary prolactin: distribution, regulation, function and clinical aspects. *Endocr Rev.* 17, 639-669.

6 References

26. Bole-Feysot C, Goffin V, et al. (1998) Prolactin and its receptor: actions, signal transduction pathways and phenotypes observed in PRL receptor knockout mice. *Endocr Rev.* 19, 225-226.
27. Lewis UJ, Singh RN, et al. (1984) Glycosylated ovine prolactin. *Proc Natl Acad Sci USA.* 81, 385-389.
28. Oetting WS, Tuazon PT, et al. (1986) Phosphorylation of prolactin. *J Biol Chem.* 261, 1649-1652.
29. Khurana S, Liby K, et al. (1999) Proteolysis of human prolactin: resistance to cathepsin D and formation of a nonangiostatic, C-terminal 16K fragment by thrombin. *Endocrinology.* Sep, 140(9), 4127-4132.
30. Mitra I. (1980) A novel "cleaved prolactin" in the rat pituitary. I. Biosynthesis, characterization and regulatory control. *Biochem Biophys Res Commun.* 95, 1750-1759.
31. Baldocchi RA, Tan L, et al. (1998) Mass spectrometric analysis of the fragments produced by cleavage and reduction of rat prolactin: evidence that the cleaving enzyme is cathepsin D. *Endocrinology.* 133, 935-938.
32. Buschmann I and Schaper W. (1999) Arteriogenesis Versus Angiogenesis: Two Mechanisms of Vessel Growth. *Physiology.* Jun (14), 3, 121-125.
33. Sinha YN, Gilligan TA, et al. (1985) Cleaved prolactin: evidence for its occurrence in human pituitary gland and plasma. *J Clin Endocrinol Metab.* 60, 239-243.
34. Ferrara N, Clapp C and Weiner R. (1991) The 16K fragment of prolactin specifically inhibits basal or fibroblast growth factor stimulated growth of capillary endothelial cells. *Endocrinology.* 129, 896-900.
35. Clapp C, Martial JA, et al. (1993) The 16-kilodalton N-terminal fragment of human prolactin is a potent inhibitor of angiogenesis. *Endocrinology.* 133, 1292-1299.
36. D'Angelo GD, Struman I, et al. (1995) Activation of mitogen-activated protein kinases by vascular endothelial growth factor and basic fibroblast growth factor in capillary endothelial cells is inhibited by the antiangiogenic factor 16-kDa N-terminal fragment of prolactin. *Proc Natl Acad Sci USA.* 92, 6374-6378.
37. Duenas Z, Torner L, et al. (1999) Barrios Inhibition of rat corneal angiogenesis by 16-kDa

6 References

prolactin and by endogenous prolactin-like molecules. *Investig Ophthalmol Vis Sci.* 40, 2498-2505.

38. Faupel-Badger JM, Ginsburg E, et al. (2010) 16 kDa prolactin reduces angiogenesis, but not growth of human breast cancer tumors *in vivo*. *Horm Cancer.* Apr, 1(2), 71–79.

39. Martini JF, Piot C, et al. (2000) The antiangiogenic factor 16K PRL induces programmed cell death in endothelial cells by caspase activation. *Mol Endocrinol.* 14, 1536-1549.

40. Tabruyn SP, Sorlet CM, et al. (2003) The antiangiogenic factor 16K human prolactin induces caspase-dependent apoptosis by a mechanism that requires activation of nuclear factor-kappaB. *Mol Endocrinol.* Sep, 17(9), 1815-1823.

41. Tabruyn SP, Nguyen NQ, et al. (2005) The antiangiogenic factor, 16-kDa human prolactin, induces endothelial cell cycle arrest by acting at both the G0-G1 and the G2-M phases. *Mol Endocrinol.* 19 (7), 1932-1942.

42. Fett JD. (2002) Peripartum cardiomyopathy. Insights from Haiti regarding a disease of unknown etiology. *Minn Med.* Dec, 85(12), 46-48.

43. Elkayam U, Akhter MW, et al. (2005) Pregnancy-associated cardiomyopathy: clinical characteristics and a comparison between early and late presentation. *Circulation.* 111, 2050-2055.

44. Reimold SC and Rutherford JD. (2001) Peripartum cardiomyopathy. *N Engl J Med.* 344, 1629-1630.

45. Pearson GD, Veille JC, et al. (2000) Peripartum cardiomyopathy. National heart, lung, and blood institute and office of rare diseases (National Institutes of Health). Workshop recommendations and review. 283, 1183-1188.

46. Elkayam U, Akhter MW, et al. (2005) Pregnancy-associated cardiomyopathy clinical characteristics and a comparison between early and late presentation. *Circulation.* 111, 2050-2055.

47. Negoro S, Kunisada K, et al. (2001) Activation of signal transducer and activator of transcription 3 protects cardiomyocytes from hypoxia/reoxygenation-induced oxidative stress through the upregulation of manganese superoxide dismutase. *Circulation.* 104, 979-981.

48. Bartoli M, Platt D, et al. (2003) VEGF differentially activates STAT3 in microvascular

6 References

endothelial cells. *FASEB J.* 17, 1562-1564.

49. Corbacho AM, Martinez DL, et al. (2002) Roles of prolactin and related members of the prolactin/growth hormone/placental lactogen family in angiogenesis. *J Endocrinol.* 173, 219-238.

50. Xiao S, Robertson DM, et al. (1986) Effects of activin and follicle-stimulating hormone (FSH)-suppressing protein/follistatin on FSH receptors and differentiation of cultured rat granulosa cells. *Endocrinology.* 131(3), 1009-1016.

51. Thompson TB, Woodruff TK, et al. (2003) Structures of an ActRIIB: ActivinA complex reveal a novel binding mode for TGF-beta ligand: receptor interactions. *EMBO J.* 22, 1555-1566.

52. Murata M, Eto Y, et al. (1988) Erythroid differentiation factor is encoded by the same mRNA as that of the inhibin beta A chain. *Proc Natl Acad Sci USA.* 85, 2434-2438.

53. Tasaka K, Kasahara K, et al. (1994) Characterization of activin A-, activin AB- and activin B-responding cells by their responses to hypothalamic releasing hormones. *Biochem Biophys Res Commun. Sep,* 203(3), 1739-1744.

54. Wang Q. (2000) Analysis of human follistatin structure: identification of two discontinuous N-terminal sequences coding for activin A binding and structural consequences of activin binding to native proteins. *Endocrinology. Sep,* 141(9), 3183-3193.

55. Mason, AJ. (1994) Functional analysis of the cysteine residues of activin A. *Mol Endocrinol.* 8(3), 325-332.

56. Stamler R, Keutmann HAT, et al. (2008) The structure of FSTL3.activin A complex. Differential binding of N-terminal domains influences follistatin-type antagonist specificity. *J Biol Chem.* 283, 32831-32838.

57. Greenwald J, Groppe J, et al. (2003) The BMP7/ActRII extracellular domain complex provides new insights into the cooperative nature of receptor assembly. *Mol Cell,* 11, 605-617.

58. Wadhwa M and Thorpe R. (2008) Haematopoietic growth factors and their therapeutic use *Thromb Haemost.* May, 99(5), 863-873.

59. Schubert TE, Obermaier F, et al. (2008) Murine models of anaemia of inflammation: extramedullary haematopoiesis represents a species specific difference to human anaemia of

6 References

inflammation that can be eliminated by splenectomy. *Int J Immunopathol Pharmacol.* Jul-Sep, 21(3), 577-584.

60. Liang R, Chan TK, et al. (1994) Childhood acute lymphoblastic leukaemia and aplastic anaemia. *Leuk Lymphoma.* May, 13(5-6), 411-415.

61. Keller G and Snodgrass G. (1990) Life span of multipotential hematopoietic stem cells in vivo. *J Exp Med.* 171, 1407–1418.

62. Johansson BM and Wiles MV. (1995) Evidence for involvement of activin A and bone morphogenetic protein 4 in mammalian mesoderm and hematopoietic development. *Mol Cell Biol.* 15, 141–151.

63. Nakamura K, Kosaka M, et al. (1993) Effect of erythroid differentiation factor on maintenance of human hematopoietic cells in co-cultures with allogenic stromal cells. *Biochem Biophys Res Commun.* 194, 1103–1110.

64. Broxmeyer HE, Lu L, et al. (1988) Selective and indirect modulation of human multipotential and erythroid hematopoietic progenitor cell proliferation by recombinant human activin and inhibin. *Proc Natl Acad Sci USA.* 85, 9052–9056.

65. Yu J, Shao L, et al. (1989) Characterization of the potentiation effect of activin on human erythroid colony formation in vitro. *Blood.* 73, 952–960.

66. Nishihara T, Ohsaki Y, et al. (1995) Induction of apoptosis in B lineage cells by activin A derived from macrophages. *J Interferon Cytokine Res.* 15, 509–516.

67. Hedger MP, Phillips DJ, et al. (2000) Divergent cell-specific effects of activin-A on thymocyte proliferation stimulated by phytohemagglutinin, and interleukin 1 β or interleukin 6 *in vitro.* *Cytokine.* 12, 595–602.

68. Eto Y, Tsuji T, et al. (1987) purification and characterization of erythroid differentiation factor isolated from human leukemia cell line THP-1. *Biochem Biophys Res Commun.* 142, 1095-1103.

69. Huang HM, Chang TW and Liu JC. (2004) Basic fibroblast growth factor antagonizes activin A-mediated growth inhibition and hemoglobin synthesis in K562 cells by activating ERK1/2 and deactivating p38 MAP kinase. *Biochem Biophys Res Commun.* Aug, 320(4), 1247-1252.

70. Frigon Jr NL, Shao L, et al. (1992) Regulation of globin gene expression in human K562

6 References

cells by recombinant activin A. *Blood*. **79**, 765–772.

71. Musso T, Scutera S, et al. (2008) Activin A induces Langerhans cell differentiation in vitro and in human skin explants. *PLoS One*. Sep, 3(9), e3271.

72. Vigneau C, Polgar K, et al. (2007) Mouse embryonic stem cell-derived embryoid bodies generate progenitors that integrate long term into renal proximal tubules *in vivo*. *J Am Soc Nephrol*. **18**, 1709–1720.

73. Sulzbacher S, Schroeder IS, et al. (2009) Activin A-induced differentiation of embryonic stem cells into endoderm and pancreatic progenitors—the influence of differentiation factors and culture conditions. *Stem Cell Rev*. Jun, 5(2), 159–173.

74. Shal-Tal Y, Lapter S, et al. (2001) Activin receptors. In: Oppenheim JJ, Feldman M, eds. *Cytokine Reference* (online book edition). Academic Press.

75. Ling N, Ying SY, et al. (1986) Pituitary FSH is released by a heterodimer of the beta-subunits from the two forms of inhibin. *Nature*. **321**, 779–782.

76. Mason AJ, Farnworth PG, et al. (1996) Characterization and determination of the biological activities of noncleavable high molecular weight forms of inhibin A and activin A. *Mol Endocrinol*. **10**, 1055–1065.

77. Husken-Hindi P, Tsuchida K, et al. (1994) Monomeric activin A retains high receptor affinity but exhibits low biological activity. *J Biochem*. **269**, 19380–19384.

78. Cronin CN, Thompson DA and Martin F. (1998) Expression of bovine activin-A and inhibin-A in recombinant baculovirus-infected *Spodoptera frugiperda* Sf 21 insect cells. *Int J Biochem*. **30**, 1129–1145.

79. Mason AJ, Gray AM, et al. (1990) Requirement for activin A and transforming growth factor- β 1 pro regions in homodimer assembly. *Science*. **247**, 1328–1330.

80. Ejima M, et al. (2000) Method of refolding human Activin A. United States Patent. No.:6,084,076.

81. Brodeur, GM. (2003) Neuroblastoma: biological insights into a clinical enigma. *Nat Rev Cancer*. **3**, 203–216.

82. Matthay KK. (1995) Neuroblastoma: a clinical challenge and biologic puzzle. *CA Cancer J*

6 References

Clin. 45, 172-192.

83. Schall TJ, Mak JY, et al. (1993) Receptor/Ligand interactions in the C-C chemokine family. *Adv Exp Med Biol.* 351, 29-37.

84. Carmeliet P. (2000) Mechanisms of angiogenesis and arteriogenesis. *Nat Med.* 6, 389–395.

85. Zhong JF, Zhao Y and Sutton S. (2005) Gene expression profile of murine long-term reconstituting vs. short-term reconstituting hematopoietic stem cells. *PNAS.* 102, 2448-2453.

86. Wang X. (2009) Molecular cloning of a novel secreted peptide, INM02, and regulation of its expression by glucose. *J Endocrinol.* 202, 355-364.

87. Mitelman F, Johhanson B and Mertens F. (2009) Mitelman database of chromosome aberations in cancer. <http://cgap.nci.nih.gov/Chromosomes/Mitelman>.

88. Su AI, Cooke MP, et al. (2002) Large-scale analysis of human and mouse transtriptomes. *Proc Natl Acad Sci USA.* 99, 4465-4470.

89. 10. Li H and Cai Y. (1999) Localization of a Flt3 ligand isoform in human tissues. *Zhonghua Xue Ye Xue Za Zhi.* 20(6), 285-287.

90. Von DeimLing A, Nagel J, et al. (1994) Deletion mapping of chromosome 19 in human gliomas. *Int J Cancer.* 57(5), 676-680.

91. Georgiou G and Valax P. (1996) Expression of correctly folded proteins in *Escherichia coli*. *Curr Opin Biotechnol.* 7(2), 190-197.

92. Bessette PH, Aslund F, et al. (1999) Efficient folding of proteins with multiple disulfide bonds in the *Escherichia coli* cytoplasm. *Proc Natl Acad Sci USA.* 96(24), 13703-13708.

93. De Marco A. (2009) Strategies for successful recombinant expression of disulfide bond-dependent proteins in *Escherichia coli*. *Microb Cell Fact.* 8, 26-43.

94. Fahnert B and Neubauer P (2004). Inclusion bodies: formation and utilisation. *Adv Biochem Eng Biotechnol.* 89, 93-142.

95. Przybycien TM, Dunn JP, et al. (1994) Folding and aggregation of TEM 6-lactamase: Analogies with the formation of inclusion bodies in *Escherichia coli* *Protein Eng.* 7, 131-143.

96. Panda AK. (2003) Bioprocessing of therapeutic proteins from the inclusion bodies of

6 References

Escherichia coli. Adv Biochem Eng Biotechnol. 85, 43-93.

97. Natalello A, Ami D, et al. (2006) Kinetics of aggregation and structural properties of proteins in inclusion bodies studied by fourier transform infrared spectroscopy. Microb Cell Fact. 5(1), 10-22.

98. Khan RH, Appa Rao KBC, et al. (1998) Isolation, solubilization, refolding, and chromatographic purification of human growth hormone from inclusion bodies of *Escherichia coli* cells: A Case Study. Biotechnol Prog. 14, 722-744.

99. Ferré H, Ruffet M, et al. (2005) A novel system for continuous protein refolding and on-line capture by expanded bed adsorption. Protein Sci. Aug, 14(8), 2141–2153.

100. Cleland JL, Builder SE, et al. (1992) Polyethylene glycol enhanced protein refolding. Biotechnology (N Y). Sep, 10(9), 1013-1019.

101. Gao YH, Guan YX, et al. (2003) Lysozyme refolding at high concentration by dilution and size-exclusion chromatography. J of Zhejiang Uni- Sci. 4, 2136-2141.

102. Tsumoto K. (1998) Highly efficient recovery of functional single-chain Fv fragments from inclusion bodies overexpressed in *Escherichia coli* by controlled introduction of oxidizing reagents—application to a human single-chain Fv fragment. J Immunol Methods. 219, 119-129.

103. Vincentelli R, Canaan S, et al. (2004) High-throughput automated refolding screening of inclusion bodies. Protein Sci. Oct, 13(10), 2782–2792.

104. Wang QR, Ma L, et al. (2005) Expression, refolding, purification, and bioactivity of recombinant bifunctional protein, hIL-2/GM-CSF. Protein Expr Purif. Feb, 39(2), 131-136.

105. Bassuk JA, Braun LP, et al. (1996) Renaturation of SPARC expressed in *Escherichia coli* requires isomerization of disulfide bonds for recovery of biological activity. Int J Biochem Cell Biol. Sep, 28(9), 1031-1043.

106. Fischer B, Sumner I, et al. (1993) Isolation, renaturation, and formation of disulfide bonds of eukaryotic proteins expressed in *E. coli* as inclusion bodies. Biotech.and Bioengin. 41(1), 3–13.

107. Bulaj G, Buczek O, et al. (2003) Efficient oxidative folding of conotoxins and the radiation of venomous cone snails. No Suppl. Nov, 25(100), 14562-14568.

6 References

108. Mamathambikab BC and Bardwell JC. (2008) Disulfide-linked protein folding pathways. *Annu Rev of Cell and Devel Bio.* 24, 211-235.
109. Eliana DBC. (1998) Refolding of recombinant proteins. *Curre Opin in Biotech.* 9, 157–163.
110. Zhao F and Clare DA. (2002) Purification and characterization of the fusion protein trypsin-streptavidin expressed in *Escherichia coli*. *J Protein Chem.* Aug, 21(6), 413-418.
111. Smith DB and Johnson K. (1988) Single-step purification of polypeptides expressed in *Escherichia coli* as fusions with glutathione S-transferase. *Gene.* 67, 31–40.
112. Di Guan C, Li P, et al. (1988) Vectors that facilitate the expression and purification of foreign peptides in *Escherichia coli* by fusion to maltose-binding protein. *Gene.* 67, 21–30.
113. Sachdev D, Chirgwin JM, et al. (1999) Properties of soluble fusions between mammalian aspartic proteinases and bacterial maltose binding protein. *J Protein Chem.* 18, 127–136.
114. Davis GD, Elisee C, et al. (1999) New fusion protein systems designed to give soluble expression in *Escherichia coli*. *Biotechnol Bioeng.* 65, 382–388.
115. Gusarov I and Nudler E. (2001) Control of intrinsic transcription termination by N and NusA: the basic mechanisms. *Cell.* 107, 437–449.
116. Malakhov MP, Mattern MR, et al. (2004) SUMO fusions and SUMO-specific protease for efficient expression and purification of proteins. *J Struct Funct Genomics.* 5, 75–86.
117. Zuo X, Mattern MR, et al. (2005). Expression and purification of SARS Coronavirus proteins using SUMO fusions. *Protein Express Purif.* Jul, 42(1), 100-110.
118. Lunn CA, Kathju S, et al. (1984) Amplification and purification of plasma-encoded thioredoxin from *E. coli* K12. *J Biol Chem.* 259, 10469-10474.
119. Katti SK, LeMaster DM and Eklund H. (1990) Crystal structure of thioredoxin from *Escherichia coli*. *J Mol Biol.* 212, 167–184.
120. LaVallie ER, Lu Z, et al. (2000) Thioredoxin as a fusion partner for production of soluble recombinant proteins in *Escherichia coli*. *Methods Enzymol.* 326, 322–340.
121. Fernandes PA, Ramos MJ, et al. (2004) Theoretical Insights into the Mechanism for

6 References

Thiol/Disulfide Exchange Chemistry - A European Journal. (4)1, 257-266.

122. Pramesti HT, Suciati T, et al. (2012) Recombinant human bone morphogenetic protein-2: optimization of overproduction, solubilization, renaturation and its Characterization. *Biotechnology*. 11, 133-143.
123. Choi SI, Song HW, et al. (2001) Recombinant enterokinase light chain with affinity tag: expression from *Saccharomyces cerevisiae* and its utilities in fusion protein technology. *Biotechnol Bioeng*. 75, 718–724.
124. Dougherty WG, Carrington JC, et al. (1988) Biochemical and mutational analysis of a plant virus polyprotein cleavage site. *EMBO J*. 7, 1281–1287.
125. Haun RS, Moss J, et al. (1992) Ligation-independent cloning of glutathione fusion genes for expression in *Escherichia coli*. *Gene*. 112, 37–43.
126. Wanga QM and Chenb SH. (2007) Human Rhinovirus 3C Protease as a Potential Target for the Development of Antiviral. *Age Curr Pro and Pep Sci*. 8, 19-27.
127. Nallamsetty S and Kapust RB. (2004). Efficient site-specific processing of fusion proteins by tobacco veinmottling virus protease *in vivo* and *in vitro*. *Protein Expr Purif*. 38, 108-115.
128. Erridge C, Bennett-Guerrero E and Poxton IR. (2002) Structure and function of lipopolysaccharides. *Microbes and Infection*. 4, 837-851.
129. Anspach FB. (2001) Endotoxin removal by affinity sorbents. *J Biochem Biophys Methods*. 49, 665-681.
130. Ogikubo Y, Ogikubo Y, et al. (2004) Evaluation of the bacterial endotoxin test for quantification of endotoxin contamination of porcine vaccines. *Biologicals*. 32, 88-93.
131. Brambilla R. (2009) Transgenic inhibition of astroglial NF- κ B improves functional outcome in experimental autoimmune encephalomyelitis by suppressing chronic central nervous system inflammation. *J Immunol*. 182, 2628–2640.
132. Porekar VG and Menar V. (2001) Perspectives of immobilized-metal affinity chromatography. *J. Biochem Biophys Methods*. 49, 335–360.
133. Yarrow JC, Perlman ZE, et al. (2004) A high-throughput cell migration assay using scratch wound healing, a comparison of image-based readout methods. *BMC Biotechnol. Sep*, 4-21.

6 References

134. Liang CC, Park AY, et al. (2007) *In vitro* scratch assay: a convenient and inexpensive method for analysis of cell migration in vitro. *Nature Protocols*. 2, 329 – 333.
135. Li ZP, Kessler W, et al. (2011) Simple defined autoinduction medium for high-level recombinant protein production using T7-based *Escherichia coli* expression systems. *Appl Microbiol Biotechnol*. Aug, 91(4), 1203-1213.
136. Blommel PG, Becker KJ, et al. (2007) Enhanced bacterial protein expression during auto-induction obtained by alteration of lac repressor dosage and medium composition. *Biotechnol Prog*. 23, 585-598.
137. Enami Y, Kato H, et al. (2001) Anti-transforming growth factor-beta 1 antibody transiently enhances DNA synthesis during liver regeneration after partial hepatectomy in rats. *J Hepatobiliary Pancreat Surg*. 8, 250–258.
138. McGonigle S and Shifrin V. (2008) *In vitro* assay of angiogenesis: inhibition of capillary tube formation current protocols in pharmacology. *Curr Protoc Pharmacol*. Dec, Chapter 12, Unit 12.12.
139. Baker M, Robinson SD, et al. (2011) Use of the mouse aortic ring assay to study angiogenesis. *Nat Protoc*. Dec, 7(1), 89-104.

Curriculum Vitae

Personal data

Name: Zhao, Yangxi

Gender: Female

Marital status: Married

Nationality: P. R. China

Place of birth: Sichuan, China

Date of birth: 01.03.1982

Education

Sep. 1988-Jul. 1994 Tieryuan primary school, Chengdu, China

Sep. 1994-Jul. 1997 Tieryuan junior middle school, Chengdu, China

Sep. 1997-Jul. 2000 Shude middle school, Chengdu, China

Sep. 2000-May 2002 Luzhou Medical School, Luzhou, China

Major: Anesthesiology

Oct. 2003-Sep. 2008 Leibniz University of Hanover

Major: Biology

Degree: Diplom

Feb. 2009-Jun. 2012 Ph.D study in Institute for Technical Chemistry,
Leibniz University of Hanover, under the guidance
of Prof. Dr.Thomas Scheper

Publications

Papers

Chen R, John J, Lavrentieva A, Müller S, Tomala M, Zhao YX, Zwegerdt R, Beutel S, Hitzmann B, Kasper C, Martin U, Rinas U, Stahl F, Scheper T. (2012) Effective production of cytokines using membrane adsorbers, illustrated with human basic fibroblast growth factor production from *Escherichia Coli*. Eng in Life Sci. Feb, 12(1), 29-38.

Zhao YX, Li YH, Korf-Klingebiel M, Reboll M, Woller KC, Rinas U, Scheper T. Production and purification of murine hematopoietic signal peptide-containing secreted 1 from recombinant *Escherichia coli* using thioredoxin as fusion partner. (in preparation)

Zhao YX, Korf-Klingebiel M, Reboll M, Woller KC, Rinas U, Scheper T. Expression and purification of bioactive soluble murine protein family with sequence similarity 163 member A in recombinant *Escherichia coli* using thioredoxin as fusion partner. (in preparation)

Poster

Zhao YX, Li YH, Korf-Klingebiel M, Reboll M, Woller KC, Rinas U, Scheper T. (2010) Expression, purification and refolding of hematopoietic signal peptide-containing secreted 1 from recombinant *Escherichia coli*. 28. DECHEMA-Jahrestagung, Berlin, Germany.